2019

Distribution system outage management after extreme weather events

Anmar Arif
Iowa State University

Distribution system outage management after extreme weather events

by

Anmar Arif

A dissertation submitted to the graduate faculty

in partial fulfillment of the requirements for the degree of

DOCTOR OF PHILOSOPHY

Major: Electrical Engineering

Program of Study Committee:
Zhaoyu Wang, Major Professor
Sarah M. Ryan
James McCalley
Venkataramana Ajjarapu
Lizhi Wang

The student author, whose presentation of the scholarship herein was approved by the program of study committee, is solely responsible for the content of this dissertation. The Graduate College will ensure this dissertation is globally accessible and will not permit alterations after a degree is conferred.

Iowa State University

Ames, Iowa

2019

DEDICATION

I would like to dedicate this thesis to my father and mother for their love and guidance, and to my wife Majd, who has been with me from start to finish, always supporting me.

TABLE OF CONTENTS

Page

LIST OF TABLES

Page

LIST OF FIGURES

Page

ACKNOWLEDGEMENTS

I would like to take this opportunity to express my thanks to those who helped me with various aspects of conducting my research and writing of this thesis. First, Dr. Zhaoyu Wang for his guidance, patience and support throughout this research and the writing of this thesis. His encouragements led me to believe in myself and publish many papers. I would also like to thank Iowa State University for giving me the opportunity to conduct my research in its wonderful campus, and I want to thank King Saud University and the Saudi government for supporting me in my studies. Besides my advisor, I want to thank my committee members for their efforts: Dr. Sarah Ryan, Dr. Venkataramana Ajjarapu, Dr. James McCalley, and Dr. Lizhi Wang. I want to express my gratitude to Dr. Sarah Ryan, who is my minor advisor, for teaching me everything I know about stochastic optimization, and for lending me her laptop to take the industrial engineering qualifier when I forgot mine. I want to thank Dr. Venkataramana Ajjarapu and Dr. James McCalley for taking time from their very busy schedule to read, listen, and provide great comments about my research. I also want to thank Dr. Lizhi Wang for teaching me so much about linear programming and optimization, without his teachings I would not have been able to do half of the work in this thesis. I would like to also thank my colleagues Shanshan Ma and Nichelle'Le Carrington who've been with me from the first day in the department.

No words are enough to thank my parents, I left home in 2013 and missed a lot of important events, but they always support me and help me overcome any difficulties. My father inspired me to pursue my PhD, and I hope to one day become as good a professor as he is. Finally, I want to thank my wife Majd, she not only followed me to Iowa and given me her love and support, she also helped me write this thesis by revising every word I write.

ABSTRACT

The main topic of this dissertation is the recovery operation of distribution networks after extreme weather events. The study focuses on coordinating crews, equipment, and distribution network operations. While utilities have established protocols for recovering distribution networks, areas for continued development still exist, especially with the increase of distributed generators and controllable switches. After major weather events, one of the greatest challenges that operators face is managing the large influx of crews required to repair the damage and to reestablish normal network operations. The aim of this work is to improve current practices and provide assistance to utilities in their decision-making process to efficiently restore the system. The main objectives of this research are summarized as follows: 1) develop a stochastic program to prepare human resources and equipment before extreme weather events; 2) co-optimize repair scheduling and power operation of distribution networks; and 3) design solution algorithms for solving the above problems. For an upcoming storm, utilities should have a preparation plan that includes warehousing restoration supplies, securing staging sites (depots), and prepositioning crews and equipment. Pre-storm planning enables faster and more efficient post-disaster deployment of crews and equipment resources to damage locations. To assist utilities in making this important preparation, we develop a two-stage stochastic mixed integer linear program. The first stage determines the depots, number of crews in each site, and the amount of equipment. The second stage is the recourse action that deals with acquiring new equipment and assigning crews to repair damaged components in realized scenarios. The objective of the developed model is to minimize the costs of depots, crews, equipment, and penalty costs associated with delays in obtaining equipment and power restoration. We consider the uncertainties of damaged lines, number and type of equipment required, and expected repair times.

In the post-disaster phase, two approaches are presented for co-optimizing repair and restoration

in distribution networks. First, a novel mixed integer linear program model is formulated for co-optimizing crews, resources, and distribution network operations. In addition, a framework for integrating different types of photovoltaic (PV) systems in the restoration process is developed. We consider line crews for damage repairs and tree crews for obstacle removal. The model is solved using a new algorithm that utilizes the neighborhood search method to iteratively improve the solution. The algorithm is used in a dynamically changing environment to handle the uncertainty of the repair time. In the second approach, a two-stage SMIP is developed to model the stochastic repair and restoration problem. A decomposition approach, combined with the Progressive Hedging algorithm, is used for solving the stochastic problem.

CHAPTER 1. INTRODUCTION

1.1 Research Motivations and Problem Statement

The United States has experienced a rising trend in power outages, primarily due to the combination of an aging electrical grid and a dramatic increase in severe storms. According to a report published by the Executive Office of the President, around 700 large-scale outage events occurred due to severe weather events in the United States between 2003 and 2012 [1]. In 2016, the average outage duration for the customers in the United States ranged from 27 minutes in Nebraska to 6 hours in West Virginia, to 20 hours in South Carolina due to Hurricane Matthew [2]. More recently in 2017, nearly 280,000 Texas customers were left without power after Hurricane Harvey [3]. The U.S. Department of Homeland Security announced that about 15 million customers were left without power after Hurricane Irma [4]. In 2017, 16 major events occurred in the United States that caused more than $1 billion each in damage. The 16 major events included three tropical cyclones and eight severe storms [5], as shown in Fig. 1.1. The trend continued in 2018 with 14 major events including eight severe storms, two tropical cyclones, two winter storms, drought, and wildfires [6], as shown in Fig. 1.2. The National Oceanic and Atmospheric Administration's (NOAA) National Centers for Environmental Information (NCEI) has been tracking weather and climate events that have greatly impacted the United States [5]. NOAA provided a summary for the number of events and the associated costs for the years 1980–2017, as shown in Fig. 1.3.

The loss of electricity after a hurricane or any natural disaster can cause significant inconvenience and is potentially life threatening in some cases. Improving outage management and accelerating service restoration are critical tasks for utilities. Dispatching and routing repair crews and operating the network to restore service for customers are crucial responsibilities. The routing problem is a combinatorial optimization problem, which is known to be difficult. Combining emergent distribution system operation technologies with the routing problem will further increase the complexity. The

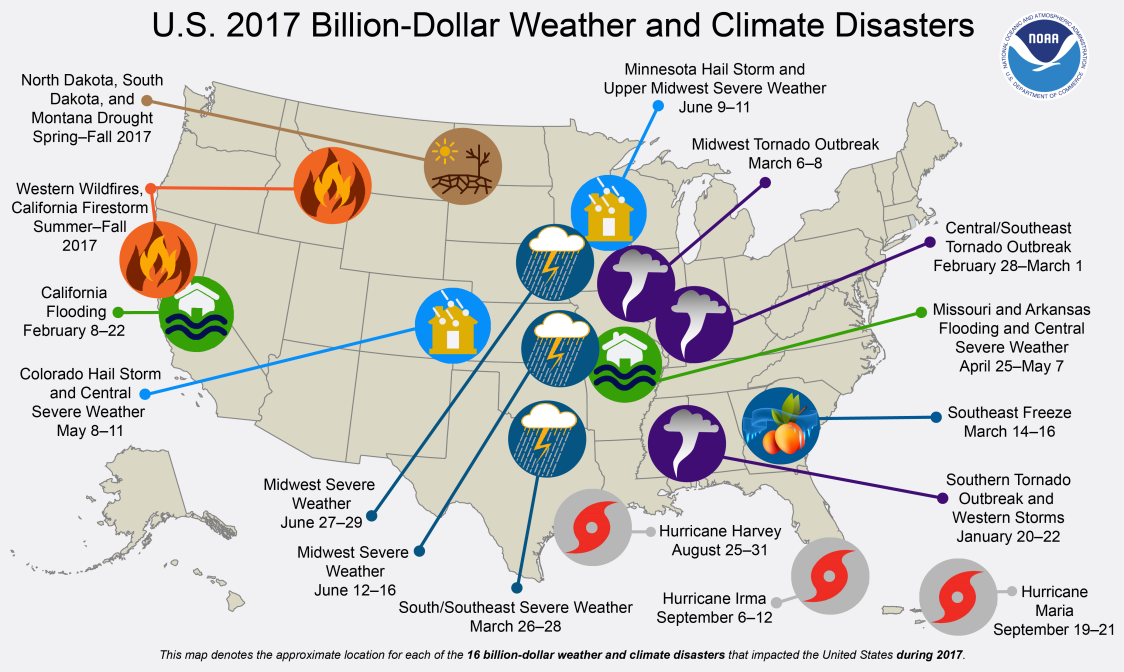

Figure 1.1 Map depicting the general area where sixteen weather and climate disasters caused at least one billion dollars in direct damages in 2017 [5].

commonly used approach is to consider the power system operation/restoration and repair crew routing as two independent problems. However, the operation of the network and the repairs are interdependent in practice. Some customers cannot be served until the damage is repaired. Utilities commonly rely on the experiences of the operators, which cannot lead to an optimal outage management plan. Therefore, an integrated framework to optimally coordinate repair and restoration needs to be designed. The addition of new technologies, such as distributed generation and automatic/controllable switches, can help facilitate a faster restoration process if coordinated well with the repairs. An optimization process that jointly considers crew scheduling and the operation of the network can help the operator in making critical and more informed decisions after outages. In addition, in order to ensure a fast response, utilities must prepare their resources before a severe weather event hits the system. A major challenge that utilities face is lack of resources, including human resources and equipment, to handle extreme events. Once utilities request assistance from neighboring companies, they are faced with another task of managing the

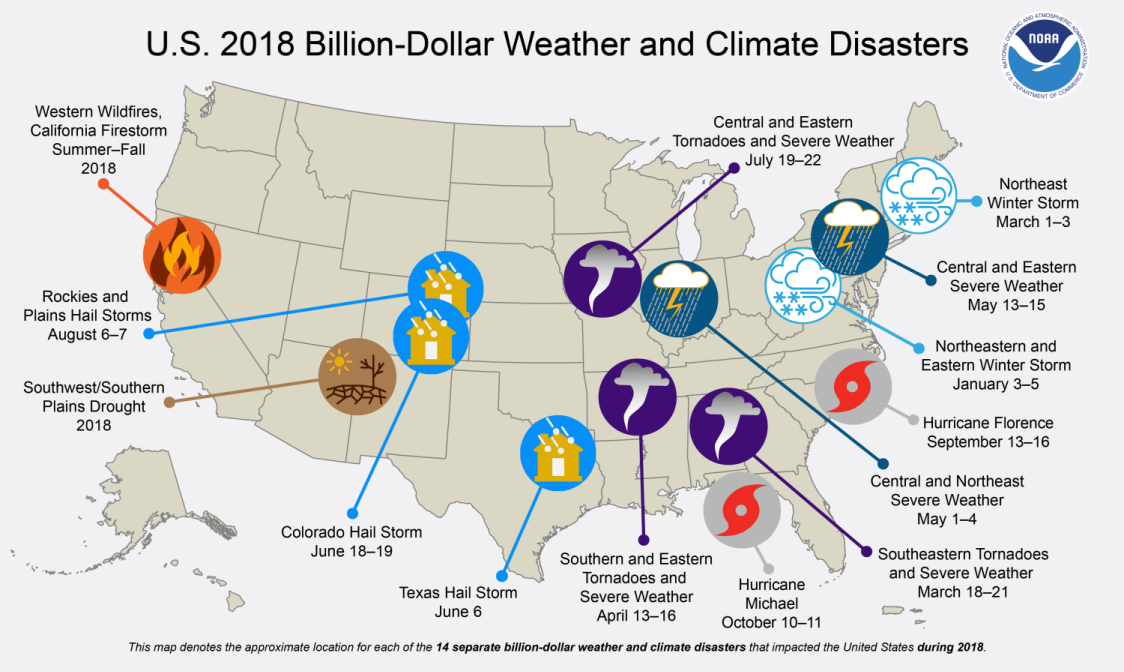

Figure 1.2 Map depicting the general area where fourteen weather and climate disasters caused at least one billion dollars in direct damages in 2018 [6].

newly acquired resources. For these reasons, preparation is essential before predicted extreme or severe weather events. Utilities need to identify the required resources and preallocate the crews and equipment. The aim of our work is to provide utilities with a better decision-making process for extreme events to improve the resiliency of the system. Resiliency is a relatively new concept in power systems that has been an active area of study in recent years. Resiliency in power systems can be defined as the ability of the system to withstand and recover quickly following disruptive events. Improving resiliency involves long-term planning, short-term planning, and post-event operations. In [7] and [8], the authors focused on long-term planning through infrastructure hardening, optimal distributed generator (DG) placement, and automatic switch installations. In this research, we focus on short-term planning and post-event operations for distribution systems, specifically the preparation of equipment and crews, and post-event repair and restoration.

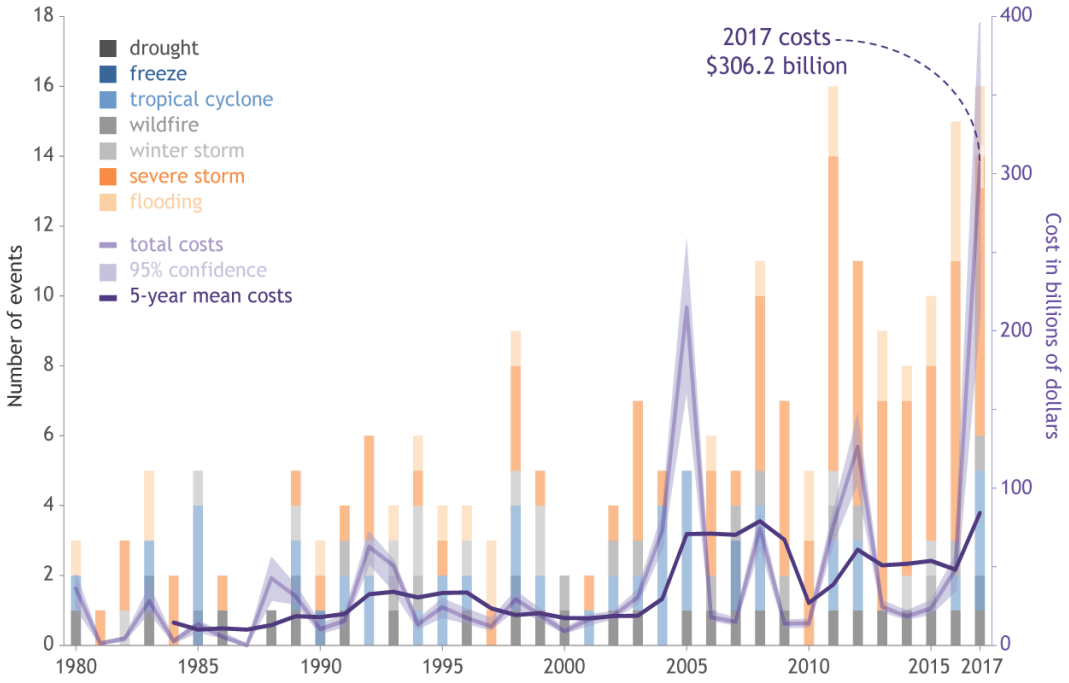

Figure 1.3 The number, type, and annual cost of billion-dollar disasters in the U.S. from 1980 to 2017, based on NCEI data from Adam Smith [5].

1.2 Research Objective

The objectives of the dissertation are listed as follows:

- Develop a two-stage multi-objective stochastic mixed integer linear program (SMIP) to prepare and pre-stage human resources and equipment. The first stage determines the staging sites, number of crews in each site, and the amount of equipment. The second stage is the recourse action that deals with acquiring new equipment and assigning crews to repair the damage. The objective of the developed model is to minimize the costs of staging areas, crews, equipment, and penalty costs associated with delays in obtaining equipment and power restoration. We consider the uncertainties of damaged lines, number and type of equipment required, and expected repair times. Pre-disaster planning enables quick deployment of crews and equipment to damage locations.

- Develop a mathematical model to co-optimize repair scheduling and the recovery operation of

distribution networks. Two approaches are proposed in this dissertation. First, a deterministic mixed integer linear program (MILP) for coordinating network reconfiguration, damage isolation, distributed generator redispatch, and crew/resource logistics is developed. Different types of photovoltaic (PV) systems and battery energy storage systems (BESS) are considered in the mathematical model. The model includes a formulation that dynamically operates automatic switches in distribution systems to form microgrids and isolates damaged lines. The developed model considers two different types of crews, namely, line crews for damage repair and tree crews for obstacle removal. In the second approach, a two-stage SMIP is developed to solve the repair and restoration problem. The first stage is to dispatch the repair crews to the damaged components. The second stage is distribution system restoration using distributed generators and reconfiguration. We consider demand uncertainty in terms of a truncated normal forecast error distribution and model the uncertainty of the repair time using a lognormal distribution.

- Design solution algorithms for solving the above problems. The combined repair and restoration problem is difficult to solve using commercial solvers. In addition, due to the nature of the problem, a fast solution is required to dispatch the crews. Here, an algorithm for each approach mentioned in the previous objective is proposed. For the MILP model, a tri-stage algorithm is developed to solve the proposed model. The first stage is an assignment problem, where the crews are assigned to the damaged components, and in the second stage, the crews are dispatched to the assigned components from the first stage. In the third stage, a neighborhood search approach is used to improve the routing decisions obtained from the second stage. The algorithm is employed in a dynamically changing environment, where the routing solution is updated as new information on the system status is obtained. For the two-stage SMIP, the problem is decomposed into two stochastic subproblems. The first subproblem is a stochastic crew assignment problem, where the main objective is to minimize the working hours. The second subproblem dispatches the crews to the assigned damaged components and operates the distribution system.

1.3 Research Contribution

The main contributions of this dissertation are listed as follows:

- A new two-stage SMIP model is developed and used to select depots and allocate crews and equipment. The model considers different types of crews (line and tree crews) and equipment (poles, transformers, and conductors). Mathematical equations for modeling the interdependencies of the depots, crews, equipment, and damaged components are formulated, in addition to symmetry-breaking constraints to improve the performance of the model. Also, we provide a procedure for estimating the number and types of required equipment after extreme weather events.

- A novel mathematical model for combining the repair crew routing and distribution network operation problems is developed. To the best of our knowledge, the proposed model is the first formulation that combines the two problems in the literature. The designed model captures the nature of the repair problem by modeling the coordination of line and tree crews, resource logistics, and isolation of the damaged components. This model can assist utilities in scheduling the repairs and reestablish normal network operations after natural disasters.

- A mathematical formulation is developed for fault isolation and service restoration. Most of the studies on distribution system restoration assume that every line is equipped with switches to isolate the faults, which is not the case in practice. The developed formulation allows the network to isolate the faults and divides the network into microgrids. The proposed model can be incorporated into various distribution system studies, such as those related to distribution system planning, networked microgrids, and distribution system repair and restoration.

- A new framework for modeling different types of PV systems is developed. Not all PV systems can be used during an outage. There are three main types of PV systems that we consider in this dissertation: 1) On-grid (grid-tied) system: this type of PV is disconnected during an outage; 2) Hybrid on/off-grid (PV with BESS): the PV system operates on-grid in normal conditions, and off-grid during an outage (serves local load only); 3) PV + BESS with grid

forming capabilities: this system can restore part of the network that is not damaged if the fault is isolated. The idea of the proposed approach is to use virtual sources, loads, and flow to identify energized buses in distribution systems.

- A new hybrid algorithm that combines mathematical programming and the neighborhood search method is designed to solve the computationally difficult repair and restoration problem. The algorithm starts by solving the co-optimization problem using an assignment-based method, and then a neighborhood search method is designed to iteratively improve the solution. The proposed method outperforms commercial solvers and can be easily updated in case of a change in outage status.

- A two-stage SMIP is developed for optimizing service restoration in distribution networks with uncertain repair time, demand, and solar irradiance. The SMIP model is decomposed into two stochastic subproblems and solved using Progressive Hedging.

1.4 Organization of the Dissertation

The rest of the dissertation is organized as follows. In Chapter 2, a review of the literature and background information on utility practices are provided. The chapter covers disaster preparation, distribution network restoration, crew routing, and previous work on the combined repair and restoration problem. Chapter 3 presents the disaster preparation problem. The chapter starts with a brief introduction on stochastic optimization, followed by a fragility analysis approach to estimate the impact of upcoming extreme events. Then, a two-stage SMIP is developed for preallocating the crews and equipment and the Progressive Hedging algorithm is introduced. Chapter 4 presents the distribution system repair and restoration problem (DSRRP). A MILP model for solving the repair and restoration problem by coordinating crews, equipment, and the recovery operation of the distribution network is developed. Chapter 5 presents the stochastic model used for solving the repair and restoration problem with uncertainty. Chapter 6 presents a summary of the dissertation, an outline of the contributions, and a discussion of future work.

CHAPTER 2. LITERATURE REVIEW

2.1 Overview

This chapter presents a review of the literature and background information on utility practices. Utility practices are discussed in Section 2.2, starting from preparation procedures to damage restoration. Section 2.3 provides a review on disaster preparation. Section 2.4 summarizes the methods for solving the crew routing problem. Section 2.5 summarizes the current research on distribution network restoration and presents some of the efforts that have been enacted to combine the crew routing and power recovery operation problems.

2.2 Utility Practices

Electric utilities have their own plans for service restoration, which may be different from one utility to another in terms of operating procedures, labor agreements, crew management, etc. Though detailed restoration procedures are different, the general steps can be summarized as follows [9, 10]:

2.2.1 Proactive Response

When a severe weather event is predicted, utilities position repair crews and supplies in (or near) the areas that are expected to suffer the greatest damage. In addition, utilities can acquire services from crews in neighboring utilities and reach out to contractors. Pre-staging crews, equipment and other resources safely before a severe event allows for a quick response and efficient resource management.

2.2.2 Outage Management

In their movement to modernize distribution networks, electric utilities have been investing in the area of distribution grid management. Three key operational technologies DMS (Distribution Management System), SCADA (Supervisory Control and Data Acquisition), and OMS (Outage Management System) have been integrated to increase distribution operation efficiency. This integrated platform is utilized in outage management processes and in normal operations. The integrated system is designed to provide real-time monitoring and control of distribution systems. It allows operators to control important operational devices such as distribution breakers, sectionalizing switches, reclosers, voltage regulators, and other devices. Reclosers and sectionalizing switches are critical for fault location, isolation, and service restoration (FLISR). Reclosers detect and interrupt faults and the sectionalizer opens and isolates the faulty section of the network. The recloser is then closed so that the healthy part of the network is supplied. OMS tracks impacted areas in the network by integrating data from geographic information systems (GIS), customer information system (CIS), Interactive Voice Response systems (IVR) for handling customer calls, SCADA, and smart meters after outages. This integration allows utilities to automatically update the work crews with information about outages and their locations. OMS also assists with crew management, restoration time estimation, and identifying critical facilities that are impacted.

2.2.3 Damage Assessment

After an extreme weather strikes the electric grid and outages occur, the OMS collects information from different sources and provides the likely locations of the problems in the grid. Field assessors are dispatched to identify the exact locations of the damage as well as document and analyze them. The damage information is communicated back to the operator. This damage assessment data is essential so that utilities can estimate the repair times and route the repair crews more effectively with the required equipment. In extreme cases, damage assessment can also be conducted through aerial survey [11].

2.2.4 Managing Tree Damage

Trees falling on distribution lines is one of the leading outage causes especially after storms and high winds. Utilities deploy tree crews to damage sites to clear the area before the repair crews (also known as line crews) start to repair the damaged components and reenergize the damaged lines. Therefore, the utilities must coordinate tree and line crews for an efficient repair and recovery operation.

2.2.5 Prioritizing Restoration

Large numbers of residential customers, hospitals, police and fire departments, schools, or other important facilities may lose energy after a severe event. Each utility has its own priority list but it can be generally summarized as follows:

- Crews first clear and isolate live power lines and any hazards to the public.
- Substations are restored. Transmission lines are restored, as well, but by different crews responsible to their owners.
- Local distribution substations are checked and repaired by service crews and engineers in case of a failure.
- The next priority is the main distribution line attended by the line crews.
- Out-of-service critical consumers like hospitals are given a higher priority while repairing the lines.
- Line crews fix tap lines based on restoring service to the greatest number of customers.
- Individual customers are last in the repair schedule.

In general, utilities schedule the repair using predefined restoration priority lists based on the priority of the consumers, number of consumers and previous experiences. Some utilities use a simple greedy algorithm to determine the restoration sequence [12], other rely on the experience of the operators. An optimization process can help the operator and greatly decrease the restoration time.

2.3 Disaster Preparation

Disaster preparation is a well-studied research area. In [13], a two-stage stochastic programming model was developed to select the storage location of medical supplies, and the required number of different types of supplies before a disaster. The objective of the developed model was to minimize the operation cost of the warehouses, the total transportation time, and the unfulfilled demand. A similar stochastic problem was tackled in [14], while considering the impact of the disaster on the warehouses. The paper used Benders Decomposition to solve the stochastic model. The authors in [15] developed a multi-objective mixed integer linear program to determine the location of emergency facilities, resource allocation and relief distribution for flood preparation. Reference [16] developed a two-stage SMIP model to acquire and allocate relief assets. The first-stage decisions included expansion of resources for warehouses, medical facilities, and shelters. In the second stage, the resources are deployed to help the population. Another SMIP approach was presented in [17]. The goal of the presented model was to place enough materials at shelter location within the first 12 hours of a forecasted hurricane to accommodate the community's need for the first 48 hours. In [18], a MILP and a Lagrangian relaxation method were developed for locating emergency shelters and medical centers, and maintaining ambulances. The authors in [19] used robust optimization to produce a logistic plan for mitigating demand uncertainty in humanitarian relief supply chains. A multi-objective robust model for humanitarian relief logistics was developed in [20]. The paper considered demand and supply uncertainty and considered the possibility that some supplies may be damaged during the event. In [21], the authors developed a p-robust optimization model, which combines robust optimization with Monte Carlo simulation, for determining the location of relief bases, number of rescue vehicles, and other relief supplies. A min-max robust model is developed in [22] to optimize the relief facility location and preposition emergency supplies for disaster preparation. However, further research is needed on disaster preparation in the context of power system and its infrastructure. In [23], the authors divided the power network into different areas/cells, and developed a MILP to find the optimal number of depots and their locations. Each area was assumed to have a specific demand and can only contain one depot. The objective was to minimize the

transportation cost between the predefined areas. A storage and customer allocation problem was presented in [24]. The authors developed a multi-objective stochastic mixed-integer program that determines which warehouse to use and the number of resources to store in each warehouse. The objectives were to minimize the amount of unsatisfied demand, the transportation cost of the resources between the warehouses, and the investments and maintenance cost of the warehouses. Reference [25] developed a SMIP model and a column generation approach for stockpiling resources before a disaster. The developed approach focused on determining the quantity and type of equipment, while neglecting the crews and the distances between the warehouses and the damaged components. In [26], a heuristic method for positioning repair crews is developed.

The distribution system preparation problem is a challenging one because it combines the combinatorial optimization problems of depot location, equipment transportation and allocation, and crew allocation. The preparation problem is inherently stochastic, as the damaged components and the required resources are not known beforehand. This makes it a complex stochastic combinatorial optimization problem. The previous work approached the preparation stage by dividing the electric network into different areas, with each area having a specific demand. This kind of approach neglects the individual components within each area and the distances between these components and the depots. Moreover, the interdependence between the location and number of crews, damaged components in the network, and the number of resources required to repair the damage was not examined in the preparation stage. Crews should be positioned near the damaged components, and the equipment should be allocated such that the crews have the required equipment for the repairs. We propose a two-stage SMIP to model the preparation problem in Chapter 3. The proposed SMIP leverages assignment, allocation, and transportation modeling techniques to model the interdependencies of the depots, crews, equipment, and damaged components.

2.4 Crew Routing and the Vehicle Routing Problem

In this dissertation, crew routing is modeled as a Vehicle Routing Problem (VRP). VRP is a combinatorial optimization problem that has been studied in operations research, applied

mathematics, and computer science for decades. VRP is an NP-hard problem which is known to be a computationally difficult problem, obtaining an optimal solution for this problem is almost impossible, and providing reliable and fast solutions is a challenging task. In its simplest form, VRP is known as the Traveling Salesman Problem (TSP) which is also a well-studied problem. TSP consists of one vehicle, a single depot (station) as a starting point, and multiple locations to be visited (damaged components in the context of repair crews). The vehicle/crew starts from the depot, travels to each damaged component to conduct the repairs, then returns to the depot. The objective is typically to find the shortest possible route. VRP is the same as TSP but with multiple crews. For a detailed review on VRP, the readers can refer to [27]. In this section, a summary of the main variations of VRP and the techniques used to solve the problem are presented. VRP has been modified in many ways by researchers through the introduction of real-world aspects. One of the classical VRP variations is the capacitated vehicle routing problem (CVRP). CVRP can be defined as a VRP where a fleet of vehicles must service a specific number of customer demands, and the total demand that each vehicle serves does not exceed the capacity of the vehicle. Adding time restrictions on VRP produces the VRP with time window (VRPTW) problem. The combination of CVRP and VRPTW is known as CVRPTW (capacitated vehicle routing problem with time windows). In real-world application, delivery companies normally have more than one depot from which they can serve their customers, A VRP with multiple depots is known as the multi-depot vehicle routing problem (MDVRP). In the context of repair crew routing, crews may have to return to depots and pick up equipment to conduct the repairs, this problem is referred to as VRP with pickup and delivery (VRPPD). Stochastic VRP (SVRP) is another variation of VRP, in which, the demand, travel time, or service time are random parameters.

In terms of modeling, VRP is commonly modeled using either Integer Programming (IP) or MILP [28]. Graph theory and network flow models [29] are also used to represent VRP. Other models include knowledge-based [30], time space [31] and Constraint Programming (CP) [32] models. CP has the same structure as mathematical programming but includes logical operations and relations. Methods for solving VRP and its variations include exact and heuristic algorithms. Though exact

methods, such as cutting-plane approaches (e.g., branch-and-cut and branch-and-bound), dynamic programming, and column generation are only used for small instances as it is impossible to solve large instances with the current technology [33]. The choice of solution method depends on the type of problem being solved and the approach must be tailored to the problem. In this dissertation, we design a hybrid method that combines mathematical programming and a metaheuristic algorithm to solve the repair and restoration problem in Chapter 4. Specifically, the problem is modeled as a MILP problem and large neighborhood search is deployed for exploring different solutions. The combination of mathematical programming and heuristic algorithms is known as matheuristic methods, which has gained considerable interest in recent years [34]. In Chapter 5, a decomposition method coupled with the Progressive Hedging algorithm is used to solve the stochastic DSRRP (S-DSRRP). Table 2.1 summarizes some of the methods used for solving VRP.

Table 2.1 Solution algorithms for solving VRP

Type	Solution Algorithm	Ref.	Problem
Exact	Lagrangian relaxation + decomposition	[35]	CVRPTW+VRPPD
	Column generation	[36]	Heterogeneous CVRP
	Branch-and-price	[28]	VRP with roaming locations
	Branch-and-cut	[37]	CVRP with unloading constraints
Heuristic	Guided Local Search	[38]	VRPTW with backhauls
	Simulated annealing	[39]	CVRP for hybrid vehicles
	Greedy randomized adaptive search	[40]	VRPTW with precedence
	Tabu search	[41]	CVRP
	Large neighborhood search	[42]	VRP with cross-docking
	Genetic Algorithm	[43]	CVRP
	Ant colony optimization	[44]	CVRP
	Particle swarm optimization	[45]	SVRP
	Cluster-first route-second	[46]	VRP with backhauls

2.5 Distribution Network Restoration

There has been considerable progress in power system restoration techniques [47, 48]. A variety of algorithms have been proposed for load restoration, including heuristic techniques [49], dynamic programming [50] and multi-agent systems [51]. Network reconfiguration is one of the most commonly

used methods to restore a power distribution system. The authors in [52] developed a reconfiguration formulation using a variation of the fixed charge network problem for service restoration. Recent studies have shown distributed generators (DGs) have the potential to assist outage management. In [53], a mixed-integer conic program and mixed-integer linear program were developed for network reconfiguration with the objective of minimizing the losses. The developed model included a spanning tree approach to enforce radiality and incorporated DGs. A MILP model and genetic algorithm were used in [54] for distribution network reconfiguration. The authors used graph theory to model the distribution network. Reference [55] developed another MILP model for distribution systems. The model included network reconfiguration, DG operation, and load management. The authors in [56] proposed a two-stage robust optimization model for distribution system restoration, and the model was solved using a column generation algorithm. The first stage determined the switching operation, and the loads were restored in the second stage. Reference [57] proposed a decentralized agent-based method for service restoration. The developed approach divided the distribution system into several zones, where each zone was represented by an agent. The role of each agent was to maintain radial topology and operation limits, and maximize the served loads.

More recently, researchers investigated the use of microgrids for distribution system restoration. The operation of multiple microgrids, with defined boundaries, in coordination with the distribution system has been investigated in [58] and [59]. The papers used stochastic programming for distribution system restoration with high penetration of DGs, including PV systems and BESS. A decentralized method for coordinating networked microgrids and the distribution system was presented in [60]. The authors modeled the operation of each microgrid as a second-order cone program and the coordination between the entities was achieved using the alternating direction method of multipliers algorithm. Other studies proposed sectionlaizing the distribution network into microgrids; i.e., microgrids with dynamic boundaries. The authors in [61] presented a MILP for microgrid formation of radial distribution networks to restore critical loads after outages. In [62], the authors developed a two-stage stochastic mixed-integer nonlinear program to sectionalize the distribution network into multiple self-supplied microgrids. The paper included dispatchable DGs,

such as microturbines and BESS, and PV systems. PVs and BESS were also considered in [63] for load restoration after wildfires. In the above references, fault isolation was not considered in the proposed models, making them hard to be implemented in practice. In [64], a multi-agent method was used for fault isolation and service restoration. The authors in [65] considered fault isolation constraints in a mixed integer second-order cone programming model. The authors assumed that all lines have switches and simplified the problem by assuming faults occur only on the buses. In [66], a heuristic method, i.e., Particle Swarm Optimization, was used for reconfiguration and fault isolation. The repair process of damaged components was either assumed to be taking place at a later time, or the times when the components are energized were assumed to be known in the aforementioned literature.

Although distribution system restoration has been long studied, there exist few efforts on integrating repair scheduling with recovery operations in power distribution systems. A pre-hurricane crew mobilization mathematical model was presented in [67] for transmission networks. The authors used stochastic optimization to determine the number of crews to be mobilized to the potential damage locations. Also, the authors proposed a post-hurricane MILP model to assign repair crews to damaged components without considering the travel times and repair sequence. In [68], the authors developed a stochastic program that assigns crews to substations in order to inspect and repair the damages, but the approach neglected crew routing. The authors in [69] used the queuing theory and stochastic point processes to determine the repair schedules. Reference [70] presented a dynamic programming model for dispatching crews to manually operate switches in the distribution network. Routing repair crews in transmission systems has been discussed by Van Hentenryck and Coffrin in [12]. The authors presented a deterministic two-stage approach to decouple the routing and restoration models. The first stage solved a restoration ordering problem using MILP. The ordering problem formulation assumed that only one damaged component can be repaired at each time step. The goal of the first stage was to find an optimal sequence of repairs to maximize the restored loads. In the second stage, the crew routing problem was solved using CP, large neighborhood search, and a randomized adaptive decomposition.

To the best of our knowledge, a single mathematical model that combines crew routing and power operation was not presented in the literature until our work in [71] and [72]. The papers in [73, 74, 75] adopted our work in [71] for different applications. The authors in [73] integrated natural gas system into the repair and restoration problem and [74] included mobile power source dispatch. In [75], a model for combining crew dispatch and switching operations is developed. In this dissertation, a new novel MILP model for unbalanced distribution systems and resource coordination is presented in Chapter 4, in addition to a neighborhood search-based algorithm for solving the co-optimization problem.

2.6 Summary

This chapter provides a description and literature review for the research topics covered in this dissertation. Section 2.2 starts with a summary of the responsibilities and measures that utilities take after weather-related outages. Disaster preparation is discussed in Section 2.3. The routing problem is discussed in Section 2.4, and distribution network repair and restoration is covered in Section 2.5.

CHAPTER 3. A STOCHASTIC MULTI-COMMODITY LOGISTIC MODEL FOR DISASTER PREPARATION IN DISTRIBUTION SYSTEMS

3.1 Overview

Outages due to weather-related events cause significant damage to the power grid infrastructure. This threat to the electric grid has raised a growing need to address disaster management and power system resilience. Disaster management consists of four phases: mitigation, preparedness, response, and recovery. For power systems, the mitigation and preparation phases include long-term and short-term pre-disaster planning. Tree trimming, pole hardening, and distributed generator installation belong to long-term pre-disaster planning. Short-term pre-disaster planning includes acquiring and allocating crews and equipment and selecting staging areas. The response and recovery phases are post-disaster actions that include damage assessment [11], crew dispatch and repair scheduling, and service restoration [72]. Effective disaster management measures can improve power system resistance during extreme events and accelerate recovery after events. The focus of this chapter is to study the short-term pre-disaster preparation problem, which is critical to achieve resiliency. Pre-disaster planning enables efficient post-disaster recovery by ensuring there are enough and optimal number of equipment and crews in the right places to quickly conduct the repairs.

After severe events, utility companies dispatch emergency crews to assess and repair the damage in order to restore power as fast as possible. A major challenge that utilities face is the lack of resources, including human resources and equipment, to handle extreme events. Once utilities request assistance from neighboring companies, they are facing another task of managing the newly acquired resources. Utilities must provide water, food, and shelter and communicate differences in work practices to the visiting crews. For these reasons, early preparation is essential to deal with upcoming extreme or severe weather events. We aim to develop a method to assist utilities in their preparation process by identifying the required resources and preallocating the crews and equipment.

Fig. 3.1 illustrates the proposed pre- and post-event framework. First, the forecasted weather and fragility models of the components are used to generate damage scenarios. For each scenario, we solve a power flow (PF) problem to identify critical components that must be repaired to restore service for high-priority customers. This information is used in the stochastic crew and resource allocation problem (SCRAP) to ensure there is enough equipment to repair the critical components. Once the weather event hits the distribution system, the repair and restoration problem is solved to restore the network to its normal state [73, 74, 76]. The distribution system repair and restoration problem is presented in Chapter 4. This chapter focuses on the steps before the weather event occurs.

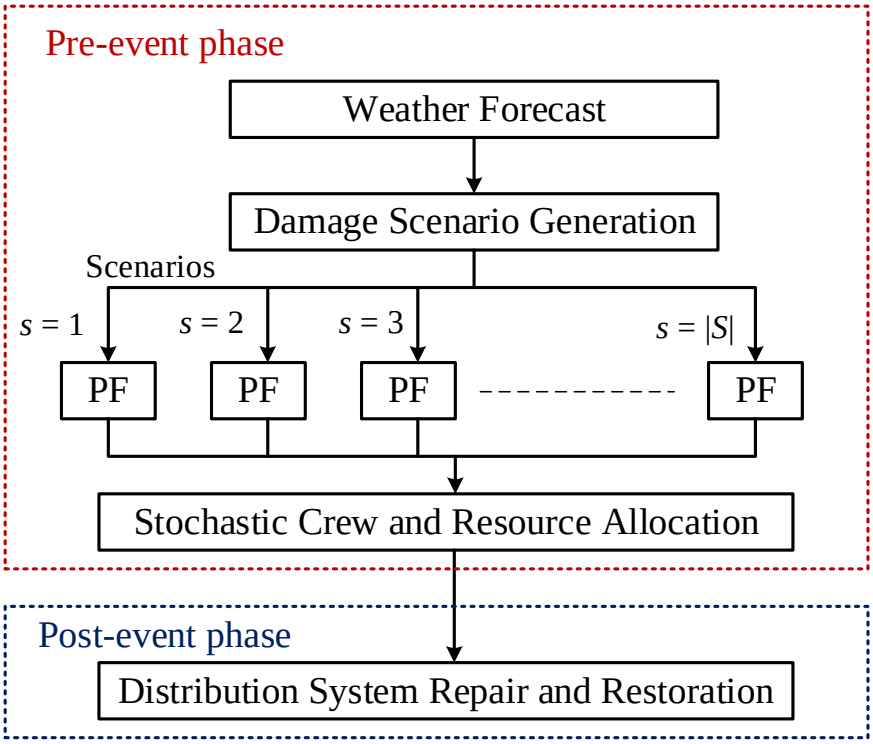

Figure 3.1 Framework for extreme event proactive recovery operation.

The rest of this chapter is organized as follows. Section 3.2 gives a brief introduction into stochastic programming. Fragility analysis and scenario generation are discussed in Section 3.3. A two-stage SMIP is developed in Section 3.4 for allocating crews and resources before a disaster. The

Progressive Hedging algorithm is introduced in Section 3.5. The method is tested on modified IEEE 123-bus distribution test system in Section 3.6.

3.2 Introduction to Two-Stage Stochastic Programming

Stochastic programming (SP) is a mathematical modeling optimization method where part of the data incorporated is uncertain. SP is a conventional and widely used approach for handling uncertainty in many real-world areas such as finance, healthcare, transportation, and energy planning [77]. Uncertainty can range from a few possible outcomes (scenarios) to an infinite number of scenarios, where the probability distributions of the data are known or estimated. One way to formulate a stochastic program is the two-stage approach, which is also known as the recourse model. In a two-stage stochastic program, a decision is made in the first stage before knowing the outcome of a random event. After the random event occurs, a recourse decision is taken in the second stage in response to the first-stage decisions and the random event. When the number of events/scenarios is finite, a two-stage stochastic linear program can be modeled as a single large linear programming model, where each constraint in the problem is duplicated for each realization of the random data. For problems where the number of realization is too large or infinite, the Monte Carlo sampling technique can be used to generate a manageable number of scenarios. The two-stage stochastic program can then be defined as follows:

$$\zeta = \min_{\boldsymbol{x},\boldsymbol{y_s}} \quad \boldsymbol{a}^T\boldsymbol{x} + \sum_{\forall s} \Pr(\text{s})\ \boldsymbol{b_s}^T\boldsymbol{y_s} \tag{3.1}$$

$$\text{s.t.} \quad (\boldsymbol{x}, \boldsymbol{y_s}) \in \mathcal{Q}_s, \forall s \tag{3.2}$$

where $\boldsymbol{a}$ and $\boldsymbol{b_s}$ are vectors containing the coefficients associated with the first stage ($\boldsymbol{x}$) and second stage ($\boldsymbol{y_s}$) variables in the objective, respectively. The restriction $(\boldsymbol{x}, \boldsymbol{y_s}) \in \mathcal{Q}_s$ represents the subproblem constraints that ensure a feasible solution. Pr(s) is the probability of occurrence for scenario s.

3.3 Damage Scenario Generation

Prepositioning crews and resources is subject to uncertain damage states of distribution lines. In this study, the uncertainty is represented by a finite set of discrete scenarios, which are obtained using a Monte Carlo sampling procedure. The Monte Carlo sampling method generates $|S|$ number of scenarios with equal probability $(1/|S|)$. The focus of this dissertation is on the impact of strong wind events, such as hurricanes and windstorms. Since the study focuses on wind-related failures, we only consider overhead distribution lines. To generate damage scenarios, we first estimate the wind speed that will affect the distribution system. In this section, we simulate hurricane events for illustration.

3.3.1 Hurricane Model

Since distribution networks cover small geographical areas, we assume that the wind speed experienced by all components in a distribution network is the same at any given moment [7]. The wind speed $w(t, s)$ that impacts the distribution network at time t and scenario s is modeled using the inland wind decay model [78], which is expressed by the following equation:

$$w(t,s) = w_b + (Rw_s^0 - w_b)\mathrm{e}^{-\alpha t} - C_w \tag{3.3}$$

where w_s^0 is the maximum sustained surface wind speed at landfall in scenario s; $\alpha = 0.095\mathrm{h}^{-1}$ is the decay constant; $w_b = 26.7$ knots (kt) is the background wind speed; and $R = 0.9$ is a reduction factor that represents the abrupt wind speed decrease as hurricanes make landfall. The value of w_s^0 can be obtained from the National Hurricane Center. In this study, we simulate this value using a logonormal distribution [79] to generate the scenarios. C_w in (3.3) represents the effect of the distance inland, which is calculated using the following equation:

$$C_w = \big(c_l t(t_0 - t)\big)\ln\big(\frac{D_I}{D_0}\big) + d_l t(t_0 - t) \tag{3.4}$$

where D_I is the distance inland to the hurricane landfall location; $D_0 = 1$ km; $t_0 = 50$ h; $c_l = 0.0109$ kt h^{-2}; and $d_l = -0.0503$ kt h^{-2}.

3.3.2 Fragility Models

Distribution systems consist of substations, distribution lines, distribution poles, and other electrical equipment associated with the protection and control of the system. Based on the study in [80], substations have low failure and damage rates during storms and hurricanes. Therefore, this study targets the failure of distribution lines. Distribution lines are modeled using edges that connect distribution buses, which connect customers to the distribution network. Distribution lines include poles and conductors between the poles. Damage of a single pole or conductor on a distribution line renders the line inoperable. Therefore, we conduct fragility analysis for each pole and conductor in the system, while assuming that the fragility of different components is independent.

3.3.2.1 Pole failure

Using the fragility model presented in [81], the probability of failure for pole z is found using the following equation:

$$p_z^p(w) = \min\{a^p e^{b^p w}, 1\} \tag{3.5}$$

where a^p and b^p are constants related to pole properties, and w is the wind speed.

3.3.2.2 Conductor failure

Conductors between distribution poles are prone to failures due to strong winds and falling trees during severe events [81]. Define p_l^w as the direct wind-induced damage probability, and p_l^t as the damage probability due to a fallen tree near conductor l [82, 7]. The wind-induced damage probability of a conductor is calculated using the ratio of the maximum perpendicular force that the conductor can endure F_l^f and the conductor wind loading F_l^w [82]. The wind loading and p_l^w are calculated by [83]:

$$q_l(w) = 0.613(G_1 G_2 G_3 w)^2 \tag{3.6}$$

$$F_l^w(w) = L_l^c \times D_l^c \times q_l(w) \times C^f \tag{3.7}$$

$$p_l^w(w) = \min\{F_l^w(w)/F_l^f, 1\} \tag{3.8}$$

Equation (3.6) calculates the dynamic pressure $q_l(w)$ (N/m^2), where G_1, G_2, and G_3 are factors related to the topography, ground roughness, and a statistical factor depending upon the level of security required. L_l^c is the length (m) and D_l^c is the diameter (m) of conductor l, and C^f is a force coefficient [83]. As for the damage due to fallen trees, the probability is modeled by [84]:

$$p_l^t(w) = \frac{e^{h(S_l^w)}}{1 + e^{h(S_l^w)}} \tag{3.9}$$

$$h(S_l^w) = a_h + c_h(k_l S_l^w) D_H^{b_h} \tag{3.10}$$

where a_h, b_h, and c_h are parameters associated with tree species, S_l^w is the estimated storm severity on conductor l (which varies from 0-1), k_l is a factor that represents the local terrain effects, and D_H is the tree diameter at breast height.

3.3.3 Equipment

The damage state of a component is determined using Bernoulli distribution (Bernoulli(p)), which takes the value of 1 (damaged) with probability p, and 0 (functional) with probability $1 - p$. For each scenario, we evaluate the status of the system using the maximum sustained wind speed $\bar{w}_s = max_{\forall t}\{w(t,s)\}, \forall s$. Therefore, the damage state of pole z in scenario s is determined by the outcome of the random variable $\psi_{z,s}^{pole} \sim$ Bernoulli($p_z^p(\bar{w}_s)$). A conductor can either be damaged by wind force $\psi_{l,s}^{wind} \sim$ Bernoulli($p_l^w(\bar{w}_s)$) or tree $\psi_{l,s}^{tree} \sim$ Bernoulli($p_l^t(\bar{w}_s)$). Consequently, the damage state of conductor l is determined as $\psi_{l,s}^{cond} = \psi_{l,s}^{wind} \vee \psi_{l,s}^{tree}$. After assessing the state of damage for each conductor and pole in the network, we can estimate the amount and type of equipment required to repair the damaged components. Although distribution networks include many types of components, we classify them into the following categories:

- Type 1: Poles for 3-phase lines
- Type 2: Poles for 1- and 2-phase lines
- Type 3: 3-phase transformers with protective equipment
- Type 4: 1-phase transformers with protective equipment
- Type 5: Conductors

The line segment connecting two distribution buses consists of poles and conductors, as shown in Fig. 3.2, where line 2–5 has one damaged pole and line 5–6 has one damaged conductor. In case of a damaged bus, such as bus 3 in Fig. 3.2, both lines 2–3 and 3–4 are affected. To avoid repetition when calculating the number of equipment required and repair time, we associate the poles on shared buses (e.g., pole at bus 3 for lines 2–3 and 3–4) with the line that has the bus with the lowest index (line 2–3). The number of type τ equipment required for line k in scenario s can be calculated using the following equations:

$$\mathcal{R}_{k,\tau,s} = \sum_{z \in \Omega_L^p(k,\tau)} \psi_{z,s}^{pole}, \forall k, \tau \in \{1..4\}, s \tag{3.11}$$

$$\mathcal{R}_{k,5,s} = n_k^{\phi} L_l^c \sum_{l \in \Omega_L^c(k)} \psi_{l,s}^{cond}, \forall k, s \tag{3.12}$$

where $\Omega_L^p(k,\tau)$ is the set of type τ equipment for the poles on line k, $\Omega_L^c(k)$ is the set of conductors on line k, and n_k^{ϕ} is the number of phases for line k. Equation (3.11) calculates the number of pole-related equipment and (3.12) calculates the amount of conductor required.

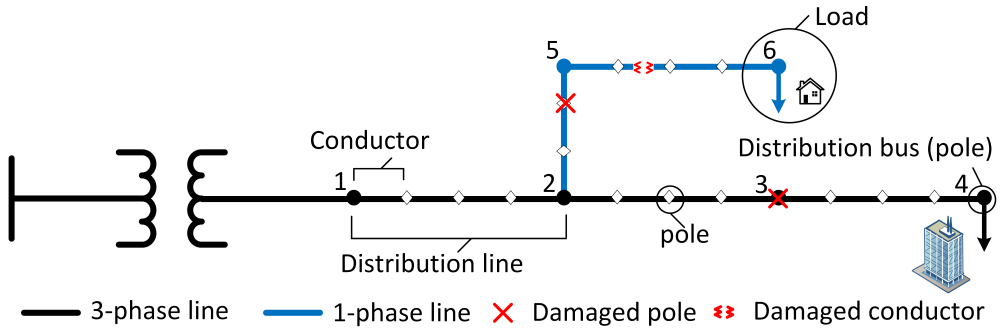

Figure 3.2 Single line diagram of a distribution network

3.3.4 Repair Time

The repair times for the damaged lines are estimated based on the number of damaged conductors and poles. The repair time for a damaged distribution pole is assumed to satisfy a normal distribution with mean 5 hours and 2.5 hours standard deviation ($r_{z,s}^p \sim \mathcal{N}(5, 2.5)$) [81]. For damaged conductors,

the repair time is assumed to satisfy a normal distribution with mean 4 hours and 2 hours standard deviation ($r^c_{l,s} \sim \mathcal{N}(4,2)$) [81]. The estimated time to repair a damaged line is found by adding the repair times of the damaged poles and conductors of the line, as follows:

$$ET^L_{k,s} = \sum_{z \in \Omega^p_L(k)} \psi^{pole}_{z,s}\ r^p_{z,s} + \sum_{l \in \Omega^c_L(k)} \psi^{cond}_{l,s}\ r^c_{l,s}, \forall k, s \tag{3.13}$$

According to the report in [85], the average time to remove a tree after a storm is 1 hour. Therefore, the tree removal time for each line, in hours, is estimated by calculating the number of downed trees on the line:

$$ET^T_{k,s} = \sum_{l \in \Omega^c_L(k)} \psi^{tree}_{l,s}\ , \forall k, s \tag{3.14}$$

3.3.5 Critical Components

After extreme events cause large-scale outages, it is imperative to quickly restore power to critical sites, such as hospitals, community shelters and emergency dispatch centers. Therefore, we must ensure that there are enough equipment and resources to repair vulnerable lines near critical sites. A MILP model is used to solve a PF problem to determine the critical lines to be repaired, so that all critical loads are restored. If one pole or conductor on a line is damaged, then the whole line is considered to be damaged and cannot be operated. The binary variable $\mathcal{U}^L_{k,s}$ is used to indicate the damage state of line k, $\mathcal{U}^L_{k,s} = 1$ if $\psi^{pole}_{z,s} = 1$ or $\psi^{cond}_{l,s} = 1$ for any $(i,l) \in k$. For example, both lines 2–5 and 5–6 are damaged in Fig. 3.2, therefore, $\mathcal{U}^L_{2\text{–}5} = \mathcal{U}^L_{5\text{–}6} = 1$. The set of damaged lines $\Omega_{DL}(s)$ can then be found by using the binary variable $\mathcal{U}^L_{k,s}$, such that $\Omega_{DL}(s) = \{k | \mathcal{U}^L_{k,s} = 1, \forall k, s\}$. Define binary variables u_k which equals 1 if line k is repaired and 0 otherwise, and y_i as the connection status of load at bus i. The MILP for identifying the critical components is formulated as follows:

$$\min \sum_{k \in \Omega_{DL}(s)} u_k \tag{3.15}$$

$$\text{subject to} \quad y_i = 1, \forall i \in \Omega_{CD} \tag{3.16}$$

subject to power operation constraints (Chapter 4)

where Ω_{CD} is the set of buses with critical loads. In this section, we provide a summary for the model. The objective (3.15) minimizes the number of lines to repair. Constraint (3.16) indicates that all critical loads must be served. Furthermore, power operation constraints such as power flow, network reconfiguration, fault isolation, and distributed generator dispatch are used in the model [76]. The power operation constraints are detailed in Chapter 4. Consider the distribution network shown in Fig. 3.3, with a critical load located at bus 7, and 5 damaged lines. In order to restore the load at bus 7 with minimal repairs, line 9–10 must be repaired ($u_{9-10} = 1$), switch 5–12 closed, and switches 1–2 and 4–5 opened to keep the damaged lines isolated. If line 9–10 requires 2 poles to repair, then the utility must have a minimum of 2 poles in their inventory. The PF model is solved for each generated scenario s. The set of critical lines $\Omega_{CL}(s)$ for scenario s can then be found as: $\Omega_{CL}(s) = \{k | u_k = 1, \forall k \in \Omega_{DL}(s), s\}$. This information is used in the SCRAP model in the following section.

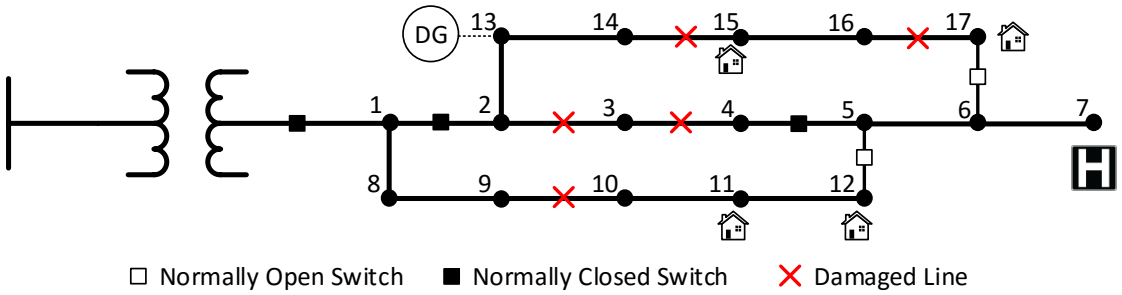

Figure 3.3 Single line diagram of a distribution network with one critical load

3.4 Stochastic Crew and Resource Allocation

The decision variables in the two-stage crew and resource allocation problem can be divided into two groups. The first group is the first-stage variables that are determined before the realization of the uncertain parameters. These variables include the number of external equipment and crews $(EI_d, LI_d, \mathcal{T}I_d)$, the number of equipment and internal crews transferred between depots d and e $(E_{d,e,\tau}, L_{d,e}, \mathcal{T}_{d,e})$, and the number of equipment in each depot d $(E^D_{d,\tau})$. Furthermore, a decision on utilizing a depot is made in the first stage using binary variable (ν_d), while the location of each

crew is determined using binary variable ($\delta_{d,c}$). The second part contains the second-stage variables, which are decided according to specific realization of the uncertainty. The second-stage variables are indexed by s to indicate the response for the specific scenario. In this stage, the crews are assigned to damaged lines ($A^L_{k,c,s}$, $A^T_{k,c,s}$) to ensure they are staged near the damaged lines, and the expected working hours for each crew ($H_{c,s}$) is estimated. Also, the number of additional equipment required ($\mathcal{E}_{d,\tau,s}$) to finish the repairs is determined in this stage. Fig. 3.4 provides an illustration for the SCRAP model, which includes the following steps: 1) depots are selected; 2) different types of equipment are allocated to depots; 3) line and tree crews are allocated to the depots; 4) equipment is assigned to crews; and 5) crews are assigned to damaged components. The two-stage stochastic crew and resource allocation problem is formulated in the following subsections, and Table 3.1 provides the nomenclature.

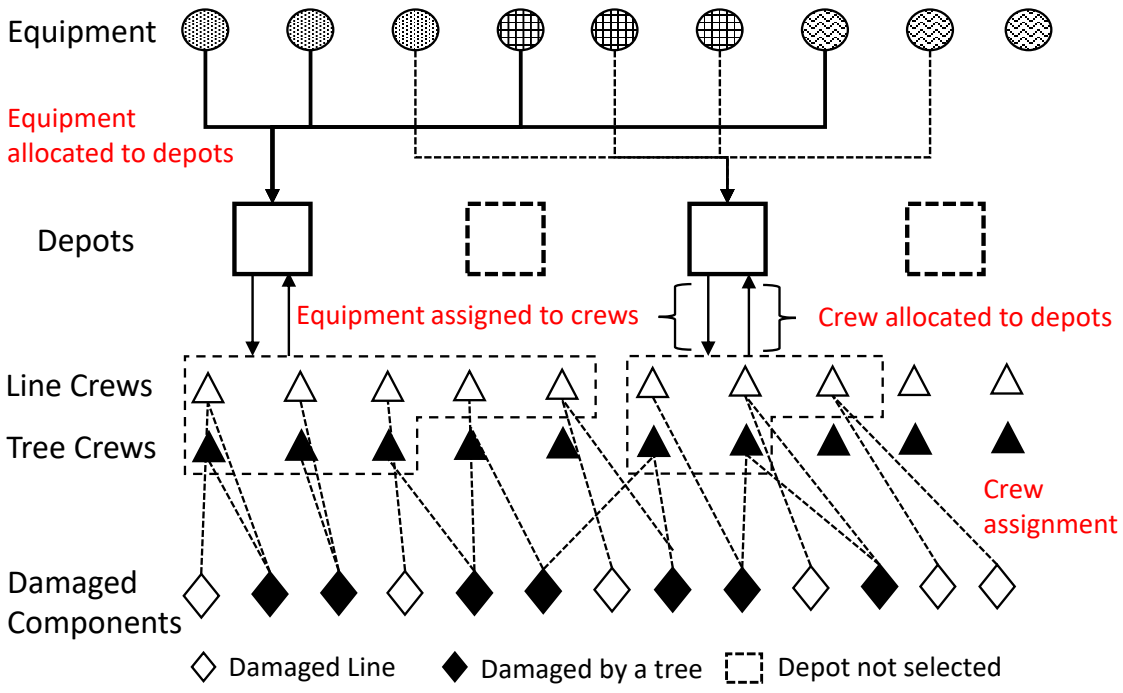

Figure 3.4 Crew and equipment allocation

Table 3.1 Nomenclature for the SCRAP Model

Indices and sets

k, c, s, τ	Indices for distribution line, crew, scenario and resource type
d/e	Indices for depot (staging site)
C^L, C^T, IC	Set of line crews, tree crews, and internal crews
Ω_{CD}, Ω_P	Set of buses with critical loads and set of depots

Parameters

$\mathcal{C}_d^E, \mathcal{C}_d^H$	The capacity of depot d for storing the supplies and capacity for accommodating the crews
$\mathcal{C}_\tau^R$	The capacity required to store resource τ
$D_{k,n}$	Distance between components k and n damaged line
$\bar{D}$	Maximum distance allowed between a crew's location and assigned damaged line
$ET_{k,s}^L, ET_{k,s}^T$	Estimated time to repair line k for line and tree crews
$E_{d,\tau}^0, L_d^0, \mathcal{T}_d^0$	Initial number of equipment, line crews and tree crews at d
M	Large positive number
$\mathcal{P}_d^D, \mathcal{P}_\tau^{EI}$	Cost of staging depot d and ordering equipment τ
$\mathcal{P}_c^H, \mathcal{P}^{EC}$	Hourly pay for crew c and cost of obtaining an external crew
$\mathcal{P}_\tau^{LF}, \mathcal{P}^R$	Penalty costs for late delivery of equipment τ and penalty on restoration time
$\mathcal{P}_{d,e,\tau}^{TE}$	Cost of transporting equipment τ between locations d to e
Pr(s)	Probability of scenario s
$\mathcal{R}_{k,\tau,s}$	The number of type τ resources required to repair line k in scenario s
$\mathcal{U}_{k,s}^T$	Binary random variable equals one if line k in scenario s is damaged by a tree
$\mathcal{U}_{k,s}^L$	Binary random variable indicating the damage state of line k in scenario s
ν^{max}	Maximum number of depots that can be selected

Table 3.1 (Continued)

Decision Variables

$A^{L/T}_{k,c,s}$	Binary variable equal to 1 if line k is assigned to line/tree crew c in scenario s
$\delta_{d,c}$	Binary variable equals 1 if crew c is positioned in depot d
$E_{d,e,\tau}$	Number of τ supplies transferred between depots d and e
$E^{C}_{c,d,\tau,s}$	The amount of type τ supplies that crew c obtains from depot d in scenario s
$\mathcal{E}_{d,\tau,s}$	Additional τ supplies required in depot d scenario s
$EI_{d,\tau}, E^{D}_{d,\tau}$	Number of τ supplies ordered to depot d and the total number of τ supplies at d
$L_{d,e}, \mathcal{T}_{d,e}$	Number of line and tree crews transferred from depot d to e
$LI_d, \mathcal{T}I_d$	Number of external line and tree crews positioned at depot d
$\mathcal{L}^{L}_{s}, \mathcal{L}^{T}_{s}$	The expected times of the last repair conducted by the line and tree crews
$H_{c,s}$	Number of hours crew c is expected to work in scenario s
ν_d	Binary variable equals 1 if depot d is staged

3.4.1 Objective

$$\min \sum_{\forall d,e,\tau} \mathcal{P}^{TE}_{d,e,\tau} E_{d,e,\tau} + \sum_{\forall d,\tau} \mathcal{P}^{EI}_{\tau} EI_{d,\tau} + \sum_{\forall d} \left(\mathcal{P}^{EC}(LI_d + \mathcal{T}I_d) + \mathcal{P}^{D}_{d}\nu_d\right) + \sum_{\forall s} \Pr(s)\left(\sum_{\forall c} \mathcal{P}^{H}_{c} H_{c,s} + \sum_{\forall d,\tau} \mathcal{P}^{LF}_{\tau} \mathcal{E}_{d,\tau,s} + \mathcal{P}^{R}(\mathcal{L}^{T}_{s} + \mathcal{L}^{L}_{s})\right) \quad (3.17)$$

The first two lines in (3.17) are for the first-stage objective, which aims to minimize the costs of equipment transportation, ordering equipment and external crews, and staging depots. The third line in (3.17) is dependent on the realization of the uncertainty, i.e., the second-stage objective. The first term in the second-stage objective minimizes the labor costs associated with the crews. The second and third terms are penalty costs. We add a penalty cost for unmet equipment demand and penalize the time needed to repair all components. The penalty $\mathcal{P}^{LF}_{\tau}$ minimizes the shortage

of equipment. The purpose of penalizing the expected time of the last repair is to minimize the system restoration time.

3.4.2 First-Stage Constraints

In the first stage, the depots are selected and both equipment and crews are allocated to the selected depots in anticipation of an extreme event. Constraints (3.18)-(3.25) represent the first-stage constraints.

3.4.2.1 Depot Selection

$$1 \leq \sum_{\forall d} \nu_d \leq \nu^{max} \tag{3.18}$$

$$0 \leq \sum_{\forall \tau} \mathcal{C}^R_\tau E^D_{d,\tau} \leq \mathcal{C}^E_d \nu_d, \forall d \tag{3.19}$$

$$0 \leq \sum_{\forall c} \delta_{d,c} \leq \mathcal{C}^H_d \nu_d, \forall d \tag{3.20}$$

The number of selected depots is limited to ν^{max} in (3.18), and at least one depot must be selected. Each depot, if selected, can contain a limited amount of equipment, as enforced by (3.19). Constraint (3.20) limits the number of crews in depots. A depot can accommodate a limited number of crews depending on its resources. The limits in (3.19) and (3.20) are multiplied by ν_d so that if the depot is not selected, it will have no crew or equipment.

3.4.2.2 Crew and Equipment Allocation

$$E^D_{d,\tau} = E^0_{d,\tau} + \sum_{\forall e, e \neq d} E_{e,d,\tau} - \sum_{\forall e, e \neq d} E_{d,e,\tau} + EI_{d,\tau}, \forall d, \tau \tag{3.21}$$

$$\sum_{\forall c \in C^L} \delta_{d,c} = L^0_d + \sum_{\forall e, e \neq d} L_{e,d} - \sum_{\forall e, e \neq d} L_{d,e} + LI_d, \forall d \tag{3.22}$$

$$\sum_{\forall c \in C^T} \delta_{d,c} = \mathcal{T}^0_d + \sum_{\forall e, e \neq d} \mathcal{T}_{e,d} - \sum_{\forall e, e \neq d} \mathcal{T}_{d,e} + \mathcal{T}I_d, \forall d \tag{3.23}$$

$$\sum_{\forall d} \delta_{d,c} = 1, \forall c \in IC \tag{3.24}$$

$$\sum_{\forall d} \delta_{d,c} \leq 1, \forall c \notin IC \tag{3.25}$$

Constraints (3.21)-(3.23) model the transportation of equipment, line crews, and tree crews, respectively. The three constraints are formulated using flow conservation equations. For instance, the constraint for the equipment (3.21) states that the amount of type τ equipment in depot d is equal to the sum of equipment initially in the depot, equipment transferred to the depot, newly obtained equipment, and minus the equipment transferred to other depots. The summations $\sum_{\forall c \in C^L} \delta_{d,c}$ and $\sum_{\forall c \in C^T} \delta_{d,c}$ are the number of line and tree crews in depot d, respectively. The first term in the right-hand side of (3.22) is the number of line crews initially present in depot d. The second term represents the number of line crews transferred to depot d and the third term is the number of line crews transferred from depot d. The last term LI_d is the number of visiting line crews to be positioned in depot d. Similarly, constraint (3.23) is designed for tree crews. Constraint (3.24) states that each internal crew must be located in one of the depots, while external crews can be either located in one depot, or not used; i.e., $\delta_{d,c} = 0$, as enforced by (3.25).

3.4.2.3 Symmetry-Breaking Constraints

The presented problem allow a large number of feasible symmetric solutions with equal objective value. Therefore, we add symmetry breaking constraints to keep at least one solution and remove all other symmetric solutions. Consider a case where there are four line crews and three potential depots. Assume that depot 1 and depot 3 are selected, and all four crews must be allocated. In this case, there are four possible solutions for allocating the crews:

$$\delta_{d,c} = \begin{pmatrix} 1 & 1 & 0 & 0 \\ 0 & 0 & 0 & 0 \\ 0 & 0 & 1 & 1 \end{pmatrix} \equiv \begin{pmatrix} 1 & 0 & 1 & 0 \\ 0 & 0 & 0 & 0 \\ 0 & 1 & 0 & 1 \end{pmatrix} \equiv \begin{pmatrix} 0 & 1 & 0 & 1 \\ 0 & 0 & 0 & 0 \\ 1 & 0 & 1 & 0 \end{pmatrix} \equiv \begin{pmatrix} 0 & 0 & 1 & 1 \\ 0 & 0 & 0 & 0 \\ 1 & 1 & 0 & 0 \end{pmatrix} \tag{3.26}$$

To deal with the symmetry problem in (3.26), we allocate the crews to the depot starting from the lowest indexed row and column. Therefore, for $\delta_{d,c} = 1$, all depots with indices $\bar{d} < d$ must

not have any crews with indices $\bar{c} > c$, i.e., $\delta_{\bar{d},\bar{c}} = 0$. The following equations are used to break the symmetry in (3.26):

$$\sum_{\forall d} \delta_{d,c+1} \geq \sum_{\forall d} \delta_{d,c}, \forall c \in C^L, c < |C^L| \tag{3.27}$$

$$\sum_{\forall d} (|\Omega_P| - d)\delta_{d,c+1} \geq \sum_{\forall d} (|\Omega_P| - d)\delta_{d,c}, \forall c \in C^L, c < |C^L| \tag{3.28}$$

$$\sum_{\forall d} \delta_{d,c+1} \geq \sum_{\forall d} \delta_{d,c}, \forall c \in C^T, c < |C^T| \tag{3.29}$$

$$\sum_{\forall d} (|\Omega_P| - d)\delta_{d,c+1} \geq \sum_{\forall d} (|\Omega_P| - d)\delta_{d,c}, \forall c \in C^T, c < |C^T| \tag{3.30}$$

Constraint (3.27) states that for similar crews, we allocate the crew with the lowest index first. Constraint (3.28) allocates the crews starting from the depots with the lowest index, and skips depots that are not staged. Constraints (3.27) and (3.28) are also enforced to the tree crews in (3.29) and (3.30). The feasible solutions are then reduced from four to one possible solution in this example, where only the first matrix in (3.26) is feasible.

3.4.3 Second Stage Constraints

After selecting the depots and allocating the crews and equipment in the first stage, the crews are assigned to repair the damaged components and the equipment are distributed to the crews in the second stage.

3.4.3.1 Crew Assignment

$$\sum_{\forall c \in C^L} A^L_{k,c,s} = \mathcal{U}^L_{k,s}, \forall k, s \tag{3.31}$$

$$\sum_{\forall c \in C^T} A^T_{k,c,s} = \mathcal{U}^T_{k,s}, \forall k, s \tag{3.32}$$

$$\sum_{\forall k} A^L_{k,c,s} \leq M \sum_{\forall d} \delta_{d,c}, \forall c \in C^L, s \tag{3.33}$$

$$\sum_{\forall k} A^T_{k,c,s} \leq M \sum_{\forall d} \delta_{d,c}, \forall c \in C^T, s \tag{3.34}$$

$$\bar{D} \geq D_{d,k}(\delta_{d,c} + A^L_{k,c,s} - 1), \forall d, k, c \in C^L, s \tag{3.35}$$

$$\bar{D} \geq D_{d,k}(\delta_{d,c} + A^T_{k,c,s} - 1), \forall d, k, c \in C^T, s \tag{3.36}$$

Equations (3.31) and (3.32) assign the line and tree crews to the damaged lines, respectively. The binary parameter $\mathcal{U}^T_{k,s}$ equals 1 (0) if line k is damaged (functional). Therefore, if $\mathcal{U}^L_{k,s}$ equals 0, then line k will not be assigned to any crews (i.e., $\sum_{\forall c \in C^L} A^L_{k,c,s} = 0$). Also, if crew c is not staged at a depot (i.e., $\sum_{\forall d} \delta_{d,c} = 0$), then crew c is not assigned to any damaged line as enforced by (3.33) and (3.34). The big M value in (3.33) can be the maximum number of damaged lines ($\max_{\forall s}(\sum_{\forall k} \mathcal{U}^L_{k,s})$). Constraints (3.35)-(3.36) are used to identify the distances between the damaged components assigned to each crew and the depots. This distance is limited to $\bar{D}$. If line crew c is positioned at depot d ($\delta_{d,c} = 1$) and is assigned to line k ($A^L_{k,c,s} = 1$), then $\bar{D} \geq D_{d,k}$.

3.4.3.2 Working Hours

In this subsection, we estimate the working hours for each crew in order to distribute the work assignments fairly between the crews and ensure that enough crews are present. The working hours constraints are modeled in (3.37)-(3.40).

$$H_{c,s} = \sum_{\forall k} (ET^L_{k,s} A^L_{k,c,s}), \forall c \in C^L, s \tag{3.37}$$

$$H_{c,s} = \sum_{\forall k} (ET^T_{k,s} A^T_{k,c,s}), \forall c \in C^T, s \tag{3.38}$$

$$\mathcal{L}^L_s \geq H_{c,s}, \forall c \in C^L, s \tag{3.39}$$

$$\mathcal{L}^T_s \geq H_{c,s}, \forall c \in C^T, s \tag{3.40}$$

The total expected working time for each line and tree crew is calculated in (3.37) and (3.38). Constraints (3.39) and (3.40) define the expected time of the last repair. The value of $\mathcal{L}^L_s$ is greater or equal to the largest $H_{c,s}$ for the line crews, and $\mathcal{L}^T_s$ is greater or equal to the largest $H_{c,s}$ for the tree crews. Since we are minimizing the expected time of the last repair, it will take the value $max_{\forall c}(H_{c,s})$ in each scenario. By minimizing $\mathcal{L}^L_s$ and $\mathcal{L}^T_s$, we minimize the restoration time of the system and ensure that we do not have a single crew or few crews in a location with many damaged components.

3.4.3.3 Equipment Assignment

$$\sum_{\forall d} E^D_{d,\tau} \geq \sum_{\forall k \in \Omega_{CL}(s)} \mathcal{R}_{k,\tau,s}, \forall \tau, s \tag{3.41}$$

$$\sum_{\forall d} (E^D_{d,\tau} + \mathcal{E}_{d,\tau,s}) \geq \sum_{\forall k} \mathcal{R}_{k,\tau,s}, \forall \tau, s \tag{3.42}$$

$$\sum_{\forall \tau} E^C_{c,d,\tau,s} \leq M\delta_{d,c}, \forall d, c \in C^L, s \tag{3.43}$$

$$\sum_{\forall c \in C^L} E^C_{c,d,\tau,s} \leq E^D_{d,\tau} + \mathcal{E}_{d,\tau,s}, \forall d, \tau, s \tag{3.44}$$

$$\sum_{\forall d} E^C_{c,d,\tau,s} \geq \sum_{\forall k} A^L_{k,c,s} \mathcal{R}_{k,\tau,s}, \forall c \in C^L, \tau, s \tag{3.45}$$

$$\{\delta, A^L, A^T, \nu\} \in \{0, 1\} \tag{3.46}$$

Constraint (3.41) indicates that the number of equipment available must be sufficient for repairing all critical lines before the extreme event occurs. Constraint (3.42) states that the total equipment that the utility has must be equal or greater than the required equipment to repair the damaged components. $\mathcal{E}_{d,\tau,s}$ identifies the additional number of equipment (unmet equipment demand) that must be ordered in each scenario to finish the repairs. Each crew can obtain equipment from the depot they are positioned at, as enforced by constraint (3.43). The crews must use the resources available in the depot (3.44). Constraint (3.45) indicates that the number of resources the crew has should be enough to repair the assigned damaged components. Finally, (3.46) defines the binary variables. After positioning the crews and resources, the utility will be ready for the recovery operation after the outages.

3.5 Progressive Hedging

The standard method for solving stochastic programs is to use a MILP solver, e.g., CPLEX, to directly solve the extensive form (3.1) of the SMIP. Solving the extensive form (EF) for large-scale problems is however computationally difficult. Rockafellar and Wets [86] developed the Progressive Hedging (PH) algorithm for solving convex stochastic problems optimally. Watson and Woodruff

adapted the algorithm [87] to approximately solve stochastic mixed-integer problems. The PH algorithm decomposes the extensive form into scenario-based subproblems, by relaxing the non-anticipativity of the first-stage variables. Hence, for $|\mathcal{S}|$ scenarios, the SMIP is decomposed into $|\mathcal{S}|$ subproblems. The authors of [88] effectively implemented PH for solving the stochastic unit commitment problem. The PH algorithm is described in Algorithm 1, using a penalty factor ρ and a termination threshold ε.

Algorithm 1 The Two-Stage PH Algorithm

1: Let $\tau := 0$
2: For all $s \in \mathcal{S}$, compute:
3: $\boldsymbol{x_s^{(\tau)}} := \arg\min_{\boldsymbol{x}} \left\{ \boldsymbol{a}^T\boldsymbol{x} + \boldsymbol{b_s}^T\boldsymbol{y_s} : (\boldsymbol{x}, \boldsymbol{y_s}) \in \mathcal{Q}_s \right\}$
4: $\bar{\boldsymbol{x}}^{(\tau)} := \sum_{s\in\mathcal{S}} \Pr(s)\boldsymbol{x_s^{(\tau)}}$
5: $\boldsymbol{\eta_s^{(\tau)}} := \rho(\boldsymbol{x_s^{(\tau)}} - \bar{\boldsymbol{x}}^{(\tau)})$
6: $\tau := \tau + 1$
7: For all $s \in \mathcal{S}$ compute:
8: $\boldsymbol{x_s^{(\tau)}} := \arg\min_{\boldsymbol{x}} \left\{ \boldsymbol{a}^T\boldsymbol{x} + \boldsymbol{b_s}^T\boldsymbol{y_s} + \boldsymbol{\eta_s^{(\tau-1)}}\boldsymbol{x} + \frac{\rho}{2}||\boldsymbol{x} - \bar{\boldsymbol{x}}^{(\tau-1)}||^2 : (\boldsymbol{x}, \boldsymbol{y_s}) \in \mathcal{Q}_s \right\}$
9: $\bar{\boldsymbol{x}}^{(\tau)} := \sum_{s\in\mathcal{S}} \Pr(s)\boldsymbol{x_s^{(\tau)}}$
10: $\boldsymbol{\eta_s^{(\tau)}} := \boldsymbol{\eta_s^{(\tau-1)}} + \rho(\boldsymbol{x_s^{(\tau)}} - \bar{\boldsymbol{x}}^{(\tau)})$
11: **if** $\sum_{s\in\mathcal{S}} \Pr(s)||\boldsymbol{x_s^{(\tau)}} - \bar{\boldsymbol{x}}^{(\tau)}|| < \varepsilon$ **then**
12: terminate
13: **else**
14: **if** $\tau \geq \tau_1$ **then**
15: **if** $\nu_{d,1}^{\tau} = \nu_{d,s}^{\tau}, \forall d, s$ **then**
16: **fix** $\nu_d = \nu_{d,s}^{\tau}, \forall d, s$
17: **end if**
18: **end if**
19: **if** $\tau \geq \tau_2$ **then**
20: **if** $\delta_{d,c,1}^{\tau} = \delta_{d,c,s}^{\tau}, \forall d, c, s$ **then**
21: **fix** $\delta_{d,c} = \delta_{d,c,s}^{\tau}, \forall d, c, s$
22: **end if**
23: **end if**
24: go to **Step 5**
25: **end if**

The first step initializes the iteration number τ and the individual scenarios are solved in Steps 2–3. In Step 4, the first stage solution obtained from Step 3 is aggregated. Step 5 calculates the multiplier η_s. The multiplier is used in Step 8 to update $\boldsymbol{x}$, where the scenarios are solved independently in parallel. Steps 9 and 10 update the first-stage solution and the multiplier, respectively. The program terminates once all first-stage decisions $\boldsymbol{x_s}$ converge to the same $\bar{\boldsymbol{x}}$ in Step

11, i.e., $\sum_{s\in\mathcal{S}} \Pr(s)||\boldsymbol{x}_{\boldsymbol{s}}^{(\tau)} - \bar{\boldsymbol{x}}^{(\tau)}|| < \varepsilon$. The PH algorithm may experience slow convergence with large problems that include many scenarios. A detailed analysis of PH showed that individual first-stage variables frequently converge to specific values across all scenario subproblems [89]. Therefore, we fix some of the first-stage variables if they converge to the same values after certain numbers of iterations. In the SCRAP model, we fix the variable ν_d (depot selected) if it converges to the same values after τ_1 iterations, as shown in Steps 14–18. In Steps 19–23, the crew allocation and selection variable $\delta_{d,c}$ is fixed after τ_2 iterations if the variable converges to the same value across all scenario subproblems. Once the variables are fixed, they are treated as parameters in the following iterations. In this study, the values of τ_1 and τ_2 are set to be 5 and 20, respectively.

The stochastic programs presented in this dissertation are implemented in the Python Optimization Modeling Objects (Pyomo) software [89]. Similarly to AMPL [90] and GAMS [91], Pyomo allows users to formulate mathematical models to solve complex optimization problems. Pyomo offers the PySP software package for easily modeling stochastic programming problems [92]. PySP provides the command *runph* to solve stochastic programs using PH. Moreover, PySP supports distributed optimization, therefore, the scenario subproblems in PH can be solved in parallel. We implement the variable fixing operations using the "Watson-Woodruff" (WW) plugin in PySP.

3.6 Simulation and Results

The preallocation model is simulated on the modified IEEE 123-bus distribution feeder [76, 93]. The size of the IEEE 123-bus feeder is scaled up, as shown in Fig. 3.5. The modified network, shown in Fig. 3.6, includes 4 dispatchable DGs, 18 new switches, 5 PVs and 2 battery energy storage devices. Note that Fig. 3.6 does not reflect the actual x- and y-coordinates. The 4 DGs are rated at 300 kW and 250 kVAr. The PV at bus 62 is rated at 900 kW and the other PVs are rated at 50 kW. The battery systems at bus 2 and 62 are rated at 50 kW/132 kWh and 500 kW/ 2100 kWh, respectively. Additional details about the network can be found in [93].

We assume that a category 3 hurricane is forecasted to make its way towards the test system. Monte Carlo sampling is used to generate 100 damage scenarios with equal probability. First,

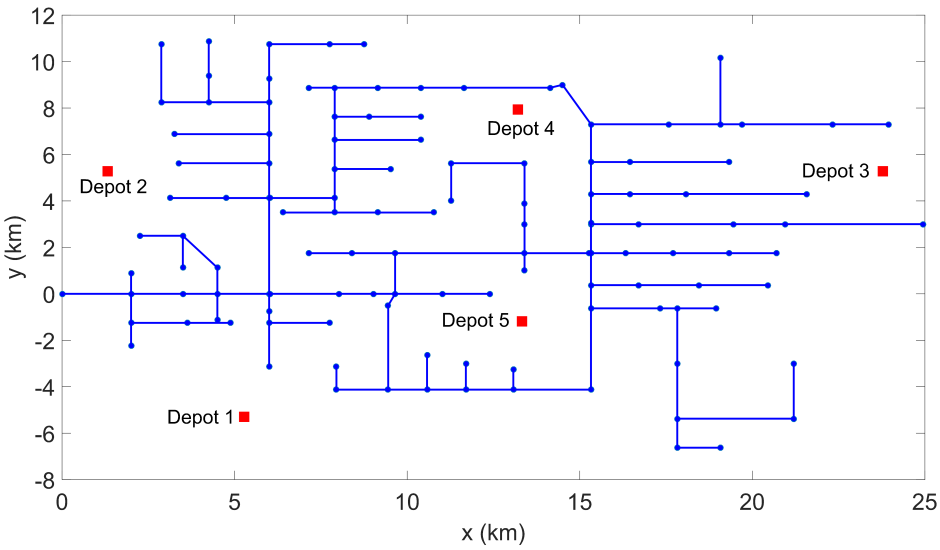

Figure 3.5 Modified IEEE 123-bus distribution feeder and location of depots

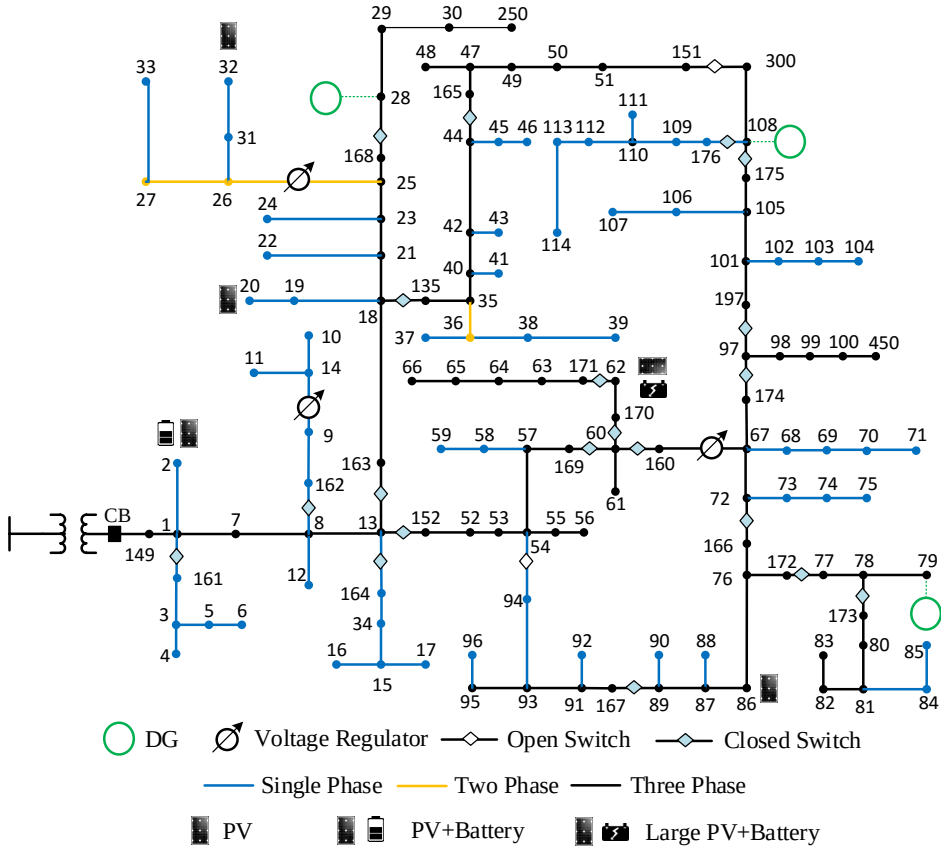

Figure 3.6 Modified IEEE 123-bus distribution feeder

lognormal distribution with $\mu = 4.638$ and $\sigma = 0.039$ [79] is used to generate 100 scenarios of possible wind speeds at landfall. Then, the models presented in Section 3.3 are used to evaluate the impact of the extreme event. The number of scenarios are reduced to 30 using the tool SCENRED2 in the General Algebraic Modeling System (GAMS) [91] to reduce the computational complexity. The simulation data used in equations (3.5)–(3.10) are listed in Table 3.2.

Table 3.2 Simulation data for the fragility models

Model	Parameter	Value	Ref.
Pole failure	a^p	0.0001	[81]
	b^p	0.0421	
Conductor failure	G_1	1	[83]
	G_2	0.83	
	G_3	1	
	C^f	1.2	
	L_l^c	45.72 m	[94]
	D_l^c	0.0183 m	
	F_l^{force}	62.8 kN	
	$\{a_h, b_h, c_h\}$	{-2.752, 0.680, 0.663}	[84]
	S_l^w	0–1	
	k_l	0.57–1.43	[95]
	D_H	0.15 m	[82]

After generating the damage scenarios, the PF problem (3.15) is solved for each scenario to find the critical lines to be repaired. Then, the SMIP model presented in Section 3.4 is used to model the preallocation problem. It is assumed that there are 5 potential staging areas, the location of each depot is shown in Fig. 3.5. We set the maximum distance between the staged crews and damaged components to be 16 km ($\bar{D}$ =16 km) in this simulation. Depot 1 is assumed to be the main location of the utility and must be staged ($\nu_1 = 1$). Depot 1 has 5 line crews, 3 tree crews, and a stockpile of 25 poles (10 for 3-phase lines and 15 for 1- and 2-phase lines), 4 km of conductor, 8 single-phase transformers, and 3 three-phase transformers. The utility can obtain additional resources based on the results of the SCRAP model. The data for the costs used in the SCRAP model are presented in Table 3.3 [26, 96, 97, 98]. The penalty costs for the unmet equipment demand is assumed to be 10 times the actual cost of the equipment. As for the penalty cost on the restoration time, we estimate

the per hour outage cost \$/h. For the IEEE-123 bus system considered in this study, the average daily load is 2772.75 kW. Using the average per hour cost [99] of \$2/kWh for regular loads and \$16/kWh for critical loads, the estimated per hour cost is found to be \$14610.5/h. We set $\mathcal{P}^R$ to equal half of the estimated per hour cost so that the penalty cost is divided between line repairs and tree removal in (3.17).

Table 3.3 Simulation data for SCRAP on the IEEE 123-bus feeder

Parameter	Value
Depot supply capacity (unit)	$\mathcal{C}_d^E = \{600,400,400,250,250\}$
Depot crew capacity (crew)	$\mathcal{C}_d^H = \{8,7,7,5,5\}$
Capacity required (unit)	$\mathcal{C}_\tau^R = \{10,8,5,4,6\}$
Staging areas costs (\$)	$\mathcal{P}_d^D = \{0,170K,170K,90K,90K\}$
Equipment costs (\$/unit*)	$\mathcal{P}_\tau^{EI} = \{2K,1.2K,2.5K,1.2K,3.3K\}$
Labor cost (\$/crew)	Line crew: 225, Tree crew: 120
Transportation costs (\$/tkm)	0.098
Contracting costs	\$4285/crew

*For the conductor, 1km = 1 unit.

3.6.1 Preparation

The SCRAP model is solved using Pyomo with IBM's CPLEX 12.6 mixed-integer solver on a high-performance computing system. The simulation is performed on Iowa State University's Condo cluster, whose individual blades consist of two 2.6 GHz 8-Core Intel E5-2640 v3 processors and 128GB of RAM. Table 3.4 presents the results of the preparation problem using SCRAP and PH with 30 scenarios and 1 scenario, which we refer to as deterministic allocation (DA). The single scenario for DA is obtained by reducing the number of scenarios to 1 using SCENRED2. Moreover, the robust stochastic optimization (RSO) method presented in [20] is used to solve the preparation problem. The staging sites and the number of crews are found to be the same for both stochastic and deterministic solutions. However, SCRAP invested around \$30,000 more in equipment. The deterministic solution is biased towards a single scenario and did not consider extreme cases where the required number of equipment is high. On the other hand, RSO favors a solution that would

perform better with worst-case scenarios. RSO invested around $40,000 more than SCRAP on equipment. However, this can lead to over-preparation and overinvestment.

The results of the SCRAP model indicate that Depot 4 should be staged in preparation to the weather event in support to the main location (Depot 1). Five new external line crews are contracted with one positioned at Depot 1 and four positioned at Depot 4. In addition, one tree crew is transferred from Depot 1 to Depot 4. Six 3-phase poles (type 1) are ordered to Depot 4 and fourteen type 2 poles are ordered, one to Depot 1 and thirteen to Depot 4. Also, two single-phase transformers are transferred to Depot 4 from Depot 1. Finally, around 200 meters of conductor is transferred from Depot 1 to Depot 4, and approximately 1800 meters of conductor is ordered to Depot 4.

Table 3.4 Pre-event Preparation Results

		SCRAP		DA		RSO	
Staged Depots		1	4	1	4	1	4
Line Crews		6	4	6	4	6	4
Tree Crews		2	1	2	1	2	1
Equipment	1	10	6	10	0	15	8
	2	16	13	13	6	26	15
	3	3	0	3	0	3	0
	4	6	2	7	1	6	3
	5	3.8 km	2 km	2.5 km	1.5 km	5 km	3 km
Costs		$146,766		$117,443		$183,371	

To show the importance of considering uncertainty in the problem, we calculate the expected value of perfect information (EVPI)). EVPI is the difference between the wait-and-see (WS) and the stochastic solutions. It represents the value of knowing the future with certainty. WS is the expected value of reacting to random variables with perfect foresight. It is obtained by calculating the means of all deterministic solutions of the scenarios. WS provides a lower bound for the objective value and cannot be obtained in practice. As for evaluating the performance of the deterministic solution across different scenarios, we set the first-stage variables obtained from DA as fixed parameters and solve the stochastic problem. Let $\zeta = \mathrm{F}(\mathrm{x}, \boldsymbol{\xi})$ be the stochastic programming problem with first-stage variables $\boldsymbol{x}$ and random variables $\boldsymbol{\xi}$. If x^{DA} is the first-stage solution

obtained by solving the deterministic problem, then the expected value of the deterministic solution (ED) is $\zeta^{ED} = \mathrm{F}(\mathrm{x}^{\mathrm{DA}}, \boldsymbol{\xi})$. The same approach is used to calculate the objective value of RSO. From Table 3.5, the stochastic solution from SCRAP with PH is less than ED, which is expected since SCRAP considers the variability of the extreme event outcome unlike the deterministic solution. The difference between PH and ED is \$163,017, which is around 80% of the difference between ED and WS. This indicates that the stochastic model leads to a better preparation strategy by acquiring and positioning enough equipment. Solving the two-stage stochastic problem is more beneficial than solving a deterministic problem. PH achieved a solution only 0.36% less than EF with a considerably lower computation time. RSO achieved a solution that outperforms the deterministic one, however, the EVPI for RSO is \$95,513 and \$38,415 for SCRAP-PH. In addition, RSO requires more computation time when compared to SCRAP-PH.

Table 3.5 Performance of the Stochastic Program

Method	Objective Value	Computation Time	EVPI
WS	\$513,170	N/A	N/A
SCRAP-EF	\$549,554	300 min	\$36,384
SCRAP-PH	\$551,585	106 min	\$38,415
RSO	\$608,683	335 min	\$95,513
ED	\$714,602	2 min	\$201,432

3.6.2 Stability Test

The stability test in [100] is used in this study to check the sensitivity of solution stability to the number of scenarios. The idea of the test is to solve the stochastic problem with multiple independent sets of scenarios and compare the objective values. The model is stable if the objective values are approximately equal [100]. We generate 8 sets of scenarios, each set includes 30 to 100 scenarios. The simulation results are shown in Fig. 3.7, which shows that the variation of the objective value is small. Therefore, the method is stable and 30 scenarios are adequate for representing the uncertainties.

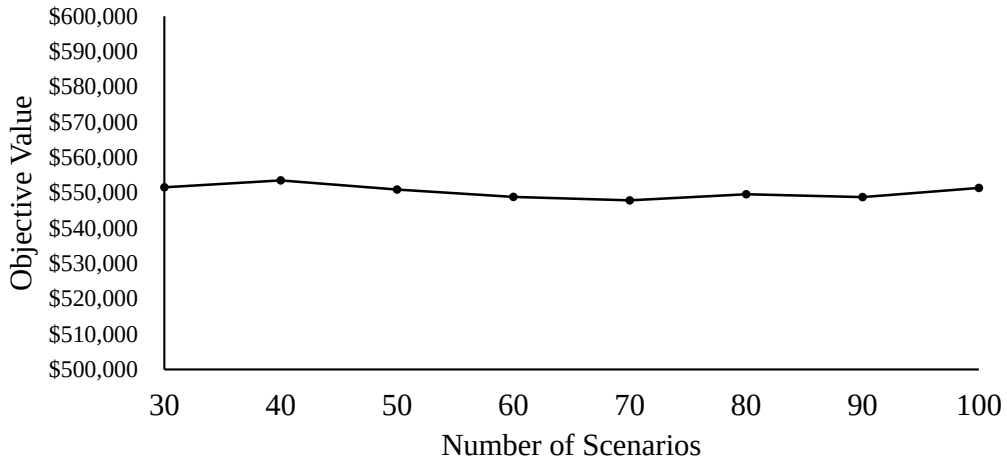

Figure 3.7 Sensitivity analysis of optimal objective value versus the number of scenarios.

3.6.3 Restoration

After the event hits the system, it is up to the utility to dispatch the crews and manage the equipment. The efficiency of this process depends on the location of the crews and the amount of stored equipment. To assess the devised preparation plan, we solve the repair and restoration problem [76]. A new random scenario is generated on the IEEE 123-bus system, with crews and equipment allocated according to the results in Table 3.4. In the generated scenario, 13 three-phase poles, 18 single-phase poles, 2 single-phase transformers, and 4343.4 meter of conductor are damaged. The method presented in [76] (Chapter 4) is used to dispatch the crews and operate the network to restore energy to customers as fast as possible. Four preparation methods are tested: 1- SCRAP; 2- RSO; 3- DA; 4- without preparation (the utility starts with its crews and equipment positioned at Depot 1). The results are shown in Table 3.6 and Fig. 3.8. The "+" sign in Table 3.6 indicates a surplus of equipment (number of available equipment is higher than the amount required) and "-" indicates a shortage of equipment. Both SCRAP and RSO over prepare with a large surplus of 11 single-phase poles for SCRAP and 23 single-phase and 10 three-phase poles for RSO. However, the restoration process is faster with 80 MWh served in the first 48 hours for both methods. Without preparation and DA have a shortage of 3 three-phase poles and 0.34 km of conductor. Moreover, without preparation, there is a shortage of 3 single-phase poles. We assume that the equipment

required to finish repairs can be obtained 12 hours after the event. With 10 line crews and 3 tree crews, the system can be completely restored within 48 hours (27 and 30 hours with SCRAP/RSO and DA, respectively). On the other hand, it takes more than 48 hours to restore the system for 5 line crews and 3 tree crews. The percentage of load served comparing the three preparation strategies is shown in Fig. 3.8, where SCRAP has the best performance.

Table 3.6 Repair and Restoration Performance After The Event

Preparation	Equipment	Load served (kWh)
SCRAP	{+3,+11,+3,+6,+0.32 km}	80,136 kWh
RSO	{+10,+23,+3,+7,+3.7 km}	80,136 kWh
DA	{-3,+1,+3,+6,-0.34 km}	77,448 kWh
W/O Preparation	{-3,-3,+3,+6,-0.34 km}	46,667 kWh

"-": shortage; "+": surplus; the load served is for the first 48 hours. Equipment: {poles for 3-phase lines, poles for single-phase lines, 3-phase transformers, single-phase transformers, conductor}.

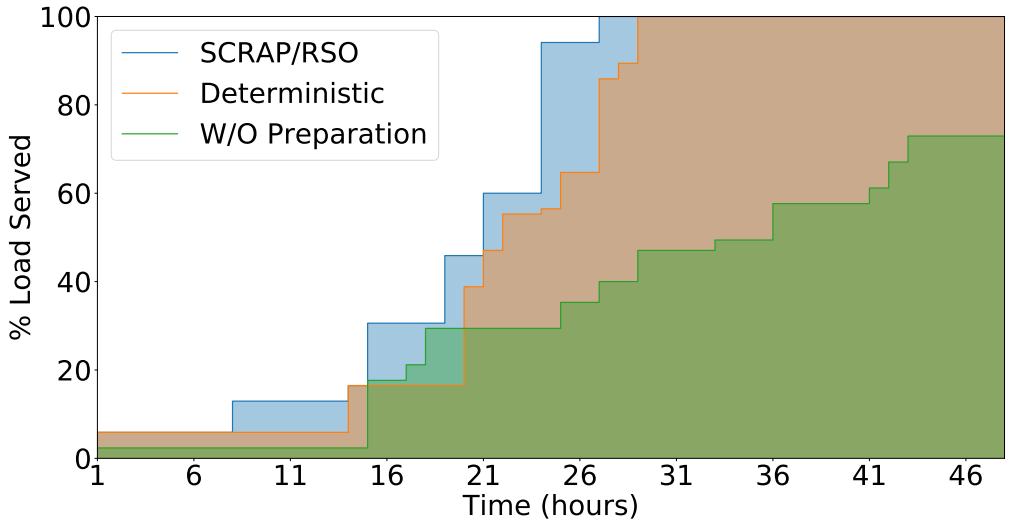

Figure 3.8 Post-event percentage of load served

3.7 Summary

In this chapter, a new study for disaster preparation considering crews and equipment allocation is presented. The study starts with analyzing the fragility of distribution networks to extreme

events in order to estimate their impacts on the network. Several outcome scenarios are generated providing information on the number of equipment required, estimated repair times, and critical lines. A two-stage stochastic mathematical model is developed to select staging locations, and allocate crews and equipment. A study case is presented on the IEEE 123-bus system where the performance of the proposed model is tested. The results demonstrate the effectiveness of the proposed approach for both meeting the equipment demand and post-event recovery operation. By using an effective preparation procedure, we can ensure that enough equipment is present for repairing the damaged components in the network and facilitate a faster restoration process.

CHAPTER 4. DISTRIBUTION NETWORK REPAIR AND RESTORATION

4.1 Overview

This chapter proposes an optimization strategy to assist utility operators to recover power distribution systems after large outages. Specifically, a MILP model is developed for co-optimizing crews, resources, and network operations in Section 4.2. The MILP model coordinates damage isolation, network reconfiguration, distributed generator redispatch, PV systems operations, and crew/resource logistics. We consider two different types of crews, namely, line crews for damage repair and tree crews for obstacle removal. Furthermore, a new algorithm is developed in Section 4.3 for solving DSRRP. The algorithm starts by assigning the crews to the damaged components in the first stage. In the second stage, DSRRP is solved with the crews dispatched to the assigned components from the first stage. In the third stage, a neighborhood search approach [101] is used to iteratively improve the routing decisions obtained from stage two. The simulation and results for validating the proposed method are presented in Section 4.4. Currently, utilities schedule the repairs using a list of predefined restoration priorities based on previous experiences, and network operation and repair scheduling are split into two different processes. This kind of approach does not capture the interdependence nature of the crew routing and network operation problems. Utilities commonly rely on the experiences of the operators. Our aim is to provide utilities with a better distribution system restoration decision-making process for coordinating crew scheduling, resource logistics, and network operations.

4.2 Mathematical Formulation

During extreme events, outage reports are received directly from customers using an interactive voice response (IVR) system. The customer information system collects the information and sends it to the outage management system (OMS). Additional information on the system status

is also obtained from advanced metering infrastructure (AMI) and the supervisory control and data acquisition (SCADA) system, which confirms the occurrence of outages or restorations using measurements from field devices. Using the collected data, the OMS can estimate the locations of the outages, and then damage assessors are dispatched to locate the damaged components and estimate the required resources and repair time. Now that the location of the damaged components and the status of the system are known, the DSRRP model is solved to obtain the repair and restoration solution. The crew schedule is sent to the work management system (WMS), which communicates the tasks to the crews. The restoration plan and operations are sent to the distribution management system (DMS) and the system operator to confidently control the switches and DGs. The proposed model can be implemented inside the OMS. Fig. 4.1 shows an example on how to integrate the proposed method in the utilities' tools.

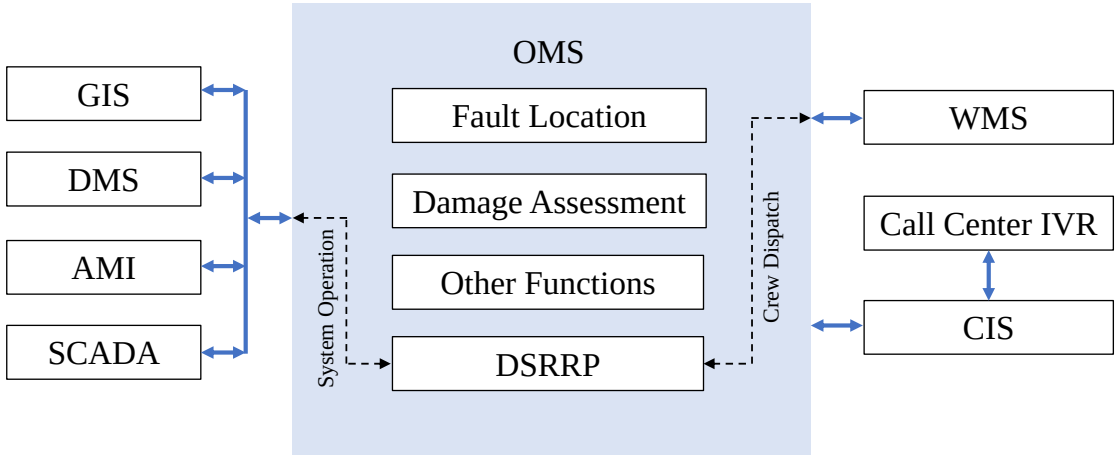

Figure 4.1 Integration of the DSRRP model into the OMS.

In this study, we assume that the assessors have located the damaged lines, and estimated the repair time and required resources. This section presents the DSRRP model. The nomenclature is given in Table 4.1.

Table 4.1 Nomenclature for the DSRRP model

Sets and Indices

m/n	Indices for damaged components and depots
c, τ, d	Index for crews, resources and depots
i/j	Indices for buses
k	Index for distribution line connecting i and j
t, φ	Index for time and phase number
C^L, C^T	Set of line and tree crews
N	Set of damaged components and the depot
$N(c)$	Set of components assigned to crew c
Ω_B, Ω_P	Set of buses and depots
Ω_{DL}, Ω_{DT}	Set of damaged lines and lines damaged by trees.
Ω_{ES}, Ω_{PV}	Set of BESSs and PVs
Ω_G, Ω_{Sub}	Set of buses with dispatchable generators and substations
$\Omega_{K(.,i)}$	Set of lines with bus i as the to bus
$\Omega_{K(i,.)}$	Set of lines with bus i as the from bus
$\Omega_{K(l)}$	Set of lines in loop l
Ω_{SW}	Set of lines with switches

Parameters

Cap_τ^R	The capacity required to carry resource τ
Cap_c^C	The maximum capacity of crew c
$\underline{E}/\overline{E}_i^S$	The minimum/maximum energy state of BESS i
$Ir_{i,t}$	Solar irradiance at bus i and time t
$\mathcal{R}_{m,\tau}$	The number of type τ resources required to repair damaged component m
$E_{d,\tau}^D$	The number of type τ resources that are located in depot d
ρ_i^D, ρ^{SW}	The cost of shedding the load at bus i and cost of switching
$P/Q_{i,\varphi,t}^D$	Diversified active/reactive demand at bus i, phase φ and time t
$P/Q_{i,\varphi,t}^U$	Undiversified active/reactive demand at bus i and phase φ
$S, \bar{P}_i^{PV}$	The kVA and kW rating of PV i
$Q_{i,\varphi}^C$	Reactive power for capacitor bank at bus i
S_i^{ES}	The kVA rating of BESS i
$ET_{m,c}$	The estimated time needed to repair (clear the trees at) damaged component m for line (tree) crew c
$tr_{m,n}$	Travel time between m and n

Table 4.1 (Continued)

ϕ_c^0/ϕ_c^1	Start/End location of crew c
Z_k	The impedance matrix of line k
$\boldsymbol{p}_k$	Vector with binary entries for representing the phases of line k
$\boldsymbol{a}_k$	Vector representing the ratio between the primary and secondary voltages for each phase of the voltage regulator on line k
$\delta_{d,c}$	Binary parameter equals 1 if crew c is positioned in depot d
$\eta_c, \eta_d, \Delta t$	Charging and discharging efficiency, and the time step duration

Decision Variables

$A_{m,c}^{L/T}$	Binary variable equal to 1 if component m is assigned to line/tree crew c
$E_{c,d,\tau}^{C}$	Number of type τ resources that crew c obtains from depot d
$\gamma_{k,t}$	Binary variable indicates whether switch k is operated in time t
$\boldsymbol{S}_k$	A vector representing the apparent power of each phase for line k at time t
$\boldsymbol{U}_{i,t}$	A vector representing the squared voltage magnitude of each phase for bus i at time t
$\mathcal{X}_{i,t}$	Binary variable equal to 0 if bus i is in an outage area at time t
$CE_{c,m,\tau}$	The number of type τ resources that crew c has before repairing damaged component m
$E_{i,t}^{S}$	Energy state of BESS i at time t
$\alpha_{m,c}$	Arrival time of crew c at damaged component m
$f_{m,t}$	Binary variable equal to 1 if damaged component m is repaired at time t
$\mathcal{L}^L, \mathcal{L}^T$	The expected times of the last repair conducted by the line and tree crews
$P_{i,\varphi,t}^{ch/dch}$	Active power charge/discharge of the BESS at bus i
$P/Q_{i,\varphi,t}^{L}$	Active/reactive load supplied at bus i, phase φ and time t
$P/Q_{i,\varphi,t}^{PV}$	The active/reactive power output of the PV at bus i
$P/Q_{i,\varphi,t}^{G}$	Active/reactive power generated by DG at bus i, phase φ and time t
$P/Q_{k,\varphi,t}^{K}$	Active/reactive power flowing on line k, phase φ and time t
$\mathcal{P}_{c,d}$	A positive penalty term for the excess capacity that crew c requires from depot d
$\bar{tr}$	Maximum travel time for the crews
$u_{k,t}$	Binary variables indicating the status of the line k at time t
$u_{i,t}^{C}$	Binary variable equals 1 if capacitor bank at bus i is connected
$u_{i,t}^{ES}$	Binary variable equals 1 if the BESS is charging and 0 for discharging
$v_{i,t}^{S}, v_{k,t}^{f}$	Virtual power generated at bus i and the virtual flow on line k
$x_{m,n,c}$	Binary variable indicating whether crew c moves from damaged components m to n.
$y_{i,t}$	Connection status of the load at bus i and time t
$z_{d,c}$	Binary variable equal to 1 if crew c require additional resources from depot d

4.2.1 Objective

In order to limit the number of switching operations, we include the cost of switching in the objective function. Therefore, the cost of switching is combined with the cost of load shedding as follows.

$$\min \sum_{\forall t} \Big(\sum_{\forall \varphi} \sum_{\forall i} (1 - y_{i,t}) \rho_i^D P_{i,\varphi,t}^D + \rho^{SW} \sum_{k \in \Omega_{SW}} \gamma_{k,t} \Big) \tag{4.1}$$

The first term in objective (4.1) minimizes the cost of load shedding, while the second term minimizes the cost of operating the switches. The base load shedding cost is assumed to be \$14/kWh [7], and the base cost is multiplied by the load priority to obtain ρ_i^D. The switch operation cost is set to be \$8/time [102].

4.2.2 Distribution Network Operation

4.2.2.1 Cold-load Pickup

After an extended period of outage, the effect of cold load pickup (CLPU) may happen, which is caused by the loss of diversity and simultaneous operation of thermostatically controlled loads. As depicted in Fig. 4.2, the normal steady-state load consumption is defined as the diversified load, and undiversified load is the startup load consumption upon restoration. The time when the load experiences an outage is t_0, t_1 is the time when the load is restored, and t_3 is the time when the load returns to normal condition. The typical behavior of CLPU can be represented using a delayed exponentially decaying function [47], which is shown in Fig. 4.2, where $t_2 - t_1$ is the exponential decay delay, and $t_3 - t_1$ is the CLPU duration. This exponential function can be approximated using a linear combination of multiple blocks. In this study, we employ two blocks to represent CLPU as suggested in [47]. The first block is for the undiversified load P^U and the second for the diversified load P^D (i.e., the steady-state load consumption) as shown in Fig. 4.2.

The use of two blocks decreases the computational burden imposed by nonlinear characteristics of CLPU and provides a conservative approach to guarantee the supply-load balance. For a time

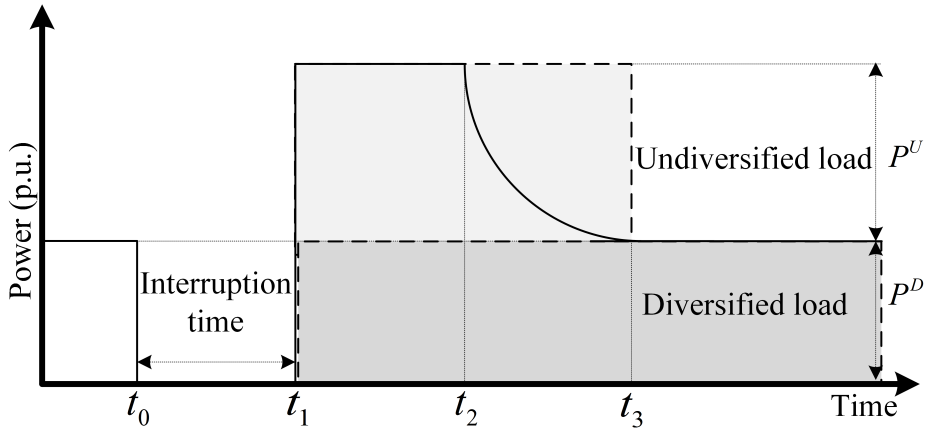

Figure 4.2 CLPU condition as a delayed exponential model, and the shaded areas represent the two-block model.

horizon T and time step Δt, the CLPU curve is sampled as shown in Fig. 4.3, where λ is the number of time steps required for the load to return to normal condition. The value of λ equals the CLPU duration divided by the time step. The CLPU constraint for active power can be formulated as follows:

$$P^L_{i,\varphi,t} = y_{i,t} P^D_{i,\varphi,t} + (y_{i,t} - y_{i,\max(\mathrm{t}-\lambda,0)}) P^U_{i,\varphi,t}, \ \forall i, \varphi, t \tag{4.2}$$

where $y_{i,0}$ is the initial state of load i immediately after an outage event; i.e., $y_{i,0} = 1$ and $P^L_{i,\varphi,0} = P^D_{i,\varphi,0}$ if the load is not affected by the outage. If a load goes from a de-energized state to an energized state at time step $t = h$ ($y_{i,h-1} = 0$ and $y_{i,h} = 1$), it will return to normal condition at time step $h + \lambda$, as $y_{i,h} - y_{i,max(h+\lambda-\lambda,0)} = 0$. Before time step $h + \lambda$, $P^U_{i,\varphi,t}$ is added to $P^D_{i,\varphi,t}$ to represent the undiversified load. The function $\max(t - \lambda, 0)$, is used to avoid negative values. We assume that the duration of the CLPU decaying process is one hour in the simulation [47]. Moreover, the study in [103] showed that the total load at pickup time can be up to 200% of the steady state value, thus, $P^U_{i,\varphi,t}$ is set to be equal to $P^D_{i,\varphi,t}$. Similarly, the CLPU constraint for reactive power [104] is formulated in (4.3). Also, we impose that once a load is served it cannot be shed using constraint (4.4).

$$Q^L_{i,\varphi,t} = y_{i,t} Q^D_{i,\varphi,t} + (y_{i,t} - y_{i,\max(\mathrm{t}-\lambda,0)}) Q^U_{i,\varphi,t}, \ \forall i, \varphi, t \tag{4.3}$$

$$y_{i,t+1} \geq y_{i,t} \ , \ \forall i,t \tag{4.4}$$

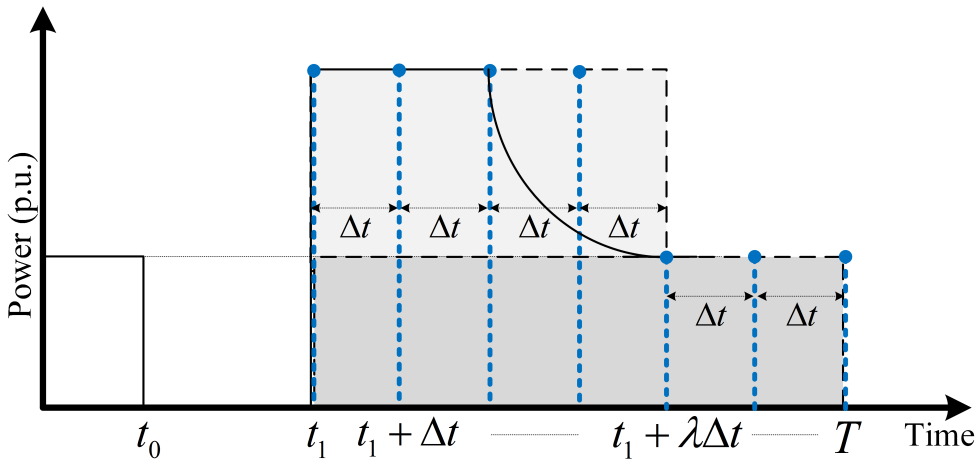

Figure 4.3 Two-blocks CLPU condition as a delayed exponential model, with time step Δt.

4.2.2.2 Unbalanced Power Flow Equations

$$0 \leq P^{G}_{i,\varphi,t} \leq P^{G_{max}}_{i} \ , \ \forall i,\varphi,t \tag{4.5}$$

$$0 \leq Q^{G}_{i,\varphi,t} \leq Q^{G_{max}}_{i} \ , \ \forall i,\varphi,t \tag{4.6}$$

$$-u_{k,t}p_{k,\varphi}P^{K_{max}}_{k} \leq P^{K}_{k,\varphi,t} \leq u_{k,t}p_{k,\varphi}P^{K_{max}}_{k} \ , \ \forall k,\varphi,t \tag{4.7}$$

$$-u_{k,t}p_{k,\varphi}Q^{K_{max}}_{k} \leq Q^{K}_{k,\varphi,t} \leq u_{k,t}p_{k,\varphi}Q^{K_{max}}_{k} \ , \ \forall k,\varphi,t \tag{4.8}$$

$$\sum_{\forall k \in K(.,i)} P^{K}_{k,\varphi,t} + P^{G}_{i,\varphi,t} + P^{PV}_{i,\varphi,t} + P^{dch}_{i,\varphi,t} = \sum_{\forall k \in K(i,.)} P^{K}_{k,\varphi,t} + P^{L}_{i,\varphi,t} + P^{ch}_{i,\varphi,t}, \forall i,\varphi,t \tag{4.9}$$

$$\sum_{\forall k \in K(.,i)} Q^{K}_{k,\varphi,t} + Q^{G}_{i,\varphi,t} + Q^{PV}_{i,\varphi,t} + Q^{ES}_{i,\varphi,t} + u^{C}_{i,t}Q^{C}_{i,\varphi} = \sum_{\forall k \in K(i,.)} Q^{K}_{k,\varphi,t} + Q^{L}_{i,\varphi,t}, \forall i,\varphi,t \tag{4.10}$$

$$\boldsymbol{U}_{j,t} - \boldsymbol{U}_{i,t} + \bar{\boldsymbol{Z}}_k \boldsymbol{S}^{*}_{k} + \bar{\boldsymbol{Z}}^{*}_{k} \boldsymbol{S}_{k} \leq (2 - u_{k,t} - \boldsymbol{p}_k)M, \forall k \in \Omega_L \backslash \Omega_V, t \tag{4.11}$$

$$\boldsymbol{U}_{j,t} - \boldsymbol{U}_{i,t} + \bar{\boldsymbol{Z}}_k \boldsymbol{S}^{*}_{k} + \bar{\boldsymbol{Z}}^{*}_{k} \boldsymbol{S}_{k} \geq -(2 - u_{k,t} - \boldsymbol{p}_k)M, \forall k \in \Omega_L \backslash \Omega_V, t \tag{4.12}$$

Constraints (4.5)–(4.8) define the active and reactive power limits of the DGs and lines. The limits on the line-flow constraints are multiplied by $u_{k,t}$ so that if a line is damaged or a switch is opened, there will be no power flowing on it. Constraints (4.9)–(4.10) are 3-phase active and reactive power node balance constraints. Binary variable $u^{C}_{i,t}$ determines the connection status of

the capacitor bank. Constraints (4.11)–(4.12) represent Kirchhoff's voltage law [105]. For each line i to j, Kirchhoff voltage law is applied as follows:

$$\boldsymbol{V}_j = \boldsymbol{V}_i - \boldsymbol{Z}_k \boldsymbol{I}_k \tag{4.13}$$

where $\boldsymbol{V}_i = [V_i^a, V_i^b, V_i^c]^T \in \mathbb{C}^{3\times 1}$ is the 3-phase complex voltage of bus i, $\boldsymbol{I}_k = [I_k^a, I_k^b, I_k^c]^T \in \mathbb{C}^{3\times 1}$ is the 3-phase current, and $\boldsymbol{Z}_k \in \mathbb{C}^{3\times 3}$ is the impedance matrix of line k that connects buses i and j. Let $\odot$ and $\oslash$ be the element wise multiplication and division, the current can then be calculated as follows:

$$\boldsymbol{I}_k = \boldsymbol{S}_k^* \oslash \boldsymbol{V}_i^* \tag{4.14}$$

where S_k is the 3-phase apparent power flowing from bus i to j. We assume that the line losses is small compared to the power flow. By combining (4.13) and (4.14), and multiplying by the complex conjugate of each side, we can obtain the following equation:

$$\boldsymbol{V}_j \odot \boldsymbol{V}_j^* = \boldsymbol{V}_i \odot \boldsymbol{V}_i^* - \boldsymbol{Z}_k(\boldsymbol{S}_k^* \oslash \boldsymbol{V}_i^*) \odot \boldsymbol{V}_i^* - \boldsymbol{Z}_k^*(\boldsymbol{S}_k \oslash \boldsymbol{V}_i) \odot \boldsymbol{V}_i + \boldsymbol{c_k(S_k, V_i, Z_k)} \tag{4.15}$$

where $\boldsymbol{c_k(S_k, V_i, Z_k)}$ is a higher-order term which can be neglected if the line losses is small compared to power flow. Equation (4.15) is expanded as follows:

$$\begin{aligned}
\begin{bmatrix} (V_j^a)^2 \\ (V_j^b)^2 \\ (V_j^c)^2 \end{bmatrix} = \begin{bmatrix} (V_i^a)^2 \\ (V_i^b)^2 \\ (V_i^c)^2 \end{bmatrix} - \begin{bmatrix} Z_k^{aa}(S_k^a \frac{V_i^a}{V_i^a})^* + Z_k^{ab}(S_k^b \frac{V_i^a}{V_i^b})^* + Z_k^{ac}(S_k^c \frac{V_i^a}{V_i^c})^* \\ Z_k^{ba}(S_k^a \frac{V_i^b}{V_i^a})^* + Z_k^{bb}(S_k^b \frac{V_i^b}{V_i^b})^* + Z_k^{bc}(S_k^c \frac{V_i^b}{V_i^c})^* \\ Z_k^{ca}(S_k^a \frac{V_i^c}{V_i^a})^* + Z_k^{cb}(S_k^b \frac{V_i^c}{V_i^b})^* + Z_k^{cc}(S_k^c \frac{V_i^c}{V_i^c})^* \end{bmatrix} \\
- \begin{bmatrix} (Z_k^{aa})^* S_k^a \frac{V_i^a}{V_i^a} + (Z_k^{ab})^* S_k^b \frac{V_i^a}{V_i^b} + (Z_k^{ac})^* S_k^c \frac{V_i^a}{V_i^c} \\ (Z_k^{ba})^* S_k^a \frac{V_i^b}{V_i^a} + (Z_k^{bb})^* S_k^b \frac{V_i^b}{V_i^b} + (Z_k^{bc})^* S_k^c \frac{V_i^b}{V_i^c} \\ (Z_k^{ca})^* S_k^a \frac{V_i^c}{V_i^a} + (Z_k^{cb})^* S_k^b \frac{V_i^c}{V_i^b} + (Z_k^{cc})^* S_k^c \frac{V_i^c}{V_i^c} \end{bmatrix}
\end{aligned} \tag{4.16}$$

Define $\boldsymbol{U}_i$ for each bus as $\boldsymbol{U}_i = [|V_i^a|^2, |V_i^b|^2, |V_i^c|^2]^T$, and by assuming that the voltages are nearly balanced ($V_i^a/V_i^b \approx V_i^b/V_i^c \approx V_i^c/V_i^a \approx e^{j2\pi/3}$), the following equation is obtained:

$$\boldsymbol{U}_j = \boldsymbol{U}_i - \bar{\boldsymbol{Z}}_k \boldsymbol{S}_k^* - \bar{\boldsymbol{Z}}_k^* \boldsymbol{S}_k \tag{4.17}$$

where $\bar{\boldsymbol{Z}}_k = \boldsymbol{A} \odot \boldsymbol{Z_k}$ and $\boldsymbol{A}$ is defined as follows:

$$\boldsymbol{A} = \begin{bmatrix} 1 & e^{-j2\pi/3} & e^{j2\pi/3} \\ e^{j2\pi/3} & 1 & e^{-j2\pi/3} \\ e^{-j2\pi/3} & e^{j2\pi/3} & 1 \end{bmatrix}$$

The big M method is used to decouple the voltages between lines that are disconnected or damaged in (4.11) and (4.12). Also, if line $k(i,j)$ is a two-phase line (e.g., phases a and c), then the voltage constraint is only applied to these two phases, which is realized by including $\boldsymbol{p_k}$. The vector $\boldsymbol{p_k} \in \{0,1\}^{3\times 1}$ represents the phases of line k; e.g., for line k with phases a, c, $\boldsymbol{p_k} = [1,0,1]$. The per-phase form of (4.11) and (4.12) is detailed in (4.18)-(4.23), where $\bar{R}$ and $\bar{X}$ are the real (resistance) and imaginary (reactance) parts of $\bar{Z}$.

$$U_{i,a,t} - U_{j,a,t} - 2(\bar{R}_k^{aa} P_{k,a,t}^K + \bar{R}_k^{ab} P_{k,b,t}^K + \bar{R}_k^{ac} P_{k,c,t}^K + \bar{X}_k^{aa} Q_{k,a,t}^K + \bar{X}_k^{ab} Q_{k,b,t}^K + \bar{X}_k^{ac} Q_{k,c,t}^K) \leq M(2 - u_{k,t} - p_{k,a}), \forall k, t \quad (4.18)$$

$$U_{i,a,t} - U_{j,a,t} - 2(\bar{R}_k^{aa} P_{k,a,t}^K + \bar{R}_k^{ab} P_{k,b,t}^K + \bar{R}_k^{ac} P_{k,c,t}^K + \bar{X}_k^{aa} Q_{k,a,t}^K + \bar{X}_k^{ab} Q_{k,b,t}^K + \bar{X}_k^{ac} Q_{k,c,t}^K) \geq -M(2 - u_{k,t} - p_{k,a}), \forall k, t \quad (4.19)$$

$$U_{i,b,t} - U_{j,b,t} - 2(\bar{R}_k^{ba} P_{k,a,t}^K + \bar{R}_k^{bb} P_{k,b,t}^K + \bar{R}_k^{bc} P_{k,c,t}^K + \bar{X}_k^{ba} Q_{k,a,t}^K + \bar{X}_k^{bb} Q_{k,b,t}^K + \bar{X}_k^{bc} Q_{k,c,t}^K) \leq M(2 - u_{k,t} - p_{k,b}), \forall k, t \quad (4.20)$$

$$U_{i,b,t} - U_{j,b,t} - 2(\bar{R}_k^{ba} P_{k,a,t}^K + \bar{R}_k^{bb} P_{k,b,t}^K + \bar{R}_k^{bc} P_{k,c,t}^K + \bar{X}_k^{ba} Q_{k,a,t}^K + \bar{X}_k^{bb} Q_{k,b,t}^K + \bar{X}_k^{bc} Q_{k,c,t}^K) \geq -M(2 - u_{k,t} - p_{k,b}), \forall k, t \quad (4.21)$$

$$U_{i,c,t} - U_{j,c,t} - 2(\bar{R}_k^{ca} P_{k,a,t}^K + \bar{R}_k^{cb} P_{k,b,t}^K + \bar{R}_k^{cc} P_{k,c,t}^K + \bar{X}_k^{ca} Q_{k,a,t}^K + \bar{X}_k^{cb} Q_{k,b,t}^K + \bar{X}_k^{cc} Q_{k,c,t}^K) \leq M(2 - u_{k,t} - p_{k,c}), \forall k, t \quad (4.22)$$

$$U_{i,c,t} - U_{j,c,t} - 2(\bar{R}^{ca}_k P^K_{k,a,t} + \bar{R}^{cb}_k P^K_{k,b,t} + \bar{R}^{cc}_k P^K_{k,c,t} + \bar{X}^{ca}_k Q^K_{k,a,t} + \bar{X}^{cb}_k Q^K_{k,b,t} + \bar{X}^{cc}_k Q^K_{k,c,t}) \geq -M(2 - u_{k,t} - p_{k,c}), \forall k, t \quad (4.23)$$

4.2.2.3 Voltage Regulators

Voltage regulators are used by utilities to maintain the voltage in the system within specific limits. The voltage regulators are capable of raising or lowering the voltage by ±10%. This is achieved by controlling the tap position of the voltage regulation transformers by increments of 0.625%. The ratio of the voltage regulator transformer is given by $(1 + 0.00625Tap_{k,\varphi,t})$, where $Tap_{k,\varphi,t} \in \{-16, -15, ..., 16\}$ is the tap position. If U_i is the primary voltage and U_j is the secondary voltage of voltage regulator k, then:

$$U_j = (1 + 0.00625Tap_{k,\varphi,t})^2 \, U_i \quad (4.24)$$

However, equation (4.24) is nonlinear. To linearize (4.24), we first define all possible ratios between the primary and secondary squared voltages as $r^v \in \mathbb{R}^{33\times 1} = [0.81, 0.8213, ..., 1.21]$. Then, binary variable $t^v_{k,r,\varphi,t} \in \{0,1\}^{33}$ is used to indicate the tap position of the voltage regulator. The mathematical model for the voltage regulators is then formulated as follows:

$$-M(1 - t^v_{k,p,\varphi,t}) + r^v_p U_{i,\varphi,t} \leq U_{j,\varphi,t} \leq r^v_p U_{i,\varphi,t} + M(1 - t^v_{k,p,\varphi,t}), \forall k \in \Omega_V, \varphi, t, p \in \{1...33\} \quad (4.25)$$

$$\sum_{p=1}^{33} t^v_{k,p,\varphi,t} = 1, \forall k \in \Omega_V, \varphi, t \quad (4.26)$$

Constraints (4.25) models the relationship between the voltage magnitudes on both sides for a 3-phase voltage regulator, with i as the primary side and j as the secondary side. If $t^v_{k,p,\varphi,t} = 0$, then (4.25) does not impose any relationship between the two voltages. On the other hand, if $t^v_{k,p,\varphi,t} = 1$, the constraint becomes $U_{j,\varphi,t} = r^v_p U_{i,\varphi,t}$. Constraint (4.26) states that the tap can be in one position.

Additionally, we can impose a limit on the number of tap changes allowed for the regulators as follows:

$$-t^{v}_{max} \leq \sum_{p=1}^{33} r^{v}_{p}(t^{v}_{k,p,\varphi,t} - t^{v}_{k,p,\varphi,t-1}) \leq t^{v}_{max}, \forall k \in \Omega_V, \varphi, t \tag{4.27}$$

where t^{v}_{max} is the maximum number of tap changes for each regulator per hour. Constraints (4.25) and (4.26) represent an exact linaerization of (4.24), however, it does impose some computational complexity. Therefore, if we assume that the tap setting is continuous [106], then equation (4.24) can be approximated using the following constraint:

$$(0.9)^2 U_{i,\varphi,t} \leq U_{j,\varphi,t} \leq (1.1)^2 U_{i,\varphi,t}, \forall k \in \Omega_V, \varphi, t \tag{4.28}$$

Constraint (4.28) forces the voltage on the secondary side of the voltage regulator to be within $\pm 10\%$ of the primary side.

4.2.2.4 Reconfiguration and Fault Isolation

Automatic sectionalizing switches can reduce the number of affected customers during an outage. The switches isolate the faulted parts of the network so that the healthy parts of the network can be supplied. The automatic operation of the sectionalizing switches is coordinated with the circuit breakers or reclosers which interrupts the high current that results from a fault. Note that the fault considered in this dissertation is a permanent fault due to failure of a component. Consider the network shown in Fig. 4.4, the substation at bus 1 is supplying the system when a permanent fault occurs at line 5–6. The circuit breaker (CB) between 1–2 opens to interrupt the fault current. After that, the sectionalizing switches at lines 3–4 and 6–7 are opened to isolate the fault. Finally, the CBs are closed to operate the healthy part of the network. The purpose of the developed model is to find the network shown in Step 3 (in Fig. 4.4) after a fault occurs. The following constraints are used to reconfigure the distribution network and isolate the failed lines [107]:

$$\mathcal{X}_{i,t} U_{min} \leq \boldsymbol{U}_{i,t} \leq \mathcal{X}_{i,t} U_{max} \ , \ \forall i, t \tag{4.29}$$

$$2u_{k,t} \geq \mathcal{X}_{i,t} + \mathcal{X}_{j,t}, \forall k \in \Omega_{DL}, t \tag{4.30}$$

$$u_{k,t} = 1, \forall k \notin \{\Omega_{SW} \cup \Omega_{DL}\}, t \tag{4.31}$$

$$\gamma_{k,t} \geq u_{k,t} - u_{k,t-1}, \forall k \in \Omega_{SW}, t \tag{4.32}$$

$$\gamma_{k,t} \geq u_{k,t-1} - u_{k,t}, \forall k \in \Omega_{SW}, t \tag{4.33}$$

$$\sum_{k \in \Omega_{K(l)}} u_{k,t} \leq |\Omega_{K(l)}| - 1, \forall l, t \tag{4.34}$$

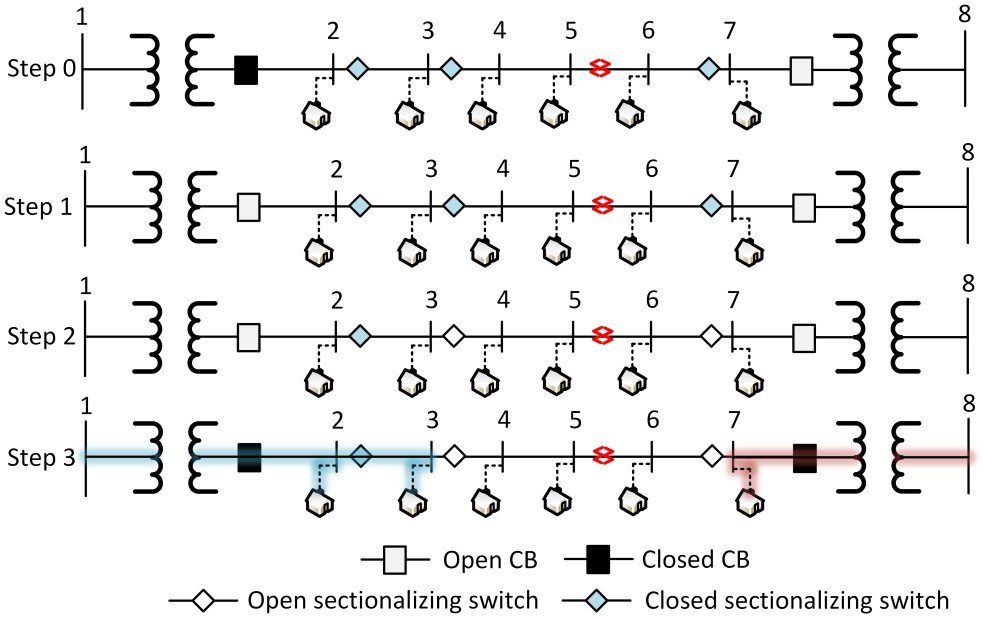

Figure 4.4 Distribution system switch operation for fault isolation.

Constraint (4.29) ensures that the voltage is within a specified limit, and is set to equal to 0 if the bus is in an on-outage area. Constraint (4.30) sets the values of $\mathcal{X}_i$ and $\mathcal{X}_j$ to be 0 if the line is damaged, therefore, the voltages on the buses between damaged lines are forced to be 0 using constraint (4.29). Subsequently, the zero voltage propagates on the rest of the network through constraints (4.11)–(4.26) until a circuit breaker or sectionalizer stops the propagation. If the voltages on two connected buses are zero, then the power flow is forced to be zero through constraints (4.11) and (4.12)Constraint (4.31) defines the default status of the lines that are not damaged or not switchable. Constraint (4.32)–(4.33) are used in order to limit the number of switching operations. We define a variable $\gamma_{k,t}$ which is equal to 1 if the line switches its status

from 0 (off) to 1 (on), or 1 (on) to 0 (off). This variable is included in the objective to minimize the number of switching operation. Constraint (4.34) is the radiality constraint. Radiality is enforced by introducing constraints for ensuring that at least one of the lines of each possible loop in the network is open [108]. A depth-first search method is used to identify the possible loops in the network and the lines associated with them [109]. Alternatively, the radiality constraints can be represented by (4.34a)-(4.34d) based on the spanning tree approach [53].

$$0 \leq \beta_{i,j,t} \leq 1, \forall i,j \in \Omega_B, t \tag{4.34a}$$

$$\beta_{i,j,t} + \beta_{j,i,t} = u_{k,t,s},\ \forall k,t \tag{4.34b}$$

$$\beta_{i,j,t} = 0,\ \forall i \in \Omega_B, j \in \Omega_{Sub}, t \tag{4.34c}$$

$$\sum_{\forall i \in \Omega_B} \beta_{i,j,t} \leq 1,\ \forall j \in \Omega_B, t \tag{4.34d}$$

Two variables $\beta_{i,j,t}$ and $\beta_{j,i,t}$ are defined to model the spanning tree. For a radial network, each bus cannot be connected to more than one parent bus and the number of lines equals the number of buses other than the root bus. Constraint (4.34b) relates the connection status of the line and the spanning tree variables $\beta_{i,j,t}$ and $\beta_{j,i,t}$. If the distribution line is connected, then either $\beta_{i,j,t}$ or $\beta_{j,i,t}$ must equal one. Constraint (4.34c) designates substations as root buses and indicates that they do not have parent buses. Constraint (4.34d) requires that every bus does not have more than one parent bus. The spanning tree constraints guarantee that the number of buses in a spanning tree, other than the root, equals the number of lines [53]. In this dissertation, we use constraint (4.34) to ensure the radiality as the spanning tree constraints in (4.34a)–(4.34d) will add $|\Omega_B| \times |\Omega_B| \times |T|$ variables.

4.2.3 PV Systems

In this study, we consider three types of PV systems:

- Type 1: on-grid (grid-tied) PV (Ω^G_{PV}): during an outage, the PV is switched off. This type of PVs is the most commonly used one especially for residential customers [110]. The on-grid system uses a standard grid-tied inverter and does not have any battery storage.

- Type 2: hybrid on-grid/off-grid PV + BESS (Ω^H_{PV}): this system is an on-grid system that can disconnect from the grid after an outage and uses battery backup supply.
- Type 3: grid-forming PV + BESS (Ω^C_{PV}): this system is an on-grid system that can support a large section of the network [111]. After an outage, the PV and battery system can provide energy to the healthy parts of the network.

4.2.3.1 PV active and reactive power

The active and reactive powers of a PV depend on the rating of the solar cell and the solar irradiance. The active output power from the PVs is determined using constraints (4.35) and (4.36). The PV inverters can provide reactive power support, which is constrained by (4.37) and (4.38) [112].

$$P^{PV}_{i,\varphi,t} = \frac{Ir_{i,t}}{(1000W/m^2)}\overline{P}^{PV}_i, \forall i \in \Omega_{PV}\backslash\Omega^G_{PV}, \varphi, t \tag{4.35}$$

$$P^{PV}_{i,\varphi,t} = \mathcal{X}_{i,t}\frac{Ir_{i,t}}{(1000W/m^2)}\overline{P}^{PV}_i, \forall i \in \Omega^G_{PV}, \varphi, t \tag{4.36}$$

$$|Q^{PV}_{i,\varphi,t}| \leq \sqrt{(S^{PV}_i)^2 - (\hat{P}^{PV}_{i,t})^2}, \forall i \in \Omega_{PV}\backslash\Omega^G_{PV}, \varphi, t \tag{4.37}$$

$$|Q^{PV}_{i,\varphi,t}| \leq \mathcal{X}_{i,t}\sqrt{(S^{PV}_i)^2 - (\hat{P}^{PV}_{i,t})^2}, \forall i \in \Omega^G_{PV}, \varphi, t \tag{4.38}$$

$$\text{where} \qquad \hat{P}^{PV}_{i,t} = \frac{Ir_{i,t}}{(1000W/m^2)}\overline{P}^{PV}_i$$

PVs of types Ω^G_{PV} and Ω^H_{PV} are able to disconnect from the grid and serve the on-site load. On the other hand, on-grid PVs are disconnected and the on-site load is not served by the PVs during an outage, therefore, the right-hand side in (4.36) and (4.38) are multiplied by $\mathcal{X}_i$. Note that $|f(x)| \leq x$ is equivalent to $-x \leq f(x) \leq x$.

4.2.3.2 PV connectivity

In this dissertation, we assume that the network can be restored using the grid-forming sources in $\Omega^C_{PV} \cup \Omega_G \cup \Omega_{Sub}$. A PV of type Ω^G_{PV} or Ω^H_{PV} can connect to the grid only after the PV bus is

energized. Consider the network shown in Fig. 4.5. Due to line damage, the network is divided into four islands. Island A can be energized by the substation, therefore, the PV at bus 10 can be connected with the grid. Island B must be isolated because of the damaged line. Island C does not have any grid-forming generators; hence, it will not be active and the grid-tied PV will be disconnected. However, the PV+BESS system at bus 7 can energize the local load. Island D can be energized by the grid-forming PV+BESS system at bus 4.

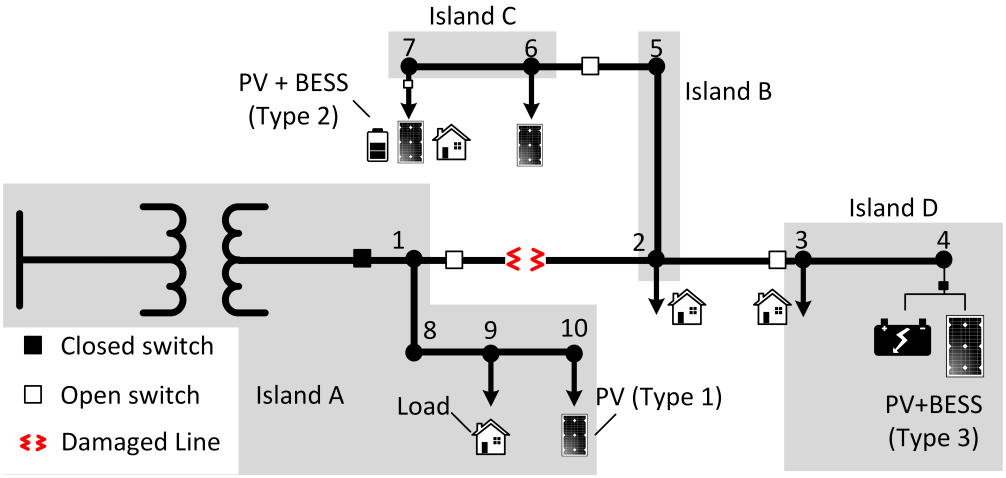

Figure 4.5 A single line diagram of a network with one damaged line.

The connectivity constraints of the PVs are represented by constraints (4.39)-(4.42). The idea of the approach is to use virtual sources, loads, and flow to identify the energized buses in the network. The constraints for the virtual framework are formulated as follows:

$$v^{S}_{i,\varphi,t} + \sum_{k \in K(.,i)} v^{f}_{k,\varphi,t} = \mathcal{X}_{i,t} + \sum_{k \in K(i,.)} v^{f}_{k,\varphi,t}, \forall i, \varphi, t \tag{4.39}$$

$$\sum_{\forall \varphi} \sum_{\forall t} v^{S}_{i,\varphi,t} = 0, \forall i \in \Omega_B \backslash \{\Omega^{C}_{PV} \cup \Omega_G \cup \Omega_{Sub}\} \tag{4.40}$$

$$-(u_{k,t}\ p_{k,\varphi})M \leq v^{f}_{k,\varphi,t} \leq (u_{k,t}\ p_{k,\varphi})M, \forall k \in \Omega_K, \varphi, t \tag{4.41}$$

$$\mathcal{X}_{i,t} \geq y_{i,t}, \forall i \in \Omega_B \backslash \{\Omega_G \cup \Omega^{C}_{PV} \cup \Omega^{H}_{PV}\}, t \tag{4.42}$$

To identify whether an island is energized by grid-forming generators or not, we create a virtual network. First, each grid-forming generator is replaced by a virtual source/generator with infinite capacity. Other power sources without grid-forming capability (e.g., grid-tied PVs) are removed. Also, virtual loads with magnitude of 1 are placed on each bus, and the actual loads are removed. For example, the network shown in Fig. 4.5 is transformed to the network shown in Fig. 4.6.

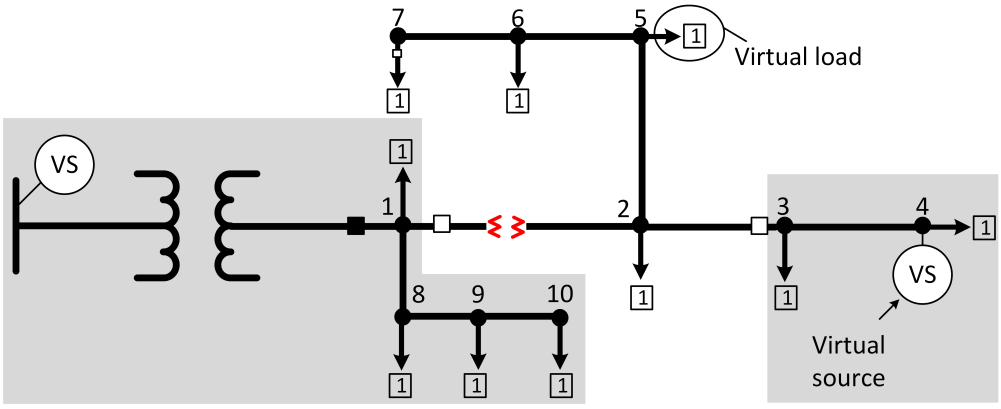

Figure 4.6 A virtual network created for the network shown in Fig. 4.5.

In the mathematical model, we add a node-balance equation for each virtual bus. If the virtual load at a bus is served, then that bus is energized. Therefore, for islands without grid-forming generators, all buses will be de-energized as the virtual loads in the island cannot be served. Constraint (4.39) is the node balance constraint for the virtual network. Constraints (4.40) states that buses without grid-forming power generators do not have virtual sources. The variable v_k^f represents the virtual flow on line k and each bus is given a load of 1 that is multiplied by $\mathcal{X}_i$. Therefore, $\mathcal{X}_i = 1$ (bus i is energized) if the virtual load can be served by a virtual source and 0 (bus i is de-energized) otherwise. The virtual flow limits is defined in (4.41). If bus i is de-energized, then the load must be shed (4.42), unless bus i has a local power source.

4.2.4 Battery Energy Storage

$$0 \leq P_{i,\varphi,t}^{ch} \leq u_{i,t}^{ES} \overline{P}_i^{ch}, \ \forall i \in \Omega_{ES}, \varphi, t \tag{4.43}$$

$$0 \leq P^{dch}_{i,\varphi,t} \leq (1 - u^{ES}_{i,t})\overline{P}^{dch}_{i}, \forall i \in \Omega_{ES}, \varphi, t \tag{4.44}$$

$$E^{S}_{i,t} = E^{S}_{i,t-1} + \Delta t(\eta_c \sum_{\forall \varphi} P^{ch}_{i,\varphi,t} - \frac{\sum_{\forall \varphi} P^{dch}_{i,\varphi,t}}{\eta_d}), \forall i \in \Omega_{ES}, t \tag{4.45}$$

$$\underline{E}^{S}_{i} \leq E^{S}_{i,t} \leq \overline{E}^{S}_{i}, \forall i \in \Omega_{ES}, t \tag{4.46}$$

$$(Q^{ES}_{i,\varphi,t})^2 + (P^{ch}_{i,\varphi,t} + P^{dch}_{i,\varphi,t})^2 \leq (S^{ES}_{i})^2, \forall i \in \Omega_{ES}, \varphi, t \tag{4.47}$$

Binary variable u^{ES} represents the charging (1) and discharging (0) state of the BESS. Limits on the charge and discharge powers are imposed using constraints (4.43) and (4.44), respectively. Constraint (4.45) represents the dynamic state of energy for each BESS, where the efficiencies η_c and η_d are assumed to be 0.95. The energy is limited to a minimum and maximum value in (4.46). $E^{S}_{i,t}$ is assumed to be between 0.2 and 0.9 of the rated capacity in this study. The active and reactive power should not exceed the rating of the BESS, as enforced by (4.47) [113]. Constraint (4.47) is quadratic, therefore, it is linearized using the circular constraint linearization method presented in [56]. Subsequently, constraint (4.47) is replaced by (4.47a)-(4.47c).

$$-u^{ES}_{i,t} S^{ES}_{i} \leq Q^{ES}_{i,\varphi,t} \leq u^{ES}_{i,t} S^{ES}_{i}, \forall i \in \Omega_{ES}, \varphi, t \tag{4.47a}$$

$$|(P^{ch}_{i,\varphi,t} + P^{dch}_{i,\varphi,t}) + Q^{ES}_{i,\varphi,t}| \leq \sqrt{2} S^{ES}_{i}, \forall i \in \Omega_{ES}, \varphi, t \tag{4.47b}$$

$$|(P^{ch}_{i,\varphi,t} + P^{dch}_{i,\varphi,t}) - Q^{ES}_{i,\varphi,t}| \leq \sqrt{2} S^{ES}_{i}, \forall i \in \Omega_{ES}, \varphi, t \tag{4.47c}$$

4.2.5 Routing Constraints

The routing problem can be defined by a complete graph with nodes and edges $G(N, E)$. The node set N in the undirected graph contains the depot and damaged components, and the edge set $E = \{(m, n) | m, n \in N; m \neq n\}$ represents the edges connecting each two components. The graph G can be obtained from a transportation network ($\hat{G}$). Transportation networks can be represented by nodes (depots, damaged components, intersection nodes) and paths connecting the nodes. Consider the transportation network shown in Fig. 4.7a, where there are two damaged components and one depot. The information that is required by the DSRRP model is the travel time between the

damaged components and the depot. Therefore, we can convert $\hat{G}$ to the network G shown in Fig. 4.7b by finding the shortest paths between damaged components and the depot [74], which can be obtained using shortest path algorithms such as Dijkstra's algorithm [114].

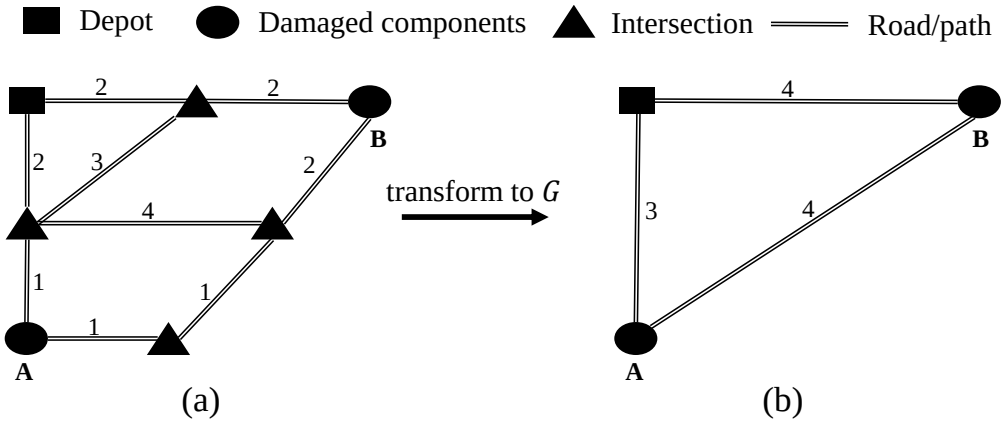

Figure 4.7 Example of (a) a transportation network transformed to (b) graph G for the crew routing model.

In the example shown in Fig. 4.7, the shortest path between the depot and damaged component A has a total length of 3 units. Therefore, the depot is connected directly to damaged component A in G with a length of 3 units. The same procedure is conducted to form the rest of the network G. If a path between two nodes in $\hat{G}$ is completely blocked or severely damaged, then the travel time of the path can be set to a large value $|T|$, where T is the time horizon. In practice, utilities use geographic information system (GIS) software to map the distribution network. Real-time data about road conditions, location of the crews, and status of the components are fed into the GIS. The utilities can then use the GIS to estimate the travel times.

Our purpose is to find an optimal route for each crew to reach the damaged components. The value of $x_{m,n,c}$ determines whether the path crew c travels includes the edge (m, n) with m preceding n. The routing constraints for the first stage problem are formulated as follows:

$$\sum_{\forall m \in N} x_{\phi_c^0, m, c} = 1, \forall c \tag{4.48}$$

$$\sum_{\forall m \in N} x_{m, \phi_c^1, c} = 1, \forall c \tag{4.49}$$

$$\sum_{\forall n \in N \setminus \{m\}} x_{m,n,c} - \sum_{\forall n \in N \setminus \{m\}} x_{n,m,c} = 0, \forall c, m \in N \setminus \left\{\phi_c^0, \phi_c^1\right\} \tag{4.50}$$

$$\sum_{\forall c \in C^L} \sum_{\forall m \in N \setminus \{n\}} x_{m,n,c} = 1, \forall n \in \Omega_{DL} \tag{4.51}$$

$$\sum_{\forall c \in C^T} \sum_{\forall m \in N \setminus \{n\}} x_{m,n,c} = 1, \forall n \in \Omega_{DT} \tag{4.52}$$

Constraint (4.48)–(4.49) guarantee that each crew starts and ends its route at the defined start (ϕ_c^0) and end (ϕ_c^1) locations. Constraint (4.50) is the flow conservation constraint; i.e., once a crew arrives at a damaged component, the crew moves to the next location after finishing the repairs. Constraint (4.51) ensures that each damaged component is repaired by only one line crew, while (4.52) ensures that each damaged component that needs removing a fallen tree first, is assigned to one tree crew.

4.2.5.1 Arrival Time

$$\alpha_{m,c} + ET_{m,c} + tr_{m,n} - (1 - x_{m,n,c})\, M \leq \alpha_{n,c} \forall m \in N \setminus \{\phi_c^1\}, n \in N \setminus \left\{\phi_c^0, m\right\}, c \tag{4.53}$$

$$\sum_{c \in C^L} \alpha_{m,c} \geq \sum_{c \in C^T} \alpha_{m,c} + ET_{m,c} \sum_{\forall n \in N} x_{m,n,c}, \forall m \in \Omega_{DT} \tag{4.54}$$

Constraint (4.53) is used to calculate the arrival time (the time when crew c starts repairing component m) for each crew at each damaged component. For a crew that travels from damaged component m to n, $\alpha_{n,c}$ equals $\alpha_{m,c} + ET_{m,c} + tr_{m,n}$. Big M is used to decouple the times to arrive at components m and n if the crew does not travel from m to n. Constraint (4.54) indicates that the line crews start repairing the damaged components after the tree crews clear the obstacles.

4.2.5.2 Resource Constraints

$$E_{d,\tau}^D \geq \sum_{\forall c \in C^L, \phi_c^0 = d} E_{c,\phi_c^0,\tau}^C + \sum_{\forall c \in C^L} E_{c,d,\tau}^C, \forall d, \tau \tag{4.55}$$

$$\sum_{\forall \tau} Cap_\tau^R \;\; CE_{c,m,\tau} \leq Cap_c^C, \forall m, c \in C^L \tag{4.56}$$

$$\sum_{\forall n \in N} x_{n,m,c} \mathcal{R}_{m,\tau} \leq CE_{c,m,\tau}, \forall m, \tau, c \in C^L \tag{4.57}$$

$$
\begin{aligned}
&-M(1-x_{m,n,c}) \le CE_{c,m,\tau} - \mathcal{R}_{m,\tau} - CE_{c,n,\tau} \le M(1-x_{m,n,c}),\\
&\forall m \in N\backslash\{\phi_c^1\}, n \in N\backslash\left\{\phi_c^0, m\right\}, c \in C^L, \tau
\end{aligned} \tag{4.58}
$$

$$
\begin{aligned}
&-M(1-x_{d,n,c}) \le CE_{c,d,\tau} + E^C_{c,d,\tau} - CE_{c,n,\tau} \le M(1-x_{d,n,c}),\\
&\forall d, n \in N\backslash\left\{\phi_c^0, \phi_c^1, d\right\}, c \in C^L, \tau
\end{aligned} \tag{4.59}
$$

$$
-M(1-x_{\phi_c^0,n,c}) \le E^C_{c,\phi_c^0,\tau} - CE_{c,n,\tau} \le M(1-x_{\phi_c^0,n,c}), \forall n \in N\backslash\left\{\phi_c^0\right\}, c \in C^L, \tau \tag{4.60}
$$

Constraint (4.55) states that the total resources that the crews obtain from depot d must be less or equal to the amount of available resources in the depot. The amount of resources that a crew can carry must be limited by the crew's capacity, which is realized by constraint (4.56). Constraint (4.57) indicates that the crews must have enough resources to repair the damaged components. Constraint (4.58) ensures that if a crew travels from m to n, then the resources that the crew has when arriving at location n is $CE_{c,n,\tau} = CE_{c,m,\tau} - \mathcal{R}_{m,\tau}$. If a crew goes to depot d to pick up supplies and travels to damaged component n, then $CE_{c,n,\tau} = CE_{c,d,\tau} + E^C_{c,d,\tau}$, which is enforced by (4.59). Constraint (4.60) ensures that the number of resources that the crew has at the first damaged component is equal to the resources obtained at the starting location.

4.2.6 Connecting Routing and System Operation

Constraints (4.61)–(4.64) are used to connect the crew scheduling and power operation problems.

$$
\sum_{\forall t} f_{m,t} = 1\ ,\ \forall m \in \Omega_{DL} \tag{4.61}
$$

$$
\sum_{\forall t} t f_{m,t} \ge \sum_{\forall c}(\alpha_{m,c} + ET_{m,c}\sum_{\forall n \in N} x_{m,n,c}), \forall m \in \Omega_{DL} \tag{4.62}
$$

$$
0 \le \alpha_{m,c} \le M\sum_{n \in N} x_{n,m,c},\ \forall m \in N\backslash\left\{\phi_c^0, \phi_c^1\right\}, c \tag{4.63}
$$

$$
u_{m,t} = \sum_{\bar{t}=1}^{t} f_{m,\bar{t}}\ ,\ \forall m \in \Omega_{DL}, t \tag{4.64}
$$

$$
\{f, x, u, y, \mathcal{X}, \gamma\} \in \{0,1\}, \{CE, E^C\} \ge 0 \tag{4.65}
$$

Let $f_{m,t}$ denote the time when the damaged component is repaired by the line crews, which equals 1 in one time interval as enforced by (4.61). Equation (4.62) determines the time when a

damaged component is repaired by setting $\sum_{\forall t} tf_{m,t}$ to be greater than or equal to $\alpha_{m,c} + ET_{m,c}$ for the crew assigned to damaged component m. Constraint (4.63) is used to set $\alpha_{m,c} = 0$ if crew c does not travel to component m, so it would not affect constraint (4.62). Fig. 4.8 demonstrates the time sequence of the repair process and how to find the time when the component is repaired.

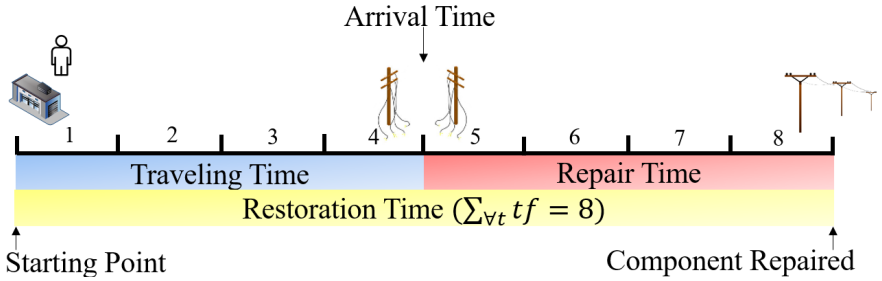

Figure 4.8 Time sequence of the repair process.

Starting from the depot, if both travel time and repair time are 4 hours, the restoration time is $\sum_{\forall t} t\ f_{m,t} = 8$. Finally, constraint (4.64) indicates that the restored component becomes available after it is repaired, and remains available in all subsequent periods. For example, if a component is repaired at $t = 3$, then $f_{m,t} = [0, 0, 1, 0, 0, 0]$ and $u_{m,t} = [0, 0, 1, 1, 1, 1]$.

4.2.7 Big M

The value used for M depends on the constraint. An inappropriately large M may increase the computation time, and a small value may introduce infeasibility. In constraint (4.11) and (4.12), the maximum and minimum values for the voltage are 1.05 and 0.95 per unit. Hence, the largest possible difference between any two squared voltages $(U_{j,\varphi,t} - U_{i,\varphi,t})$ is 0.4 per unit. Accordingly, the minimum value of M in (4.11) and (4.12) is 0.4 per unit, and the same value can be used in (4.25). For the big M value in (4.41), the maximum virtual flow is equal to the number of buses, thus, M is equal to $|\Omega_B|$.

In the routing constraints, the crews must arrive at the damaged components before starting the repairs. For example, if the time horizon is $T = 10$, and the repair time for some damaged component m is $ET_m = 1$, then the crew should arrive at $\alpha_{m,c,s} = 9$ at the latest in order to repair the component. Note that the time horizon should be chosen such that all damaged components

can be repaired in the optimization problem. Therefore, the minimum value of M in (4.63) equals the time horizon minus the minimum repair time. The minimum repair time is used to obtain the largest difference between T and the repair times of the components. Denote the value of M in (4.63) as M_{27}. For (4.53), the value of M should be larger than the time horizon T. In a worst-case scenario, the arrival time of crew c at damaged component m is $\alpha_{m,c} = M_{27}$, and the crew does not repair damaged component n, as per equation (4.63), $\alpha_{n,c} = 0$. Consequently, (4.53) is translated to $M_{27} + ET_{m,c} + tr_{m,n} - 0 \leq M$. Hence, the minimum value of M in (4.53) equals M_{27} plus the maximum repair and travel times. The value of M in (4.58)-(4.60) can be set to equal two times the capacity of the crews, as the crews cannot carry more than their defined capacity.

4.3 Solution Algorithms

DSRRP combines two problems, the Vehicle Routing Problem for routing the crews [115], and distribution system operation for outage restoration. VRP is an NP-hard combinatorial optimization problem, where the computation time rises exponentially with the size of the problem. Adding distribution system operation constraints will further increase the complexity. A three-stage algorithm for solving the combined routing and distribution system operation problem is presented in this section, where the stages are: assignment, initial solution, and neighborhood search. The three-stage algorithm is referred to as the Reoptimization Algorithm. Furthermore, to compare the developed method with current practices, a priority-based method that mimics the utilities' scheduling procedures is developed, and the cluster-first method proposed in [71] is presented.

4.3.1 Priority-Based Routing

In general, utilities schedule the repairs using a defined restoration priority list. To compare the proposed approach to current practices, a priority-based method is developed to replicate the procedure that the utilities follow. Each utility has its own priority list but it can be generally summarized as follows [116]:

1. Repair lines connected to high-priority customers.

2. Repair 3-phase lines starting with upstream lines
3. Repair single phase lines and individual customers

Define L_r as the set of lines to repair with priority r, and W_r is a weighting factor, where $W_1 > W_2 > W_3$ (e.g., $W_1 = 10, W_2 = 5, W_3 = 1$). L_1 contains the lines that must be repaired to restore critical customers, which can be found by solving the following problem:

$$\min\{\sum_{k\in\Omega_{DL}} u_k | \text{s.t. } (4.2)\text{-}(4.12), (4.28)\text{-}(4.47), y_i = 1, \forall i \in \Omega_{HP}\} \tag{4.66}$$

Problem (4.66) finds the minimum number of lines required to repair, so that all high-priority loads are restored. L_2 represents the 3-phase lines not in L_1, and L_3 represents the rest of the lines. The following routing model is solved to find the repair schedule by utilizing the priority of each line, as follows:

$$x^r = \arg\min\{\sum_{\forall r}\sum_{\forall k\in L_r}\sum_{\forall c\in C^L} W_r \alpha_{c,k} | \text{s.t.} (4.48)\text{-}(4.64)\} \tag{4.67}$$

The objective of (4.67) is to minimize the arrival time of the line crews at each damaged components, while prioritizing the high-priority lines through multiplying the arrival time by the weight W_r. The priority-based model is similar to DSRRP, but without the power operation constraints. However, it is still difficult to solve directly in a short time using a commercial solver such as CPLEX. Therefore, the same procedure presented in Algorithm 2 is used to solve (4.67). After obtaining the route x^r, the DSRRP problem is solved by setting $x = x^r$; i.e., we solve $\min\{(4.1) | \text{ s.t. } (4.2)\text{-}(4.12), (4.28)\text{-}(4.47), (4.53)\text{-}(4.64), x_{m,n,c} = x^r_{m,n,c}, \forall c, m, n\}$.

4.3.2 Cluster-Based Routing

To reduce the computation complexity of the co-optimization problem, we propose a clustering method to assign damaged components to depots [71]. The damaged components are clustered into CS clusters, which is determined by the number of depots. By performing the pre-routing clustering, the routing problem is decomposed from a single large VRP problem to CS small VRP problems. After damages are clustered, the information is sent to the second stage to solve the

DSRRP. The clustering problem is formulated as an integer linear program. The input data of the optimization problem includes distances between depots and damaged components $D_{d,m}$, resources available at depots $E^D_{d,\tau}$ and resources required to fix the damage $\mathcal{R}_{m,\tau}$. A binary variable $cs_{d,m}$ is used to decide which cluster/depot a component m is assigned to.

$$cs_{d,m} = \begin{cases} 1\ , m \textit{ is clustered to } w \\ 0\ , \qquad o.w. \end{cases} \qquad \forall d, m \tag{4.68}$$

If the depot does not have enough resources, the damaged component is clustered to the next closest depot. The clustering problem is modeled as follows:

$$\min \sum_{\forall d} \sum_{\forall m} D_{d,m}\ cs_{d,m} \tag{4.69}$$

$$\sum_{\forall d} cs_{d,m} = 1\ ,\ \forall m \tag{4.70}$$

$$E^D_{d,\tau} \geq \sum_{\forall m} \mathcal{R}_{m,\tau}\ cs_{d,m}\ ,\ \forall d, r \tag{4.71}$$

$$cs_{w,m} \in \{0,1\}\ ,\ \forall w, m \tag{4.72}$$

The objective (4.69) is to assign the damaged components to their closest depots. Constraint (4.70) ensures that a damaged component is assigned to a single depot. The assignment is performed while considering the resource availability constraint in (4.71). The resource constraint ensures that depots have enough resources to handle the assigned damaged components. After assigning the damaged components to different depots, DSRRP is solved with the crews dispatched based on the clusters. Define $C^L(d)$ and $C^T(d)$ as the set of line and tree crews located at depot d, respectively. Therefore, the cluster-based model can be formulated as follows.

$$\begin{aligned} &\min\{(3.1)|\text{ s.t. } (4.2)\text{-}(4.12), (4.28)\text{-}(4.47), (4.53)\text{-}(4.64) \\ &\sum_{\forall c \in C^L(w)} \sum_{\forall m \in N \setminus \{n\}} x_{m,n,c} = 1, \forall n \in \Omega_{DL}, \\ &\sum_{\forall c \in C^T(w)} \sum_{\forall m \in N \setminus \{n\}} x_{m,n,c} = 1, \forall n \in \Omega_{DT}\} \end{aligned} \tag{4.73}$$

4.3.3 Reoptimization Algorithm

The tri-stage Reoptimization algorithm starts by solving an assignment problem, where the crews are assigned to the damaged components based on the expected working hours, distances between the crews and the outage locations, and the capacity of the crews. In the second stage, the DSRRP is solved with the crews dispatched to the assigned components from the first stage. In the third stage, a neighborhood search approach [101] is used to iteratively improve the routing decisions obtained from stage two. The algorithm is described in the following subsections.

4.3.3.1 Assignment-Based Routing

By assigning the damaged components to the crews, the large VRP problem can be converted to multiple small-size Traveling Salesman Problems [115]. The assignment problem is formulated as follows:

$$\min \mathcal{L}^L + \mathcal{L}^T + \sum_{\forall c} \sum_{\forall d} \mathcal{P}_{c,d} + \bar{tr} \tag{4.74}$$

$$\mathcal{L}^L \geq \sum_{\forall m} A^L_{m,c} ET_{m,c}, \forall c \in C^L \tag{4.75}$$

$$\mathcal{L}^T \geq \sum_{\forall m} A^T_{m,c} ET_{m,c}, \forall c \in C^T \tag{4.76}$$

$$\sum_{\forall c \in C^L} A^L_{m,c} = 1, \forall m \in \Omega_{DL} \tag{4.77}$$

$$\sum_{\forall c \in C^T} A^T_{m,c} = 1, \forall m \in \Omega_{DT} \tag{4.78}$$

$$\sum_{\forall \tau} Cap^R_\tau E^C_{c,d,\tau} \leq (\delta_{d,c} + z_{d,c}) Cap^C_c, \forall d, c \in C^L \tag{4.79}$$

$$z_{d,c} \leq \delta_{d,c}, \forall d, m, c \in C^L \tag{4.80}$$

$$\mathcal{P}_{c,d} \geq A^L_{m,c} tr_{d,m} - M(1 - z_{d,c}), \forall d, m, c \in C^L \tag{4.81}$$

$$\sum_{\forall c \in C^L} E^C_{c,d,\tau} \leq E^D_{d,\tau}, \forall d, \tau \tag{4.82}$$

$$\sum_{\forall w} E^C_{c,d,\tau} \geq \sum_{\forall m} A^L_{m,c} \mathcal{R}_{m,\tau}, \forall c \in C^L, \tau \tag{4.83}$$

$$\bar{tr} \geq tr_{m,n}(A^L_{m,c} + A^L_{n,c} - 1), \forall m, n, c \in C^L \tag{4.84}$$

$$\bar{tr} \geq tr_{d,m}(\delta_{d,c} + A^L_{m,c} - 1), \forall d, m, c \in C^L \tag{4.85}$$

$$\bar{tr} \geq tr_{m,n}(A^T_{m,c} + A^T_{n,c} - 1), \forall m, n, c \in C^T \tag{4.86}$$

$$\bar{tr} \geq tr_{d,m}(\delta_{d,c} + A^T_{m,c} - 1), \forall d, m, c \in C^T \tag{4.87}$$

$$\{A^{L/T}, z\} \in \{0, 1\}, \{\mathcal{P}, E^C\} \geq 0 \tag{4.88}$$

The objective (4.74) consists of four parts. The first two terms minimize the expected time of the last repair for the line crews ($\mathcal{L}^L$) and tree crews ($\mathcal{L}^T$). The variables $\mathcal{L}^L$ and $\mathcal{L}^T$ are defined in constraints (4.75) and (4.76), respectively. The third term in (4.74) is a penalty cost used to limit the number of times a crew goes back to the depot to pick up additional resources. The fourth term $\bar{tr}$ is the maximum travel time for the crews. Constraints (4.77)-(4.78) assign each damaged component to one crew. The amount of resources a crew can carry is limited by the crew's capacity in (4.79). Binary variable $z_{d,c}$ is equal to 1 if a crew requires additional resources. In such case, the crew goes back to the depot to pick up the required resources. Constraint (4.80) states that the crews can go back to the depot they started from. We set the penalty term $\mathcal{P}_{d,c}$ to be equal to the maximum travel time between the depot and the assigned damage components, as defined in (4.81). The big M constant is added so that the penalty term equals 0 if the crew does not go back to the depot for additional resources. The crews must use the resources available in the depot as enforced by (4.82). Constraint (4.83) indicates that the number of resources crew c has should be enough to repair the assigned damaged components. Constraints (4.84)-(4.87) are used to identify the maximum travel time between the damaged components that are assigned to each crew. If components m and n are assigned to crew c, then $\bar{tr} \geq tr_{m,n}$.

4.3.3.2 Large Neighborhood Search

After assigning each damaged component to a crew, DSRRP is solved with the crews dispatched to the assigned components. Subsequently, a neighborhood search method is used to improve the initial route. The optimization problem considered in this study involves a dynamically changing environment due to the uncertainty of the repair time, solar irradiance, and demand. The repair

time is updated periodically either by the repair crews or the damage assessors. Therefore, we apply the neighborhood search algorithm continuously and update the routing solution as more information is obtained. The advantage of this method is that it allows the algorithm to update the solution while the repair crews are repairing the lines, therefore, loosening the time limit restriction. The pseudo-code for the proposed algorithm (Reoptimization algorithm) is detailed in Algorithm 2.

Algorithm 2 Reoptimization Algorithm for DSRRP

Obtain the location of the outages from the damage assessors.
solve using **CPLEX** {Assignment}
$(A^L, A^T) = \arg\min\{(4.74)|\text{s.t. } (4.75)\text{-}(4.88)\}$
for all $c \in C^L$ **do**
  $N(c) = \{m|\forall m \in \Omega_{DL}, A^L_{m,c} = 1\} \cup \Omega_P$
end for
for all $c \in C^T$ **do**
  $N(c) = \{m|\forall m \in \Omega_{DT}, A^T_{m,c} = 1\} \cup \Omega_P$
end for
solve using **CPLEX** (time limit = 300 s) {Assignment-DSRRP}
$\zeta^* = \min\{(4.1)|\text{s.t. } (4.2)\text{-}(4.12), (4.25)\text{-}(4.64), \sum_{n\in N(c)} x_{m,n,c} = 1, \forall c, m \in N(c)\}$
obtain solution x^* and objective ζ^*
let $\bar{x} = x^*$ and $\bar{\zeta} = \zeta^*$
repeat
  set $count = 0$
  set $ss = ss_0$ {sample size}
  while time limit is not surpassed **do** {Neighborhood Search}
    let $\bar{N} = sample(N, ss)$, where $\bar{N} \subset N$ and $|\bar{N}| = ss$.
    solve using **CPLEX** (time limit = 120 s) with *warm start*
    $\zeta^* = \min\{(4.1)|\text{s.t. } (4.2)\text{-}(4.12), (4.25)\text{-}(4.64), x_{m,n,c} = \bar{x}_{m,n,c}, \forall c,\ m \in N\backslash\bar{N}, n \in N\backslash\bar{N}\}$
    obtain x^* and objective ζ^*
    if $\zeta^* < \bar{\zeta}$ **then**
      set $\bar{x} = x^*; \bar{\zeta} = \zeta^*; count = 0$
    else
      $count = count + 1$
    end if
    if $ss = |N|$ **then break** {solution is optimal}
    if $count = h_1$ **then** $ss = ss + 1$
    if $count = h_1 + h_2$ **then break**
  end while
  dispatch crews and set the traveled path as constant
  update the repair time and return to Step 11
until all lines are repaired

In Step 1, the assignment problem is solved using CPLEX [117] to obtain the binary variables $A^L_{m,c}$ and $A^T_{m,c}$. These variables are used to find $N(c)$, which is the set of damaged components assigned

to crew c. For example, consider the set of damaged components $\Omega_{DL} = \{1, 2, 3, 4, 5\}$, if line crew 1 is assigned with damaged components 1 and 3, then $A^L_{m,c} = \{1, 0, 1, 0, 0\}$ and $N(1) = \{1, 3\} \cup \Omega_P$. $N(c)$ is found for each crew in Steps 2-7. Consequently, a simplified DSRRP is solved in Step 8 by allowing the crews to only repair the assigned damaged components. In Step 10, the obtained route x^* and objective ζ^* are set to be the incumbent (current best solutions) route ($\bar{x}$) and objective ($\bar{\zeta}$). Steps 11-29 represent the neighborhood search algorithm. The algorithm selects a subset of damaged components $\bar{N}$, where $\bar{N} \subset N$, then removes the paths connected to $\bar{N}$ and sets the rest of the routes to be constant by forcing $x_{m,n,c} = \bar{x}_{m,n,c}, \forall c,\ m \in N \backslash \bar{N}, n \in N \backslash \bar{N}$. Afterwards, DSRRP is solved to obtain an improved solution, the process is demonstrated in Fig. 4.9, where $|\bar{N}| = 3$.

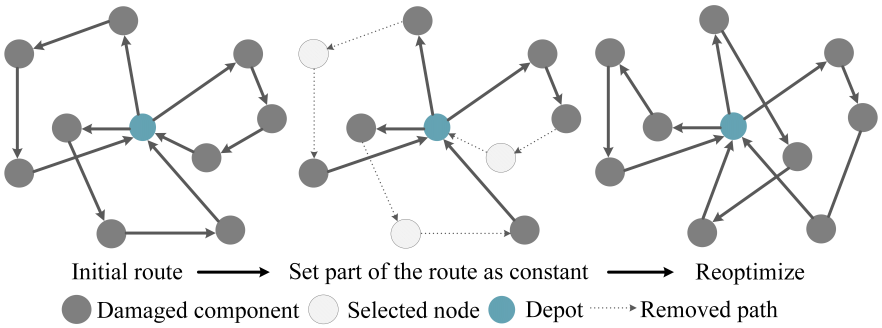

Figure 4.9 A single iteration of the neighborhood search, with $|\bar{N}| = 3$.

Steps 12 and 13 initialize a counter and the sample size (ss), respectively. In Step 15, the subset $\bar{N}$ is determined by randomly selecting ss nodes from N. The parameters ss_0, h_1, and h_2 are constants used to tune the algorithm. The value of ss_0 determines the size of the subset $\bar{N}$ in the first iteration. The size of $\bar{N}$ is increased after h_1 iterations with no change to the objective, and the neighborhood search algorithm is terminated after $h_1 + h_2$ iterations with no change to the objective. In this study, ss_0 is set to be 3, as selecting 1 damaged component will not change the route, and selecting 2 has minimal impact on the route. The values of h_1 and h_2 were determined experimentally using several test cases, both h_1 and h_2 equal 3. The DSRRP is solved in Step 16 with parts of the route set as constant. To obtain a fast solution, we warm start (provide a starting

point) CPLEX by using the incumbent solution and enforce a time limit of 120 seconds for each iteration. The objective value ζ^* obtained from Step 16 is compared to the current incumbent solution $\bar{\zeta}$. If the value is improved, we set ζ^* and x^* as the current incumbent solutions and update the counter, otherwise, the counter increases by one. The process is repeated until the counter reaches h_1, where we increase the size of the subset in Step 24. If the sample size is $|N|$; i.e., the complete problem is solved without simplification, then the solution is optimal and the neighborhood search stops. Also, the search ends once the counter reaches $h_1 + h_2$, or if the time limit is reached. The crews are then dispatched to the damaged components, and the traveled paths are set as constants in the optimization problem. After that, the repair time is updated and Steps 14-26 are repeated to update the route, as shown in Fig. 4.10. The idea of the dynamic approach is to run Steps 14-26 while maintaining the best solution in an adaptive memory. Once the operator receives an update from the field, the neighborhood search is restarted with the newly acquired information. Whenever a crew finishes repairing the assigned damaged component, the crew is provided with the current best route $\bar{x}$. A flowchart for the proposed algorithm is presented in Fig. 4.11.

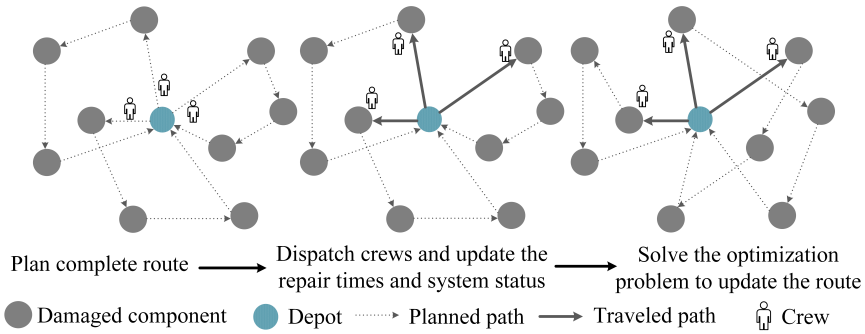

Figure 4.10 Dynamic vehicle routing problem.

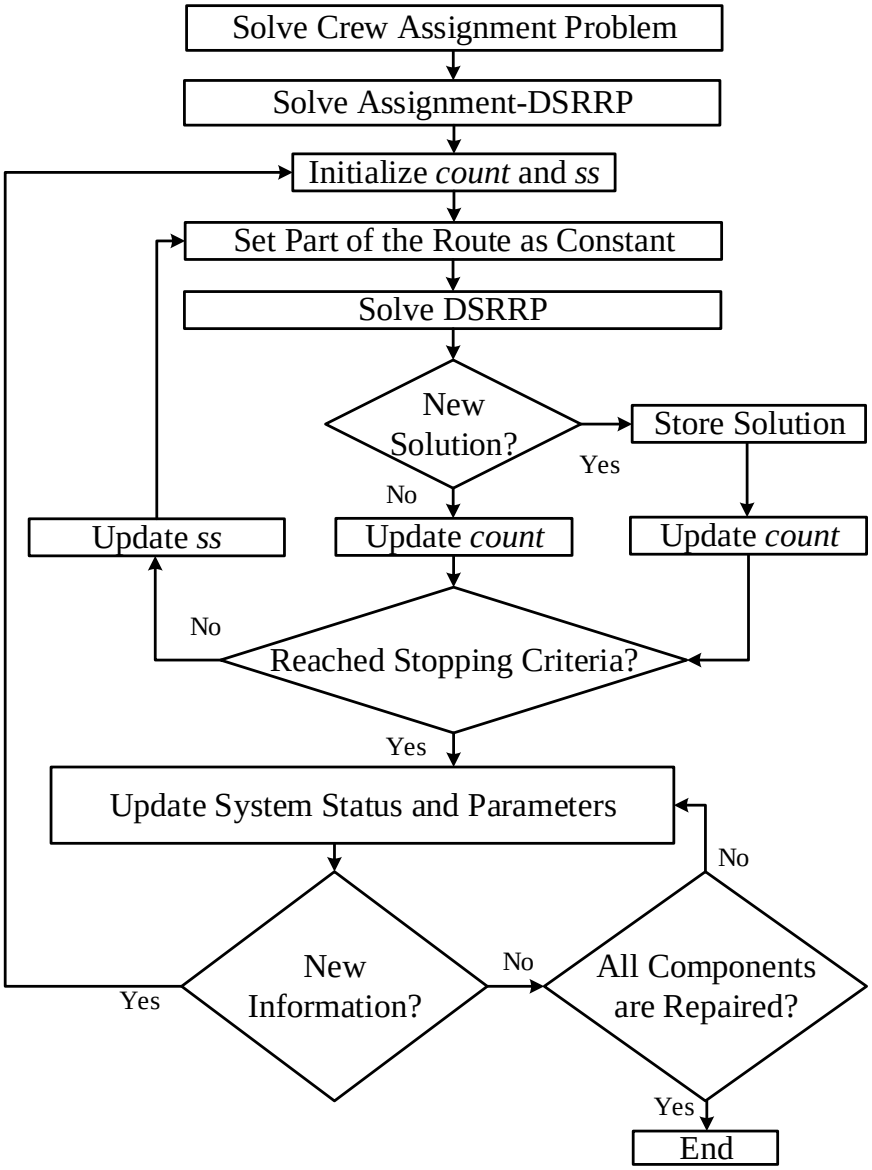

Figure 4.11 Flowchart of the Reoptimization algorithm.

4.4 Simulation and Results

4.4.1 Test Case: IEEE-123 distribution feeder

The modified IEEE 123-bus distribution feeder is used as a test case for the DSRRP problem. Detailed information on the network can be found in [93]. Since transportation networks data for the IEEE 123-bus test case is not available, the network G and the travel times are simulated by using the Euclidean distance [12]. The average speed of the crews is assumed to be 35 mph in the simulated problem. The travel time is calculated by dividing the Euclidean distances between all nodes by the speed of the crews. We then scale the travel time such that the travel time between the two furthest locations equals 2 hours. The x-coordinates and y-coordinates for the IEEE 123-bus test cases can be found in [93]. We assume that there is an available path to each damaged component. The network, shown in Fig. 4.12, is modified by including 4 dispatchable DGs, 18 new switches, 5 PVs and 2 BESSs. The 4 DGs are rated at 300 kW and 250 kVAr. PVs in On-grid and hybrid systems are rated at 50 kW, and the PV at bus 62 is rated at 900 kW. The forecasted solar irradiance used in the simulation is presented in Fig. 4.13, which is obtained from the National Solar Radiation Data Base (NSRDB) [118]. The data in Fig. 4.13 represent the solar irradiance at a location impacted by Hurricane Matthew.

The BESSs at bus 2 and 62 are rated at 50 kW/132 kWh and 500 kW/ 2100 kWh, respectively. Fig. 4.14 shows the load shedding costs of each load. The problems of optimally allocating the resources, DGs, or switches, are out of the scope of this study. We assume there are 3 depots, 6 line crews distributed equally between the depots, and 4 tree crews with 2 located in Depot 2 and 1 tree crew in each of the other depots. The time step in the simulation is 1 hour. The simulated problem is modeled in AMPL and solved using CPLEX 12.6.0.0 on a PC with Intel Core i7-4790 3.6 GHz CPU and 16 GB RAM.

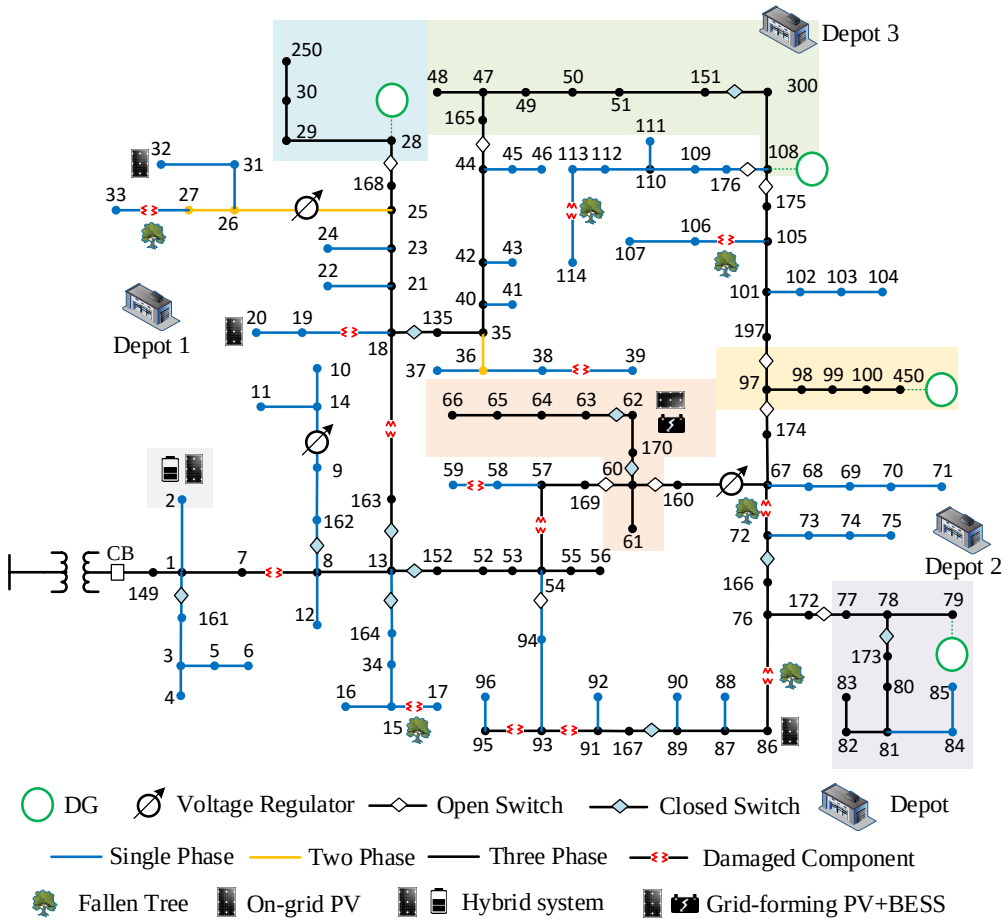

Figure 4.12 Initial state of the distribution network after 14 lines are damaged.

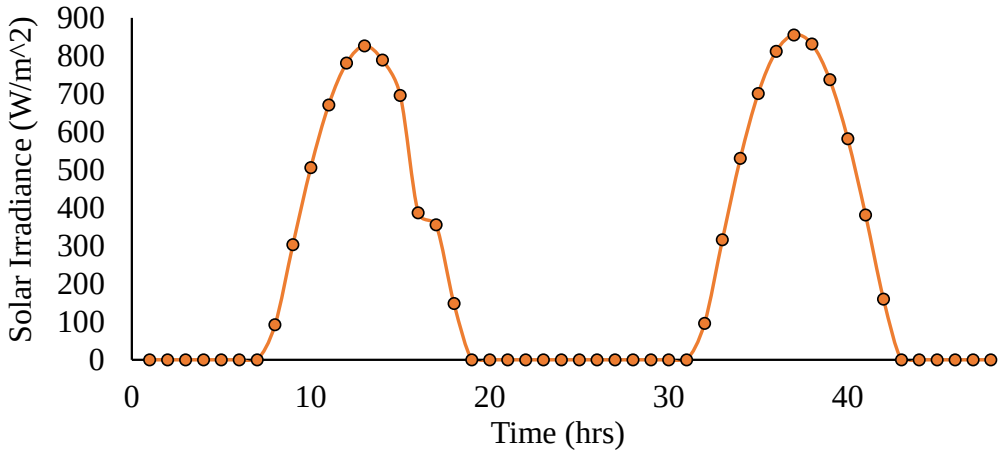

Figure 4.13 Solar irradiance for the PV systems in the simulation.

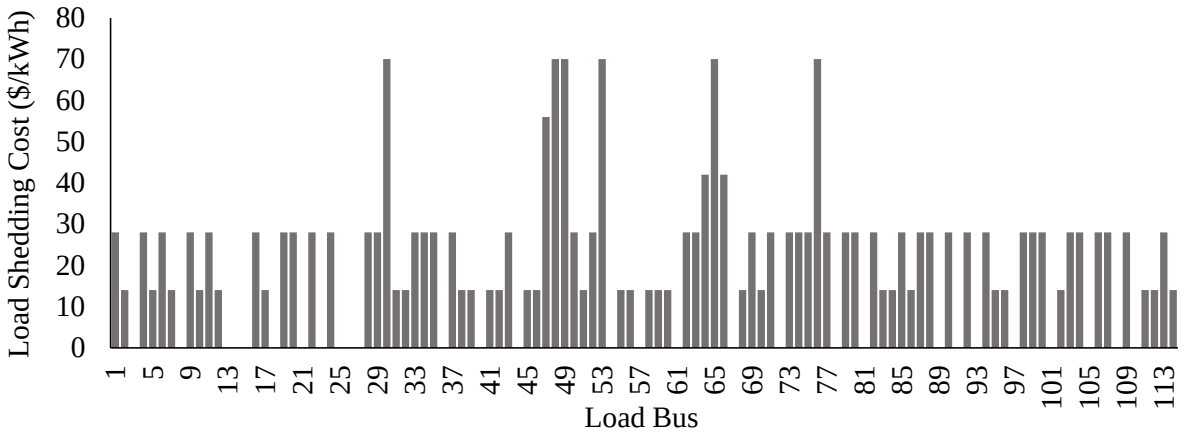

Figure 4.14 The load shedding cost in $/kWh of each load in the simulation.

4.4.2 Solution Comparison

The repair and restoration problem is solved using five methods: 1) a cluster-first DSRRP-second (C-DSRRP) approach presented in [71], the method clusters the damaged components to the depot, then solves DSRRP; 2) priority-based method; 3) an assignment-based method where the damaged components are assigned to the crews, then DSRRP is solved (A-DSRRP), which is similar to Steps 1-8 in Algorithm 1; 4) Reoptimization algorithm; 5) CPLEX with warm start using the Reoptimization algorithm solution. Once an outage occurs, the distribution network is reconfigured, and the DGs are dispatched to restore as many customers as possible, before conducting the repairs. A random event is generated on the IEEE 123-bus system, where 14 lines are damaged, four of which are damaged by trees. Fig. 4.12 shows the recovery operation of the distribution system to the outages before the repairs; i.e., the state of the system at time $t = 0$. The solution shown in Fig. 4.12 is obtained regardless of the solution algorithm used, as the algorithms will only affect the repair schedule and the network operation during the repairs.

Before the outage, all switches are closed except 151-300 and 54-94. Since line 7-8 is damaged, the circuit breaker at the substation is opened. Sectionalizer 28-168 is switched off, forming a small microgrid, to serve the loads at buses 28 to 30. Similarly, switches 44-165, 77-172, 97-174, 97-197, 108-175 and 108-176 are opened and 151-300 is closed to form additional microgrids using the DGs

in the network. Switches 60-160 and 60-169 are opened so that the PV+BESS at bus 62 can form a microgrid. The battery at bus 2 can serve the local load in the first few hours after the damage. The repair/tree-clearing times and required resources are given in Table 4.2. The estimated repair time is assumed to be accurate. It is assumed that each crew can carry 30 units of resources, and the required capacities (Cap_r^R) for the 5 types of resources are {5, 4, 3, 2, 1}. A summary of the results and performances of different solution methods is shown in Table 4.3. The time limit is set to be 3600 seconds for all methods except for the last one (CPLEX with a warm start) in order to find the optimal solution.

Table 4.2 The resources and time required to repair the damaged components

Line	Resources (units)					Repair/Clearing Time (hrs)	
	Type 1	Type 2	Type 3	Type 4	Type 5	Line Crew	Tree Crew
7–8	2	0	0	0	1	2.5	
15–17	0	2	0	1	1	1.25	1
18–19	0	2	0	1	1	0.5	
27–33	0	2	0	1	1	2.25	
38–39	0	2	0	1	1	1	0.75
54–57	2	0	0	1	2	0.75	
58–59	0	2	0	1	1	0.5	
18–163	2	0	0	0	2	1.75	
67–72	1	0	0	0	1	4	1.25
76–86	1	0	1	0	3	6	2
91–93	2	0	0	1	2	1.5	
93–95	2	0	0	0	1	2.75	
105–106	0	2	0	1	1	1.75	1
113–114	0	2	0	1	1	0.75	0.5

Table 4.3 A comparison between four methods for the IEEE 123-bus system

Method	Objective Value	Optimality Gap	Comp. Time	Load Served	Restoration Time
C-DSRRP	$241,371	21.16%	3600 s	61.86 MWh	12 hrs
Priority-based	$229,112	15.01%	662 s	62.25 MWh	9 hrs
A-DSRRP	$211,597	6.21%	206 s	62.98 MWh	9 hrs
Reoptimization	$199,210	0.00%	694 s	63.5 MWh	9 hrs
CPLEX	$199,210	0.00%	4 hrs	63.5 MWh	9 hrs

The fifth column in Table 4.3 is the amount of energy served, and the sixth column (restoration time) is the time when all loads are restored. The assignment-based approach (A-DSRRP) is the fastest but the solution is not optimal, neighborhood search in the Reoptimization algorithm improved the routing solution and obtained the best repair schedule. The Reoptimization algorithm converged after 21 iterations, as shown in Fig. 4.15.

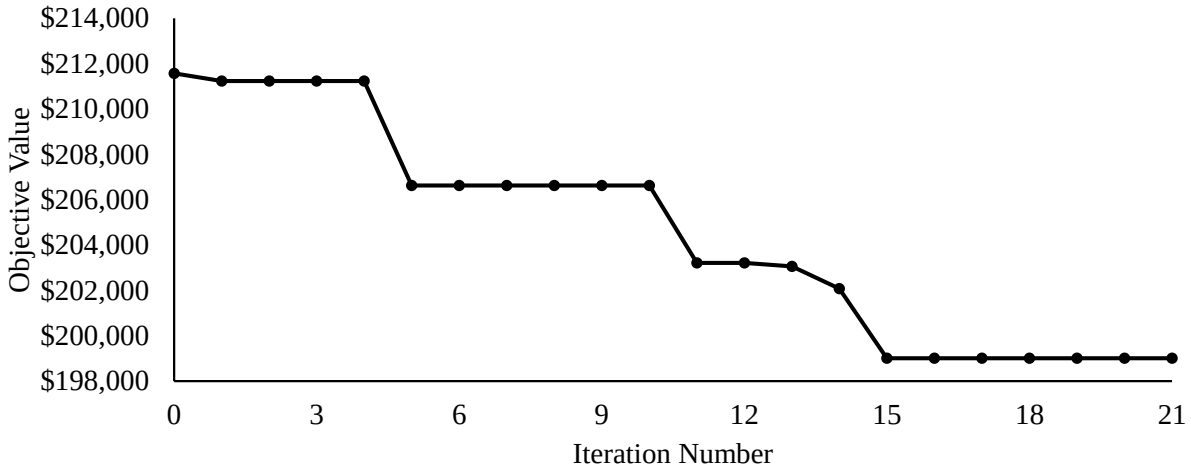

Figure 4.15 Convergence of the Reoptimization algorithm

To obtain the optimal solution, the route obtained from the proposed method is used to warm start CPLEX and solve DSRRP. CPLEX showed that the solution obtained from the Reoptimization algorithm is optimal. C-DSRRP reached the time limit but produced a feasible solution with 21.16% optimality gap, while the priority-based method achieved an objective value which is $29,902 higher

than the optimal solution. The change in percentage of load served for each method is shown in Fig. 4.16. The proposed algorithm outperformed the other methods.

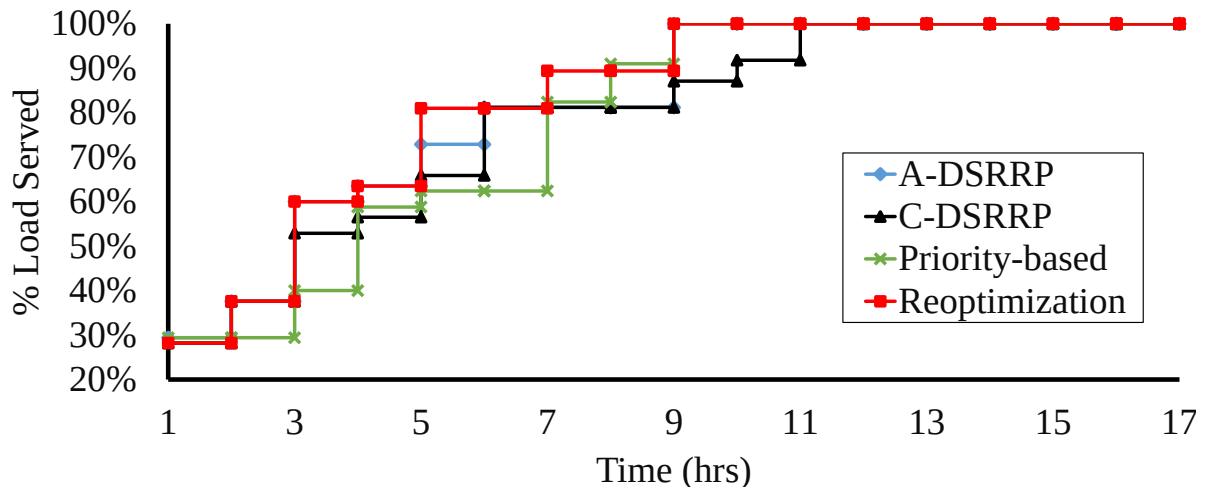

Figure 4.16 Percentage of load served at each time step

Next, we compare the Reoptimization algorithm with the priority-based method using three different damage scenarios on the IEEE 123-bus system. The simulation results are shown in Table 4.4. The proposed method outperforms the priority-based method in all instances with comparable computation times. The results indicates the importance of co-optimizing repair scheduling and the operation of the distribution system. For the first test case, the algorithm achieved the optimal solution, while the optimality gap for the priority-based method is 2.98%. The Reoptimization algorithm achieved solutions that are approximately 11% and 17% less than the priority-based method for the second and third test cases, respectively.

Table 4.4 Three test cases solved using the Reoptimization and priority-based methods

Test	Damage	Reoptimization			Priority-based		
		Obj.	% Gap	Comp. Time	Obj.	% Gap	Comp. Time
1	15 Lines	$158,023	0.00%	660 s	$162,734	2.98%	464 s
2	20 Lines	$248,986	2.53%	762 s	$279,197	14.97%	392 s
3	25 Lines	$388,760	2.27%	782 s	$467,278	22.93%	520 s

4.4.3 Dynamic Solution

In practice, the crew repair time is continuously changing. Moreover, the dispatch commands must be issued as fast as possible to reduce the outage duration. Therefore, the DSRRP must be solved efficiently and the solutions should be dynamically updated according to the current crew repair time. To simulate the change in repair time, it is assumed that once a crew reaches the damaged component, the repair time is updated to its actual value by adding a random number from the continuous uniform distribution on [-2,2] to the estimated time. For example, once crew 1 arrives at line 7-8, the repair time is changed from 2.5 to 3 hours. Similarly, the solar irradiance is updated by adding ±5% to the forecasted value. The time limit at Step 14 in Algorithm 1 is set to be 15 minutes after the first dispatch, so that the repair time is updated every 15 minutes. While the crews are repairing the damaged components, the neighborhood search algorithm keeps searching for a better solution, and the crews are dispatched using the incumbent solution. The complete route is given in Table 4.5.

Table 4.5 Routing solution for the dynamic 123-bus test case

Crew	Route
Crew 1	DP 1 → 7-8 → 15-17
Crew 2	DP 1 → 163-18 → 27-33 → DP 1 → 93-95
Crew 3	DP 2 → 54-57 → 18-19
Crew 4	DP 2 → 113-114 → DP 3 → 105-106 → DP 2 → 91-93
Crew 5	DP 3 → 38-39 → 67-72
Crew 6	DP 3 → 58-59 → 76-86
Crew 7	DP 1 → 27-33 → 15-17
Crew 8	DP 2 → 76-86
Crew 9	DP 2 → 67-72
Crew 10	DP 3 → 113-114 → 105-106

The total cost is $192,694, and the total energy served is 64.7 MWh. Table 4.6 shows the timeline of events after solving DSRRP, where all loads are restored after 8 hours. The initial states of the switches are shown in Fig. 4.12, and the subsequent switching operations are given in Table 4.6.

Table 4.6 Event timeline for the IEEE 123-bus dynamic test case

Time step	Switch operation		Repaired	% Load Served
	open	close		
1				29%
2				29%
3	18-135	44-165 108-176	38-39 163-18 58-59 113-114	39%
4	13-163 13-164	60-169 150-149	7-8 54-57	61%
5		13-164 97-197 108-175	15-17 27-33 105-106	73%
6	72-166	13-163 168-28 60-160 97-174	18-19 67-72	89%
7				89%
8		72-166 77-172	76-86 91-93 93-95	100%
9	151-300	18-135		100%

The 3-phase output of the DGs and the substation are shown in Fig. 4.17, and Fig. 4.18 shows the output of the PVs and BESSs. Crew 5 repairs line 38-39 and switch 18-135 is opened and 44-165 is closed to restore the loads at buses 35 to 46. Once line 113-114, is repaired by tree crew 10 and line crew 4, switch 108-174 is closed to restore the loads at buses 109 to 114. After repairing line 7-8 in time step 4, the CB is closed and the network starts to receive power from the substation. Switches 13-163 and 13-164 are opened to keep lines 15-17, 18-19, and 27-33 isolated. Loads at buses 52 to 59 are restored after repairing lines 54-57 and 58-59. 8 loads are restored after repairing lines 15-17 and 105-106. After 6 hours, the loads around depot 1 are restored after repairing line

18-19 and closing switch 13-163. Finally, all loads are restored after 8 hours once lines 76-86, 91-93, and 93-95 are repaired. Switch 151-300 is opened and 18-135 is closed to return the network to its original configuration, and the substation can serve all loads. Fig. 4.19 shows the distribution system status at different time points, where the shaded areas are energized. Once lines 76-86, 91-93, and 93-95 are repaired, the system returns to its normal condition.

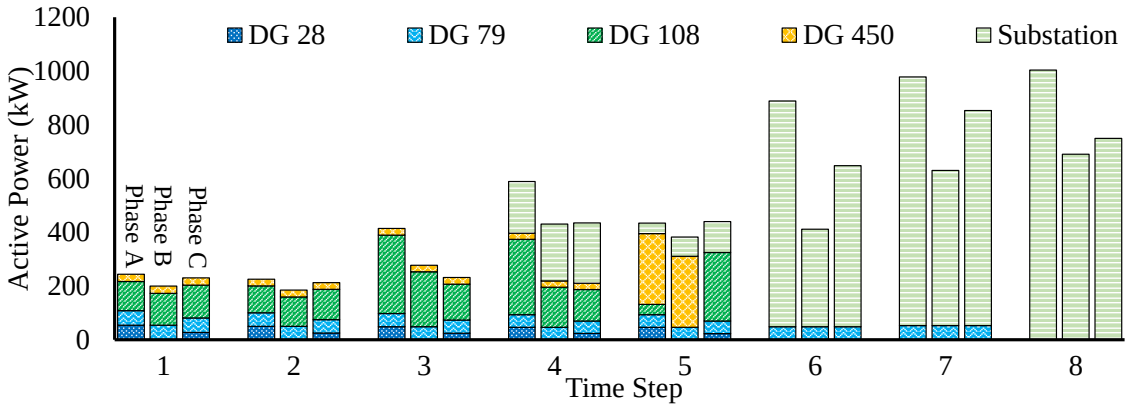

Figure 4.17 The 3-phase active power delivered by the DGs and substation.

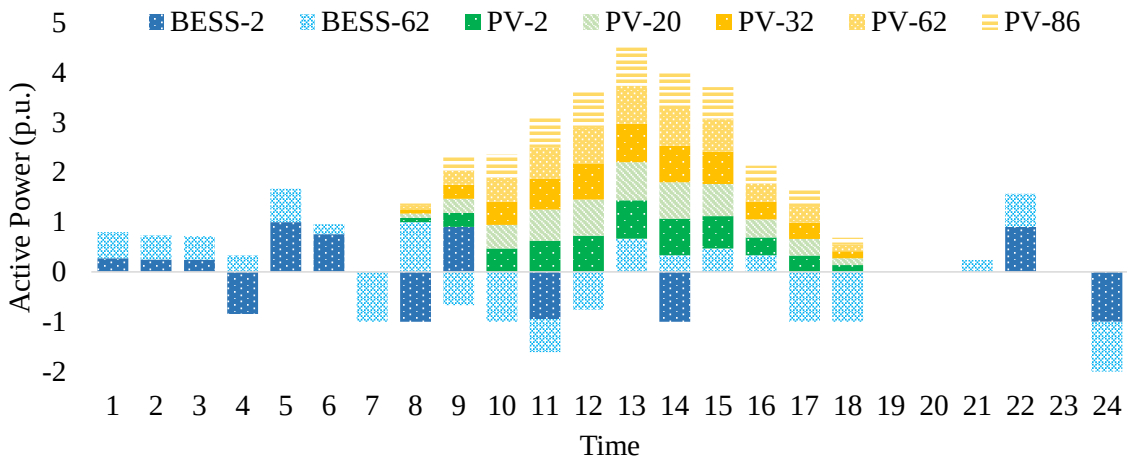

Figure 4.18 The active power delivered by the PVs and BESSs.

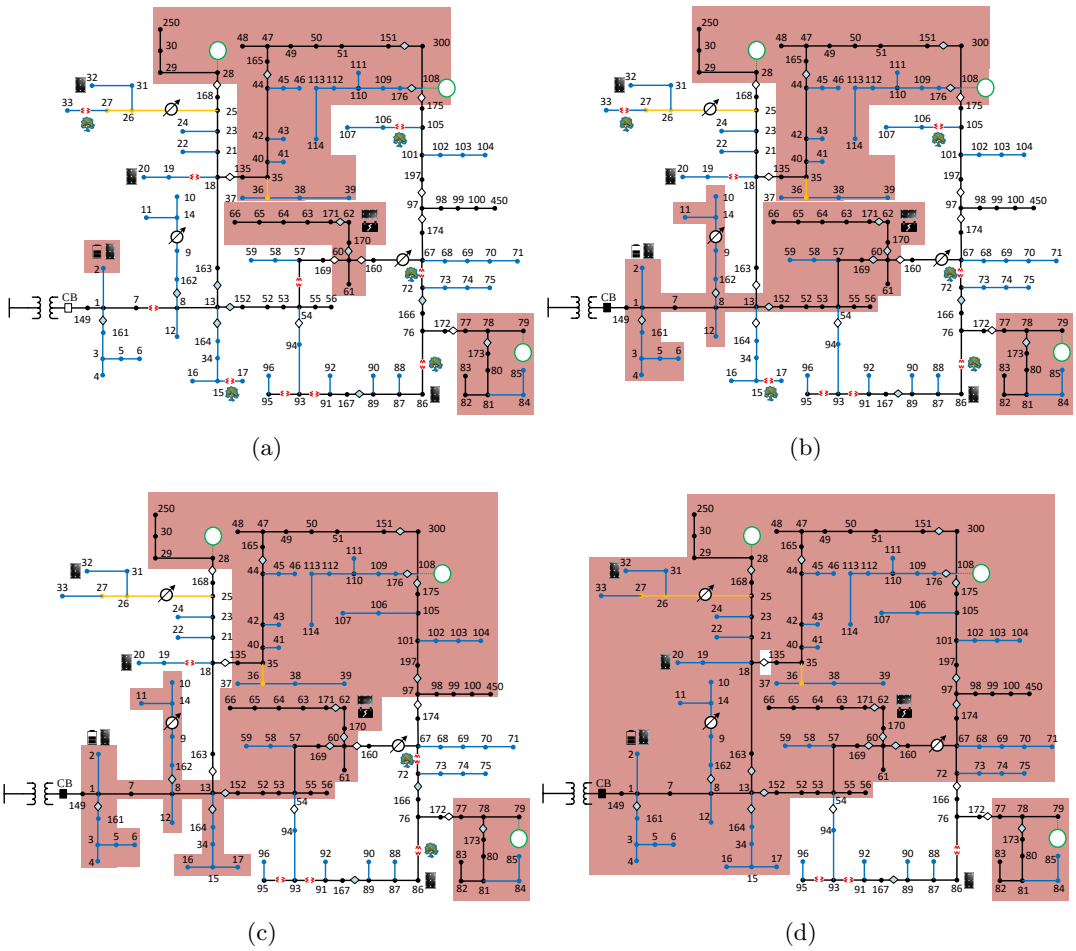

(a) (b) (c) (d)

Figure 4.19 The status of the IEEE 123-bus system after (a) 3 hours, (b) 4 hours, (c) 5 hours, and (d) 6 hours

4.4.4 Advantages of DGs and Switches

To show the importance of DGs and automatic switches, we vary the number of DGs and switches in the test case shown in Fig. 4.12, and solve the repair and restoration problem using the Reoptimization algorithm. Table 4.7 shows the results. As one would expect, the best performance is obtained with the highest number of DGs (11) and switches (23). However, having a large number of DGs is not beneficial without switches, as can be seen when the number of switches is decreased to 7, while maintaining 11 DGs. In this case, the total cost is increased by approximately 83%. The worst scenario is a low number of both DGs and switches. For example, with 7 switches and 0 DGs,

the total cost is more than 200% higher than the best-case scenario (with 11 DGs and 23 switches). This experiment supports previous work showing the importance of optimizing the number of DGs and switches [8].

Table 4.7 Objective value of DSRRP with varying numbers of DGs and switches

Number of DGs	Number of Switches		
	23	14	7
11	$ 199,210	$ 231,803	$ 363,989
4	$ 223,291	$ 289,435	$ 388,111
0	$ 345,175	$ 412,998	$ 421,692

4.4.5 Power Flow Validation

Equations (4.18)-(4.23) used in the DSRRP model can approximate the unbalanced power flow operation of three-phase unbalanced systems, however, the formulation introduces approximation errors. Therefore, we validate the unbalanced formulation by comparing the voltage magnitude that the formulation produces with the results from OpenDSS, which is an open-source software developed by the Electric Power Research Institute (EPRI). The IEEE 123 bus system is used in this section for validation. The voltage magnitude for the linear power flow results are compared with the OpenDSS results in the correlation plot in Fig. 4.20. The figure shows that the results are closely correlated. The maximum error is around 0.0076 p.u. and the average error is 0.0019 p.u. The error is mainly due to neglecting the losses in the linear formulation.

4.5 Summary

A new mathematical model that combines 3-phase unbalanced distribution system operation, fault isolation and restoration, PV and BESS systems operations, and resources coordination is developed in Section 4.2. The model included the coordination of line and tree crews as well as equipment pickup for conducting the repairs. Also, a new framework for modeling the connectivity of PV systems is designed. Furthermore, a three-stage algorithm is developed with a newly designed neighborhood search algorithm to iteratively improve the routing solution in Section 4.3. The

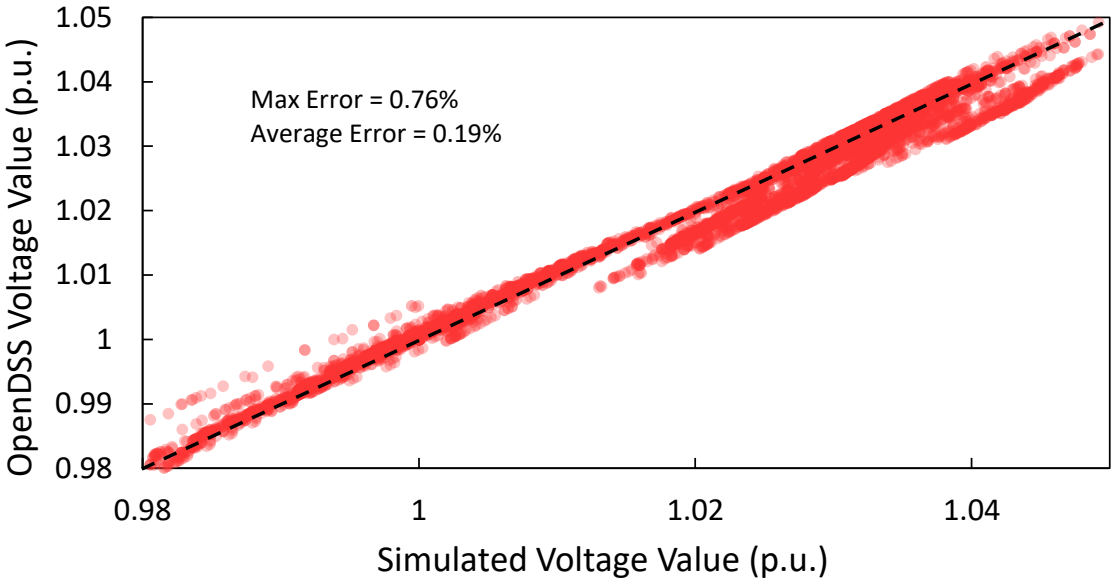

Figure 4.20 The 3-phase active power delivered by the DGs and substation.

developed approach is able to restart when the repair time is updated, and the crews are dispatched based on the incumbent solution. Test results have shown that the proposed algorithm can provide effective restoration plans within the time limit.

CHAPTER 5. DISTRIBUTION SYSTEM REPAIR AND RESTORATION USING STOCHASTIC PROGRAMMING

5.1 Overview

The aim of this chapter is to use stochastic programming to solve DSRRP. Scenario generation is discussed in Section 5.2, where we consider demand and solar irradiance uncertainties, and model the uncertainty of the repair time using a lognormal distribution. Section 5.3 proposes a two-stage stochastic mixed integer linear programming model to co-optimize distribution system operation and repair crew routing for outage restoration after extreme weather events. The first stage is to dispatch the repair crews to the damaged components. The second stage is distribution system restoration using distributed generators and reconfiguration. The stochastic DSRRP model is decomposed into two stages and solved using Progressive Hedging in Section 5.4. The proposed method is validated on modified 123-bus distribution test system in Section 5.5.

5.2 Scenario Generation

In this chapter, the uncertainties of repair time, load, and solar irradiance are represented by a finite set of discrete scenarios, which are obtained by sampling. The lognormal distribution is used to model the repair time, as recommended in [119]. The lognormal probability distribution density function is given as:

$$f(x;\mu,\sigma) = \frac{1}{x\sigma\sqrt{2\pi}} e^{-(ln\ x-\mu)^2/2\sigma^2} \tag{5.1}$$

where μ and σ are called the location parameter and the scale parameter, respectively. The lognormal distribution is a commonly used distribution for equipment and system maintainability analysis, and applies to many maintenance and repair tasks [120]. The clearing time for the tree crews is

assumed to follow a truncated normal distribution, with a minimum of 30 minutes, maximum of 3 hours, and a mean of 1 hour.

Load uncertainty is modeled in terms of load forecast error [121]. Define $P^F_{i,\varphi,t}$ as the load forecast for the load at bus i at time t, Fig. 5.1 shows an example of a 24-hour load profile. A load forecast error is generated independently for every hour. The forecast error at time t in scenario s is a realization of a truncated normal random variable $e_{t,s}$, so that the error is bounded using a fixed percentage (e.g., 15%). The active demand for the load at bus i and time t in scenario s is then obtained as follows:

$$P^D_{i,\varphi,t,s} = P^F_{i,\varphi,t}(1 + e_{t,s}) \tag{5.2}$$

where a similar equation is used to obtain the corresponding realization for reactive power. By bounding the error to ±15%, equation 5.2 states that the actual load is within 15% of the forecasted load. Fig. 5.2 shows an example of 30 generated scenarios for one load, where $P^F_{i,\varphi,t}$ is the load forecast, and $P^D_{i,\varphi,t,s}$ is the generated scenario.

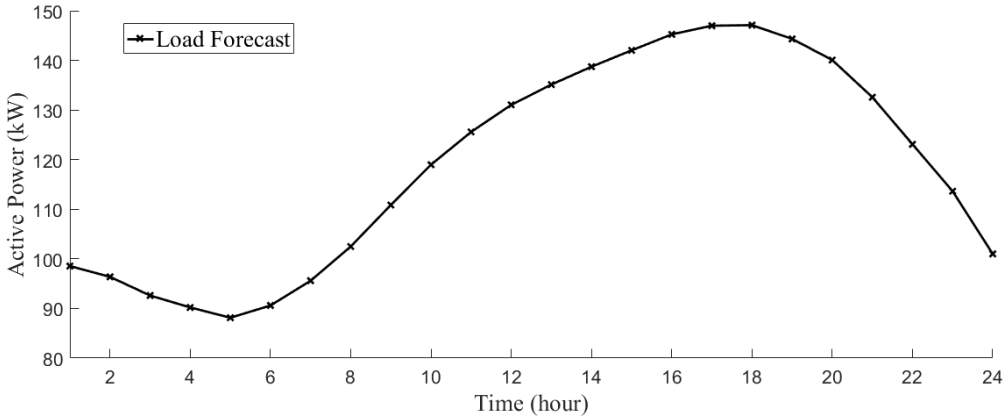

Figure 5.1 Forecast of active power consumption of a load.

In this sudy, the PVs are considered as non-dispatchable DGs. The power generated by PVs is dependent on the incident solar irradiance level, while the irradiance depends on the cloud coverage level (CCL). The sky condition can be divided into four categories: clear, partly clear, mostly cloudy, and overcast. It is assumed that the sky condition is clear after the extreme event in the test cases presented in this chapter. Monte Carlo simulation is used to generate a finite set of random

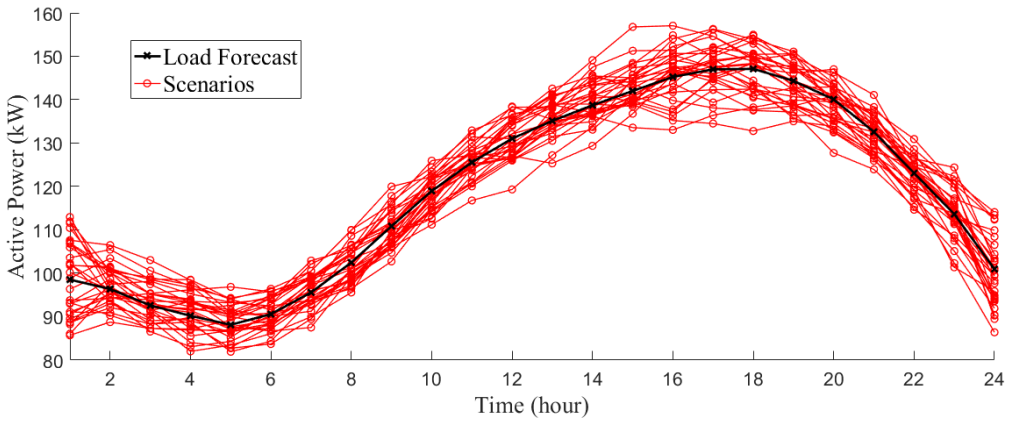

Figure 5.2 Generated scenarios of active power of a load.

scenarios representing the solar irradiance. This uncertainty is modeled through CCL in each time period. Therefore, the cloud coverage level can be represented as CCL(t,s), where t is the hour of the day and s is the scenario. The scenario generation procedure starts by randomly selecting a cloud-type according to the probabilities in Table 5.1 [122] for each scenario s. Then, CCL is determined as follows:

$$CCL(t,s) = U(CCL_{min}, CCL_{max}) \tag{5.3}$$

A random correction factor is used to the variability and forecast errors. The corrected CCL value is modeled using a normal distribution with mean $CCL(t,s)$ and standard deviation 0.05.

$$CCL_{corrected}(t,s) = max(0, \mathcal{N}(CCL(t,s), 0.05)) \tag{5.4}$$

The random values of CCL are used to calculate the current solar irradiance level using the following equation:

$$Ir(t,s) = \bar{Ir}(t)(1 - CCL_{corrected}(t,s)) \tag{5.5}$$

where $Ir(t,s)$ is the solar irradiance level at time t and scenario s, and $\bar{Ir}(t)$ is the maximum irradiance at instant t. The output power of the PVs can be calculated using equation 4.35. An example of 30 generated scenarios is shown in Fig. 5.3.

For a time horizon T and scenario index s, we can summarize the random variables as follows: 1) the repair times of damaged lines $\boldsymbol{ET_s^L} \in \mathbb{R}^{|\Omega_{DL}|}$; 2) tree clearing time $\boldsymbol{ET_s^T} \in \mathbb{R}^{|\Omega_{DT}|}$; 3) load

Table 5.1 Cloud coverage probability

CCL	Cloud type	Probability of occurrence
0.00-0.05	1	0.67
0.05-0.15	2	0.19
0.15-0.25	3	0.14

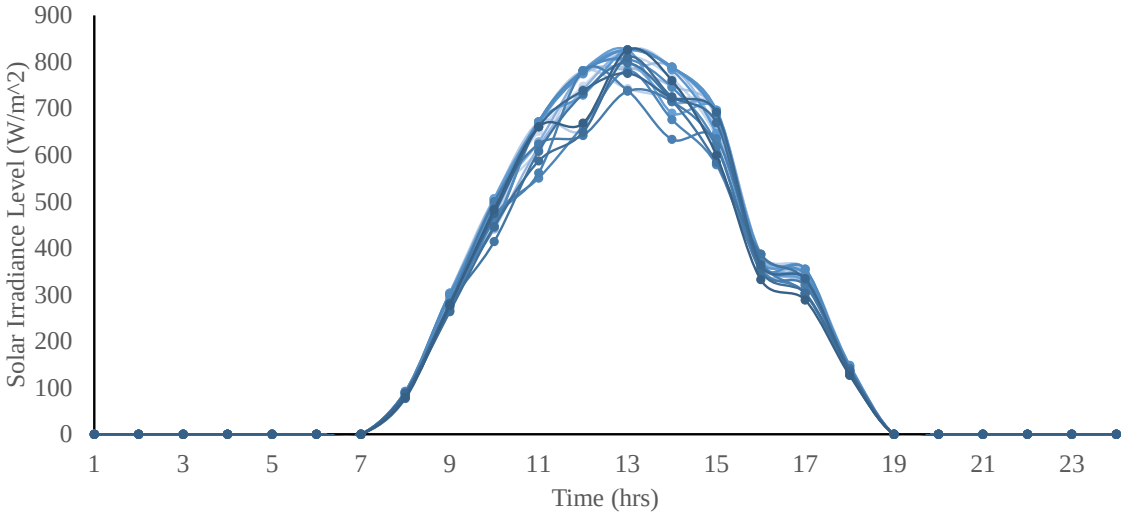

Figure 5.3 30 generated scenarios for the solar irradiance level.

forecast error $\boldsymbol{e_s} \in \mathbb{R}^T$; and 4) $\boldsymbol{Ir_s} \in \mathbb{R}^T$. By combining all random variables, the number of random variables is $(2T + |\Omega_{DL}| + |\Omega_{DT}|)$, and we assume they are mutually independent. Therefore, for $|S|$ scenarios, we can define a matrix $\boldsymbol{\xi} \in \mathbb{R}^{(2T+|\Omega_{DL}|+|\Omega_{DT}|)\times|S|}$ whose rows consist of random variables and columns consist of scenarios as follows:

$$
\boldsymbol{\xi} = \begin{array}{c}
\begin{array}{ccccc} s=1 & s=2 & s=3 & \dots & s=|\mathcal{S}| \end{array} \\
\left(\begin{array}{ccccc}
ET^L_{1,1} & ET^L_{1,2} & ET^L_{1,3} & \dots & ET^L_{1,|\mathcal{S}|} \\
ET^L_{2,1} & ET^L_{2,2} & ET^L_{2,3} & \dots & ET^L_{2,|\mathcal{S}|} \\
\vdots & \vdots & \vdots & \ddots & \vdots \\
ET^L_{\Omega_{DL},1} & ET^L_{\Omega_{DL},2} & ET^L_{\Omega_{DL},3} & \dots & ET^L_{\Omega_{DL},|\mathcal{S}|} \\
ET^T_{1,1} & ET^T_{1,2} & ET^T_{1,3} & \dots & ET^T_{1,|\mathcal{S}|} \\
ET^T_{2,1} & ET^T_{2,2} & ET^T_{2,3} & \dots & ET^T_{2,|\mathcal{S}|} \\
\vdots & \vdots & \vdots & \ddots & \vdots \\
ET^T_{\Omega_{DT},1} & ET^T_{\Omega_{DT},2} & ET^T_{\Omega_{DT},3} & \dots & ET^T_{\Omega_{DT},|\mathcal{S}|} \\
e_{1,1} & e_{1,2} & e_{1,3} & \dots & e_{1,|\mathcal{S}|} \\
e_{2,1} & e_{2,2} & e_{2,3} & \dots & e_{2,|\mathcal{S}|} \\
\vdots & \vdots & \vdots & \ddots & \vdots \\
e_{T,1} & e_{T,2} & e_{T,3} & \dots & e_{T,|\mathcal{S}|} \\
Ir_{1,1} & Ir_{1,2} & Ir_{1,3} & \dots & Ir_{1,|\mathcal{S}|} \\
Ir_{2,1} & Ir_{2,2} & Ir_{2,3} & \dots & Ir_{2,|\mathcal{S}|} \\
\vdots & \vdots & \vdots & \ddots & \vdots \\
Ir_{T,1} & Ir_{T,2} & Ir_{T,3} & \dots & Ir_{T,|\mathcal{S}|}
\end{array}\right)
\begin{array}{l}
v=1 \\ v=2 \\ \vdots \\ v=\Omega_{DL} \\ v=\Omega_{DL}+1 \\ v=\Omega_{DL}+2 \\ \vdots \\ v=\Omega_{DL}+\Omega_{DT} \\ v=\Omega_{DL}+\Omega_{DT}+1 \\ v=\Omega_{DL}+\Omega_{DT}+2 \\ \vdots \\ v=\Omega_{DL}+\Omega_{DT}+T \\ v=\Omega_{DL}+\Omega_{DT}+T+1 \\ v=\Omega_{DL}+\Omega_{DT}+T+2 \\ \vdots \\ v=\Omega_{DL}+\Omega_{DT}+2T
\end{array}
\end{array}
$$

where $\xi_{v,s}$ is the realization of random variable v in scenario s. According to the Monte Carlo sampling procedure, the probability Pr(s) of each scenario is $1/|\mathcal{S}|$.

5.3 Two-Stage Stochastic Program

The repair and restoration problem can be divided into two stages. The first stage is to route the repair crews, which is characterized by depots, repair crews, damaged components and paths between the damaged components. The second stage is distribution system restoration using DGs and reconfiguration. In practice, these two subproblems are interdependent. Therefore, we propose a single MILP formulation that integrates the two problems for joint distribution system repair and

restoration, with the objective of maximizing the picked-up loads. The utility solves the optimization problem to obtain the best route for the repair crews. The crews are then dispatched to repair the damaged components. For example, the crews may have to replace a pole or reconnect a wire. This repair process is included in the model through the repair time. Meanwhile, the utility controls the DGs and switches to restore power to the consumers. In this chapter, we modify the mathematical model presented in Chapter 4 by adding uncertainty and converting the MILP model into a two-stage stochastic MILP (SMIP). A brief explanation for the modified constraints is provided for clarity.

5.3.1 First Stage: Repair Crew Routing and Resource Constraints

The first-stage decision variables in the SMIP are used to compute the routes for each crew while satisfying equipment requirement and capacity constraints. The first-stage constraints are independent from the uncertain parameters. The constraints are listed in the following:

$$\sum_{\forall m \in N} x_{\phi_c^0,m,c} = 1, \forall c \tag{5.6}$$

$$\sum_{\forall m \in N} x_{m,\phi_c^1,c} = 1, \forall c \tag{5.7}$$

$$\sum_{\forall n \in N \backslash \{m\}} x_{m,n,c} - \sum_{\forall n \in N \backslash \{m\}} x_{n,m,c} = 0, \forall c, m \in N \backslash \left\{\phi_c^0, \phi_c^1\right\} \tag{5.8}$$

$$\sum_{\forall c \in C^L} \sum_{\forall m \in N \backslash \{n\}} x_{m,n,c} = 1, \forall n \in \Omega_{DL} \tag{5.9}$$

$$\sum_{\forall c \in C^T} \sum_{\forall m \in N \backslash \{n\}} x_{m,n,c} = 1, \forall n \in \Omega_{DT} \tag{5.10}$$

$$E_{d,\tau}^D \geq \sum_{\forall c \in C^L, \phi_c^0 = d} E_{c,\phi_c^0,\tau}^C + \sum_{\forall c \in C^L} E_{c,d,\tau}^C, \forall d, \tau \tag{5.11}$$

$$\sum_{\forall \tau} Cap_\tau^R \;\; CE_{c,m,\tau} \leq Cap_c^C, \forall m, c \in C^L \tag{5.12}$$

$$\sum_{\forall n \in N} x_{n,m,c} \mathcal{R}_{m,\tau} \leq CE_{c,m,\tau}, \forall m, \tau, c \in C^L \tag{5.13}$$

$$\begin{aligned} &-M(1 - x_{m,n,c}) \leq CE_{c,m,\tau} - \mathcal{R}_{m,\tau} - CE_{c,n,\tau} \leq M(1 - x_{m,n,c}), \\ &\forall m \in N \backslash \{\phi_c^1\}, n \in N \backslash \left\{\phi_c^0, m\right\}, c \in C^L, \tau \end{aligned} \tag{5.14}$$

$$
\begin{aligned}
&-M(1-x_{d,n,c}) \leq CE_{c,d,\tau} + E^{C}_{c,d,\tau} - CE_{c,n,\tau} \leq M(1-x_{d,n,c}),\\
&\forall d,n \in N \backslash \left\{\phi^0_c, \phi^1_c, d\right\}, c \in C^L, \tau
\end{aligned} \tag{5.15}
$$

$$
-M(1-x_{\phi^0_c,n,c}) \leq E^{C}_{c,\phi^0_c,\tau} - CE_{c,n,\tau} \leq M(1-x_{\phi^0_c,n,c}), \forall n \in N \backslash \left\{\phi^0_c\right\}, c \in C^L, \tau \tag{5.16}
$$

Constraint (5.6)–(5.7) define the starting and ending point for each crew. Constraint (5.8) is the flow conservation constraint, where a crew arrives at a damaged component and then moves to the next location after finishing the repairs. Constraints (5.9) and (5.10) ensure that each damaged component is repaired by only one line crew and one tree crew, respectively. Constraint (5.11) limits the number of resources that the crews obtain from depot d by the number of available resources in the depot. Constraint (5.12) limits the number of resources by the crew's capacity. The crews must have enough resources to repair the damaged components, as enforced by (5.13). Constraint (5.14) calculates the number of resources that crew c has when arriving at location n. Constraint (5.15) models the resource pick up constraint, where a crew can go back to the depot to obtain additional resources. Constraint (5.16) defines the initial resources that the crews have.

5.3.2 Second Stage: Distribution Network Operation

In the second stage, the distribution system is operated based on the realized scenarios. The second-stage decision variables are used to operate the switches and DGs to maximize the served loads. The variables in the second stage, indexed by s, are functions of the random variables $ET_{m,c,s}$ (repair time), $P^D_{i,\varphi,t,s}$ (demand), and $Ir_{t,s}$ (solar irradiance). Notice that $ET^L_{m,s}$ and $ET^T_{m,s}$ are combined into $ET_{m,c,s}$ by including the crew index c. The second stage objective and constraints are presented in this subsection.

5.3.2.1 Objective

$$
\min \sum_{\forall s} \Pr(s) \sum_{\forall t} \Big(\sum_{\forall \varphi} \sum_{\forall i} (1-y_{i,t,s}) \rho^D_i P^D_{i,\varphi,t,s} + \rho^{SW} \sum_{k \in \Omega_{SW}} \gamma_{k,t,s} \Big) \tag{5.17}
$$

The objective (5.17) of the second stage is to maximize the expected served loads and minimize the switching operations over the time horizon. In the second stage, DGs and line switches are

optimally operated in response to the realization of the random variables. Once a damaged line is repaired and energized, it provides a path for the power flow.

5.3.2.2 Second-Stage Constraints

$$P^{L}_{i,\varphi,t,s} = y_{i,t,s}P^{D}_{i,\varphi,t,s} + (y_{i,t,s} - y_{i,\max(\mathrm{t}-\lambda,0),\mathrm{s}})P^{U}_{i,\varphi,t,s},\ \forall i,\varphi,t,s \tag{5.18}$$

$$Q^{L}_{i,\varphi,t,s} = y_{i,t,s}Q^{D}_{i,\varphi,t,s} + (y_{i,t,s} - y_{i,\max(\mathrm{t}-\lambda,0),\mathrm{s}})Q^{U}_{i,\varphi,t,s},\ \forall i,\varphi,t,s \tag{5.19}$$

$$y_{i,t+1,s} \geq y_{i,t,s}\ ,\ \forall i,t,s \tag{5.20}$$

$$0 \leq P^{G}_{i,\varphi,t,s} \leq P^{G_{max}}_{i}\ ,\ \forall i,\varphi,t,s \tag{5.21}$$

$$0 \leq Q^{G}_{i,\varphi,t,s} \leq Q^{G_{max}}_{i}\ ,\ \forall i,\varphi,t,s \tag{5.22}$$

$$-u_{k,t,s}p_{k,\varphi}P^{K_{max}}_{k} \leq P^{K}_{k,\varphi,t,s} \leq u_{k,t,s}p_{k,\varphi}P^{K_{max}}_{k}\ ,\ \forall k,\varphi,t,s \tag{5.23}$$

$$-u_{k,t,s}p_{k,\varphi}Q^{K_{max}}_{k} \leq Q^{K}_{k,\varphi,t,s} \leq u_{k,t,s}p_{k,\varphi}Q^{K_{max}}_{k}\ ,\ \forall k,\varphi,t,s \tag{5.24}$$

$$\sum_{\forall k\in K(.,i)} P^{K}_{k,\varphi,t,s} + P^{G}_{i,\varphi,t,s} + P^{PV}_{i,\varphi,t,s} + P^{dch}_{i,\varphi,t,s} = \sum_{\forall k\in K(i,.)} P^{K}_{k,\varphi,t,s} + P^{L}_{i,\varphi,t,s} + P^{ch}_{i,\varphi,t,s}, \forall i,\varphi,t,s \tag{5.25}$$

$$\sum_{\forall k\in K(.,i)} Q^{K}_{k,\varphi,t,s} + Q^{G}_{i,\varphi,t,s} + Q^{PV}_{i,\varphi,t,s} + Q^{ES}_{i,\varphi,t,s} + u^{C}_{i,t,s}Q^{C}_{i,\varphi} = \sum_{\forall k\in K(i,.)} Q^{K}_{k,\varphi,t,s} + Q^{L}_{i,\varphi,t,s}, \forall i,\varphi,t,s \tag{5.26}$$

$$\boldsymbol{U}_{j,t,s} - \boldsymbol{U}_{i,t,s} + \bar{\boldsymbol{Z}}_{k}\boldsymbol{S}^{*}_{k,s} + \bar{\boldsymbol{Z}}^{*}_{k}\boldsymbol{S}_{k,s} \leq (2 - u_{k,t,s} - \boldsymbol{p}_{k})M, \forall k \in \Omega_L\backslash\Omega_V, t, s \tag{5.27}$$

$$\boldsymbol{U}_{j,t,s} - \boldsymbol{U}_{i,t,s} + \bar{\boldsymbol{Z}}_{k}\boldsymbol{S}^{*}_{k,s} + \bar{\boldsymbol{Z}}^{*}_{k}\boldsymbol{S}_{k,s} \geq -(2 - u_{k,t,s} - \boldsymbol{p}_{k})M, \forall k \in \Omega_L\backslash\Omega_V, t, s \tag{5.28}$$

$$(0.9)^2 U_{i,\varphi,t,s} \leq U_{j,\varphi,t,s} \leq (1.1)^2 U_{i,\varphi,t,s}, \forall k \in \Omega_V, \varphi, t, s \tag{5.29}$$

$$\mathcal{X}_{i,t,s}U_{min} \leq \boldsymbol{U}_{i,t,s} \leq \mathcal{X}_{i,t,s}U_{max}\ ,\ \forall i,t,s \tag{5.30}$$

$$2u_{k,t,s} \geq \mathcal{X}_{i,t,s} + \mathcal{X}_{j,t,s}, \forall k \in \Omega_{DL}, t, s \tag{5.31}$$

$$u_{k,t,s} = 1, \forall k \notin \{\Omega_{SW} \cup \Omega_{DL}\}, t, s \tag{5.32}$$

$$\gamma_{k,t,s} \geq u_{k,t,s} - u_{k,t-1,s}, \forall k \in \Omega_{SW}, t, s \tag{5.33}$$

$$\gamma_{k,t,s} \geq u_{k,t-1,s} - u_{k,t,s}, \forall k \in \Omega_{SW}, t, s \tag{5.34}$$

$$\sum_{k\in\Omega_{K(l)}} u_{k,t,s} \leq |\Omega_{K(l)}| - 1, \forall l, t, s \tag{5.35}$$

$$P^{PV}_{i,\varphi,t,s} = \frac{Ir_{i,t,s}}{(1000W/m^2)}\overline{P}^{PV}_i, \forall i \in \Omega_{PV}\backslash\Omega^G_{PV}, \varphi, t, s \tag{5.36}$$

$$P^{PV}_{i,\varphi,t,s} = \mathcal{X}_{i,t,s}\frac{Ir_{i,t,s}}{(1000W/m^2)}\overline{P}^{PV}_i, \forall i \in \Omega^G_{PV}, \varphi, t, s \tag{5.37}$$

$$|Q^{PV}_{i,\varphi,t,s}| \leq \sqrt{(S^{PV}_i)^2 - (\hat{P}^{PV}_{i,t,s})^2}, \forall i \in \Omega_{PV}\backslash\Omega^G_{PV}, \varphi, t, s \tag{5.38}$$

$$|Q^{PV}_{i,\varphi,t,s}| \leq \mathcal{X}_{i,t,s}\sqrt{(S^{PV}_i)^2 - (\hat{P}^{PV}_{i,t,s})^2}, \forall i \in \Omega^G_{PV}, \varphi, t, s \tag{5.39}$$

$$\text{where} \qquad \hat{P}^{PV}_{i,t,s} = \frac{Ir_{i,t,s}}{(1000W/m^2)}\overline{P}^{PV}_i$$

$$v^S_{i,\varphi,t,s} + \sum_{k\in K(.,i)} v^f_{k,\varphi,t,s} = \mathcal{X}_{i,t,s} + \sum_{k\in K(i,.)} v^f_{k,\varphi,t,s}, \forall i, \varphi, t, s \tag{5.40}$$

$$\sum_{\forall\varphi}\sum_{\forall t} v^S_{i,\varphi,t,s} = 0, \forall i \in \Omega_B\backslash\{\Omega^C_{PV} \cup \Omega_G \cup \Omega_{Sub}\}, s \tag{5.41}$$

$$-(u_{k,t,s}\ p_{k,\varphi})M \leq v^f_{k,\varphi,t,s} \leq (u_{k,t,s}\ p_{k,\varphi})M, \forall k \in \Omega_K, \varphi, t, s \tag{5.42}$$

$$\mathcal{X}_{i,t,s} \geq y_{i,t,s}, \forall i \in \Omega_B\backslash\{\Omega_G \cup \Omega^C_{PV} \cup \Omega^H_{PV}\}, t, s \tag{5.43}$$

$$0 \leq P^{ch}_{i,\varphi,t,s} \leq u^{ES}_{i,t,s}\overline{P}^{ch}_i,\ \forall i \in \Omega_{ES}, \varphi, t, s \tag{5.44}$$

$$0 \leq P^{dch}_{i,\varphi,t,s} \leq (1 - u^{ES}_{i,t,s})\overline{P}^{dch}_i, \forall i \in \Omega_{ES}, \varphi, t, s \tag{5.45}$$

$$E^S_{i,t,s} = E^S_{i,t-1,s} + \Delta t(\eta_c\sum_{\forall\varphi} P^{ch}_{i,\varphi,t,s} - \frac{\sum_{\forall\varphi} P^{dch}_{i,\varphi,t,s}}{\eta_d}), \forall i \in \Omega_{ES}, t, s \tag{5.46}$$

$$\underline{E}^S_i \leq E^S_{i,t,s} \leq \overline{E}^S_i, \forall i \in \Omega_{ES}, t, s \tag{5.47}$$

$$-u^{ES}_{i,t,s}S^{ES}_i \leq Q^{ES}_{i,\varphi,t,s} \leq u^{ES}_{i,t,s}S^{ES}_i, \forall i \in \Omega_{ES}, \varphi, t, s \tag{5.48}$$

$$|(P^{ch}_{i,\varphi,t,s} + P^{dch}_{i,\varphi,t,s}) + Q^{ES}_{i,\varphi,t,s}| \leq \sqrt{2}S^{ES}_i, \forall i \in \Omega_{ES}, \varphi, t, s \tag{5.49}$$

$$|(P^{ch}_{i,\varphi,t,s} + P^{dch}_{i,\varphi,t,s}) - Q^{ES}_{i,\varphi,t,s}| \leq \sqrt{2}S^{ES}_i, \forall i \in \Omega_{ES}, \varphi, t, s \tag{5.50}$$

$$\alpha_{m,c,s} + ET_{m,c,s} + tr_{m,n} - (1 - x_{m,n,c})\,M \leq \alpha_{n,c,s} \forall m \in N\backslash\{\phi^1_c\}, n \in N\backslash\left\{\phi^0_c, m\right\}, c, s \tag{5.51}$$

$$\sum_{c\in C^L} \alpha_{m,c,s} \geq \sum_{c\in C^T} \alpha_{m,c,s} + ET_{m,c,s}\sum_{\forall n\in N} x_{m,n,c}, \forall m \in \Omega_{DT}, s \tag{5.52}$$

$$\sum_{\forall t} f_{m,t,s} = 1\ ,\ \forall m \in \Omega_{DL}, s \tag{5.53}$$

$$\sum_{\forall t} tf_{m,t,s} \geq \sum_{\forall c} (\alpha_{m,c,s} + ET_{m,c,s} \sum_{\forall n \in N} x_{m,n,c}), \forall m \in \Omega_{DL}, s \tag{5.54}$$

$$0 \leq \alpha_{m,c,s} \leq M \sum_{n \in N} x_{n,m,c}, \ \forall m \in N \backslash \left\{\phi_c^0, \phi_c^1\right\}, c, s \tag{5.55}$$

$$u_{m,t,s} = \sum_{\bar{t}=1}^{t} f_{m,\bar{t},s} \ , \ \forall m \in \Omega_{DL}, t, s \tag{5.56}$$

Constraints (5.18–(5.19) model the CLPU effects on the loads. Constraint (5.20) prohibits load shedding once the load is served. Constraints (5.21)–(5.24) define the active and reactive power limits of the DGs and lines. Constraints (5.25)–(5.26) are the 3-phase active and reactive power node balance constraints. Kirchhoff's voltage law is represented in (5.27)–(5.28) [105]. In this chapter, we assume that the tap setting is continuous [106] for voltage regulators, then constraint (5.29) forces the voltage on the secondary side of the voltage regulator to be within ±10% of the primary side. Constraint (5.30) ensures that the voltage is within a specified limit if energized. Constraint (5.31) sets the values of $\mathcal{X}_i$ and $\mathcal{X}_j$ to be 0 if the line is damaged, therefore, the voltages on the buses between damaged lines are forced to be 0 using constraint (5.30). If the voltages on two connected buses are zero, then the power flow is forced to be zero through constraints (5.27) and (5.28), therefore, the model will isolate the faults in order to serve the loads. Constraint (5.32) sets $u_k = 1$ for lines that are not damaged or not switchable. Constraint (5.33)–(5.34) are used in order to limit the number of switching operations, where $\gamma_{k,t}$ is included in the objective to minimize the number of switching operation. Constraint (5.35) is the radiality constraint [108]. The active and reactive power of different types of PV systems are defined in (5.36)–(5.39). The connectivity of the PV systems is modeled in (5.40)–(5.42) using the virtual framework presented in Chapter 4. A load connected to a de-energized bus must be shed (5.43), unless the bus has a local power source. Constraints on BESSs are modeled in (5.44)–(5.50). The arrival time of the crews at each damaged component is calculated in (5.51). The coordination between tree and line crews is represented in (5.52). Constraints (5.53)–(5.56) are used to connect the crew scheduling constraints with power operation constraints.

5.3.3 Extensive Form

The complete two-stage stochastic program for solving stochastic DSRRP (S-DSRRP) is presented in this section. The *extensive form* (EF) of the two-stage S-DSRRP is formulated as follows:

$$\begin{aligned} \min \ & \sum_{\forall s} \Pr(s) \sum_{\forall t} \Big(\sum_{\forall \varphi} \sum_{\forall i} (1 - y_{i,t,s}) \rho_i^D P_{i,\varphi,t,s}^D + \rho^{SW} \sum_{k \in \Omega_{SW}} \gamma_{k,t,s} \Big) \\ & \text{subject to first-stage constraints (5.6)–(5.16)} \\ & \text{subject to second-stage constraints (5.18)–(5.56)} \\ & \{f, x, u, y, \mathcal{X}, \gamma\} \in \{0,1\}, \{CE, E^C\} \geq 0 \end{aligned} \tag{5.57}$$

5.4 Solution Algorithm

The routing problem is an NP-hard combinatorial optimization problem with exponential computation time. Adding uncertainty and combining distribution system operation constraints with the routing problem further increase the complexity. To solve S-DSRRP, we adapt the assignment-based approach presented in Chapter 4, and utilize the Progressive Hedging algorithm for solving the stochastic program. Our approach decomposes the S-DSRRP into two stochastic subproblems. The goal of the first subproblem is to assign the crews to the damaged components, where we consider the uncertainty of the repair time. In the second subproblem, the repair crews are dispatched based on the assignment results obtained from the first subproblem. The second subproblem is solved using parallel PH. In this section, we decompose S-DSRRP and present the procedure for solving the problem. The decomposed S-DSRRP will be referred to as DS-DSRRP.

5.4.1 Subproblem I

The first subproblem is similar to (4.74)–(4.88), where the crews are assigned to the damaged components based on the capacity, distances, and expected working hours. However, in this section we modify the MILP problem in (4.74)–(4.88) to SMIP, as the repair time is a random variable. The subproblem is formulated as follows:

$$\min \sum_{\forall s} \Pr(s) \big(\mathcal{L}_s^L + \mathcal{L}_s^T \big) + \sum_{\forall c} \sum_{\forall d} \mathcal{P}_{c,d} + \bar{tr} \tag{5.58}$$

s.t. (4.77) – (4.88)

$$\mathcal{L}_s^L \geq \sum_{\forall m} A_{m,c}^L ET_{m,c,s}, \forall c \in C^L, s \tag{5.59}$$

$$\mathcal{L}_s^T \geq \sum_{\forall m} A_{m,c}^T ET_{m,c,s}, \forall c \in C^T, s \tag{5.60}$$

The first-stage decision variables are the assignment variables $A_{m,c}^L$ and $A_{m,c}^T$. Therefore, the crews are assigned to the damaged components in the first stage. After the realization of the scenario, the working hours and the time of the last repairs are determined in the second stage. After solving this subproblem, we can calculate the set of components that each crew repairs using the following equations:

$$\Omega_{DL}(c) = \{m | \forall m \in \Omega_{DL}, A_{m,c}^L = 1\}, \forall c \in C^L \tag{5.61}$$

$$\Omega_{DT}(c) = \{m | \forall m \in \Omega_{DT}, A_{m,c}^T = 1\}, \forall c \in C^T \tag{5.62}$$

$$N(c) = \Omega_{DL}(c) \cup \Omega_P, \forall c \in C^L \tag{5.63}$$

$$N(c) = \Omega_{DT}(c) \cup \Omega_P, \forall c \in C^T \tag{5.64}$$

where $\Omega_{DL}(c)$ and $\Omega_{DL}(c)$ are the set of damaged components for each line and tree crew, respectively. $N(c)$ combines the set of depots to the set of damage components.

5.4.2 Subproblem II

The second subproblem is formulated similarly to (5.17)-(5.56). However, the crews are only dispatched to the damaged components that they are assigned to repair from Subproblem I. The second subproblem is then formulated as follows:

min (5.17)

$$\sum_{\forall m \in N(c)} x_{\phi_c^0, m, c} = 1, \forall c \tag{5.65}$$

$$\sum_{\forall m \in N(c)} x_{m, \phi_c^1, c} = 1, \forall c \tag{5.66}$$

$$\sum_{\forall n \in N(c)\backslash\{m\}} x_{m,n,c} - \sum_{\forall n \in N(c)\backslash\{m\}} x_{n,m,c} = 0, \forall c, m \in N(c)\backslash\left\{\phi_c^0, \phi_c^1\right\} \tag{5.67}$$

$$\sum_{\forall m \in N(c)\backslash\{n\}} x_{m,n,c} = 1, \forall c \in C^L, n \in \Omega_{DL}(c) \tag{5.68}$$

$$\sum_{\forall m \in N(c)\backslash\{n\}} x_{m,n,c} = 1, \forall c \in C^T, n \in \Omega_{DT}(c) \tag{5.69}$$

$$\sum_{\forall n \in N(c)} x_{n,m,c}\mathcal{R}_{m,\tau} \leq CE_{c,m,\tau}, \forall c \in C^L, m \in N(c), \tau \tag{5.70}$$

$$\begin{aligned} &-M(1-x_{m,n,c}) \leq CE_{c,m,\tau} - \mathcal{R}_{m,\tau} - CE_{c,n,\tau} \leq M(1-x_{m,n,c}), \\ &\forall m \in N(c)\backslash\{\phi_c^1\}, n \in N(c)\backslash\left\{\phi_c^0, m\right\}, c \in C^L, \tau \end{aligned} \tag{5.71}$$

$$\begin{aligned} &-M(1-x_{d,n,c}) \leq CE_{c,d,\tau} + E^C_{c,d,\tau} - CE_{c,n,\tau} \leq M(1-x_{d,n,c}), \\ &\forall d, n \in N(c)\backslash\left\{\phi_c^0, \phi_c^1, d\right\}, c \in C^L, \tau \end{aligned} \tag{5.72}$$

$$-M(1-x_{\phi_c^0,n,c}) \leq E^C_{c,\phi_c^0,\tau} - CE_{c,n,\tau} \leq M(1-x_{\phi_c^0,n,c}), \forall n \in N(c)\backslash\left\{\phi_c^0\right\}, c \in C^L, \tau \tag{5.73}$$

$$\begin{aligned} &\alpha_{m,c,s} + ET_{m,c,s} + tr_{m,n} - (1-x_{m,n,c})\,M \leq \\ &\qquad \alpha_{n,c,s}, \forall m \in N(c)\backslash\{\phi_c^1\}, n \in N(c)\backslash\left\{\phi_c^0, m\right\}, c, s \end{aligned} \tag{5.74}$$

$$\sum_{c \in C^L} \sum_{\substack{n \in \Omega_{DL}(c) \\ n==m}} \alpha_{m,c,s} \geq \sum_{c \in C^T} \sum_{\substack{n \in \Omega_{DT}(c) \\ n==m}} \alpha_{m,c,s} + ET_{m,c,s} \sum_{\forall n \in N} x_{m,n,c}, \forall m \in \Omega_{DT}, s \tag{5.75}$$

$$\sum_{\forall t} tf_{m,t,s} \geq \alpha_{m,c,s} + ET_{m,c,s}, \forall c \in C^L, m \in \Omega_{DL}(c), s \tag{5.76}$$

$$\text{s.t. } (5.11)\text{–}(5.12),\ (5.18)\text{–}(5.50),\ (5.53),\ (5.56)$$

Constraints (5.65)–(5.75) are similar to the constraints presented in Chapter 4, however, they are modified by replacing N, Ω_{DL}, and Ω_{DT} with $N(c)$, $\Omega_{DL}(c)$, and $\Omega_{DT}(c)$. We simplify constraint (5.54) by removing the $x_{m,n,c}$ term, as shown in (5.76). The rest of the constraints and the objective are not changed.

Algorithm 3 summarizes the procedure for solving S-DSRRP, starting from scenario generation to decomposition. Subproblem I is solved using the extensive form as it is not a difficult problem. However, Subproblem is solved using PH due to its complexity.

Algorithm 3 Scenario generation and S-DSRRP

for $s \in 1$ to $|S|$ **do**
  Generate the repair time for each damaged component using lognormal distribution ($\mu = 1.0570, \sigma = 1.0555$)
  Generate the tree-clearing time using a truncated normal distribution (mean = 1 hour, max = 3 hours, min = 30 minutes)
  Generate the kW and kVAr demand values for each load using (5.2)
  Generate the solar irradiance using (5.5)
end for
Solve Subproblem I using the extensive form
$\Omega_{DL}(c) = \{m | \forall m \in \Omega_{DL}, A^L_{m,c} = 1\}, \forall c \in C^L$
$\Omega_{DT}(c) = \{m | \forall m \in \Omega_{DT}, A^T_{m,c} = 1\}, \forall c \in C^T$
$N(c) = \Omega_{DL}(c) \cup \Omega_P, \forall c \in C^L$
$N(c) = \Omega_{DT}(c) \cup \Omega_P, \forall c \in C^T$
Solve Subproblem II using PH

5.5 Simulation and Results

The modified IEEE 123-bus distribution feeder, presented in Chapter 4, is used as a test case for the stochastic repair and restoration problem. Detailed information on the network can be found in [93]. The stochastic models and algorithms are implemented using the PySP package in Pyomo [89]. IBM's CPLEX 12.6 mixed-integer solver is used to solve all subproblems. The experiments were performed on Iowa State University's Condo cluster, whose individual blades consist of two 2.6 GHz 8-Core Intel E5-2640 v3 processors and 128 GB of RAM. The scenario subproblems are solved in parallel by using the Python Remote Objects library.

The same test case in Fig. 4.12, with 6 line crews, 2 tree crews, 3 depots, and 14 damaged lines is used in this section. The Monte Carlo sampling technique is used to generate 1000 random scenarios with equal probability, and the SCENRED2 toolkit in GAMS is used to reduce the number of scenarios to 30. For the repair time, a lognormal distribution is used with parameters $\mu = 1.0570$ and $\sigma = 1.0555$ [119], and unrealistic values (e.g., 0.01 hours) are truncated. On the other hand, the load forecast error is generated using a truncated normal distribution with limits $\pm 15\%$ [121]. The tree-clearing time is generated using a truncated normal distribution and the solar irradiance is generated according to (5.5). Samples of the 30 generated scenarios are shown in Table 5.2 for

the repair time. Three methods are used to solve the test case: 1) DS-DSRRP with subproblem II solved using EF; 2) DS-DSRRP with PH; 3) Reoptimization algorithm. Since the Reoptimization algorithm is deterministic, we reduce the number of scenarios to a single scenario using GAMS for this method.

Table 5.2 Samples of the repair times (in hours) for the 30 generated scenarios using the lognormal distribution

Damage	Scenario 1	Scenario 2	Scenario 3	...	Scenario 30
Line 7–8	6	6	2	...	4
Line 27–33	3	4	2	...	3
Line 18–19	5	2	2	...	2
Line 163–18	2	4	2	...	6
Line 15–17	5	6	6	...	4
Line 38–39	1	3	5	...	6
Line 58–59	6	1	3	...	1
Line 54–57	2	4	4	...	2
Line 67–72	2	1	6	...	1
Line 76–86	4	1	4	...	5
Line 91–93	4	1	5	...	1
Line 93–95	1	2	2	...	5
Line 105–106	1	2	4	...	5
Line 113–114	5	1	2	...	3

The routing solutions obtained using DS-DSRRP with PH and the Reoptimization algorithm are shown in Fig. 5.4 and Fig. 5.5, respectively. Solving the complete problem S-DSRRP without decomposition did not result in a solution after 12 hours. To show the benefits of including uncertainty and compare the deterministic method with the stochastic method, we set the first-stage variables as fixed parameters and solve the stochastic problem $\mathrm{F}(x, \boldsymbol{\xi}) = \min\{5.17, s.t.\ 5.18 - 5.56\}$. Therefore, if x^R is the routing solution in Fig. 5.5, then the expected value of the deterministic solution is $\mathrm{F}(x^R, \boldsymbol{\xi})$. A comparison between the three methods (DS-DSRRP (EF),DS-DSRRP (PH), Reoptimization) is shown in Table 5.3. The wait-and-see (WS) is found to provide a lower bound to the objective value to give us an indication on the quality of the solutions obtained using different methods.

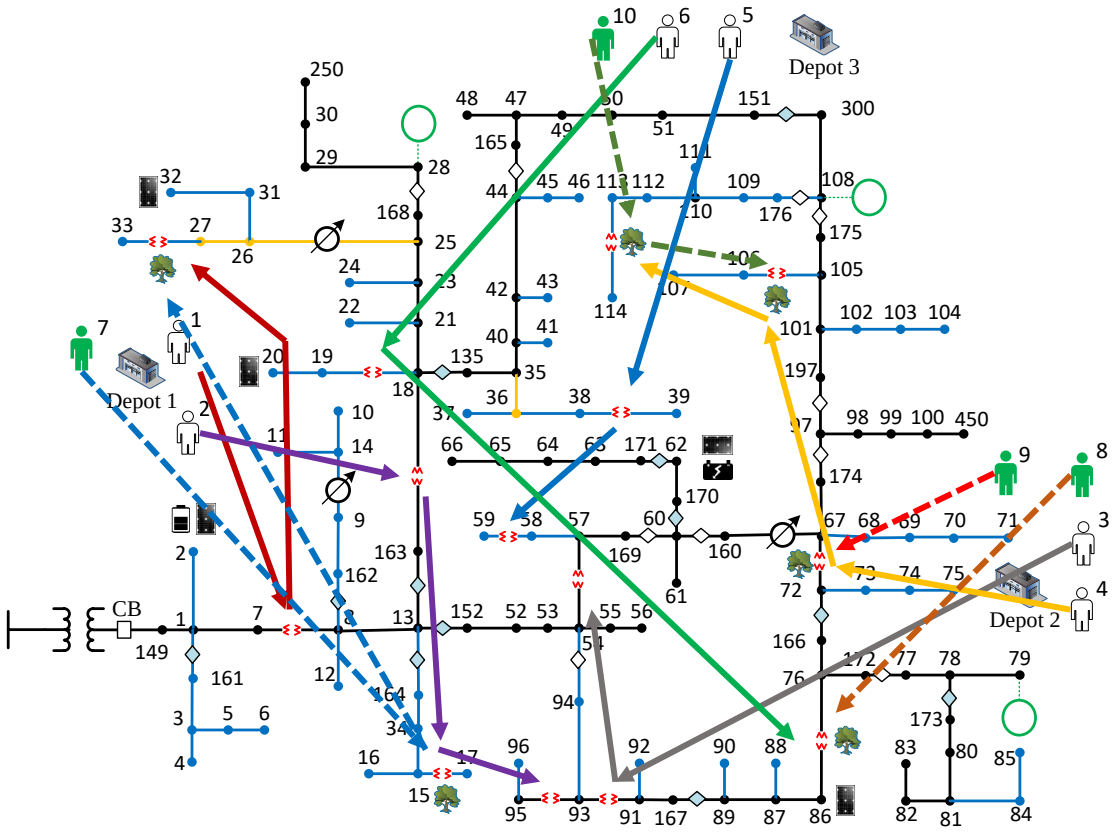

Figure 5.4 Routing solution obtained by solving DS-DSRRP using PH.

Table 5.3 Stochastic DSRRP simulation results on the IEEE 123-bus system with 14 damaged lines

	Objective Value F(x,$\boldsymbol{\xi}$)	Comp. Time	(Objective Value - WS)/WS
DS-DSRRP (EF)*	$251,246.43	12 h	5.92%
DS-DSRRP (PH)	$250,306.7	858.08 s	5.53%
Reoptimization	$258,643.3	786.2 s	9.04%

*The solver did not converge to the optimal solution after 12 hours (imposed time limit).

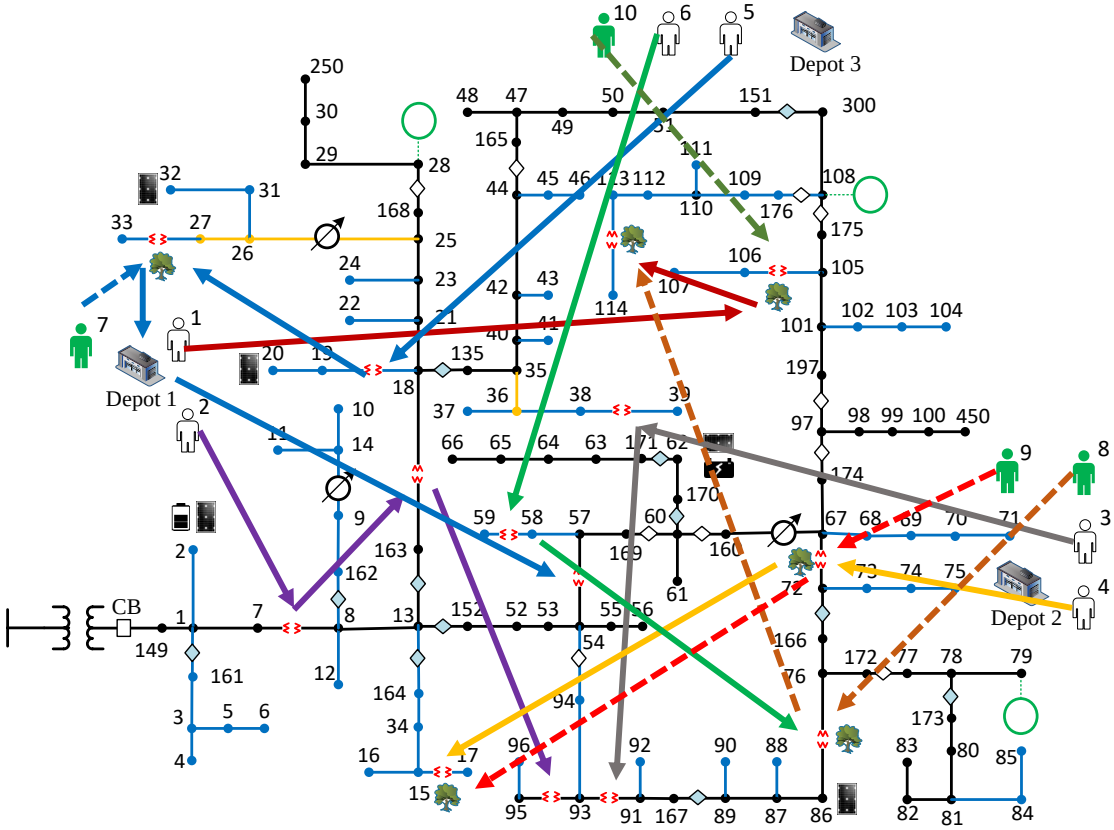

Figure 5.5 Routing solution obtained by using the Reoptimization algorithm and the expected values of the repair times.

For DS-DSRRP with EF, the solution did not converge to the optimal one after 12 hours, however, a feasible is obtained, which is 5.92% larger than the WS solution. EF requires a long computation due to the complexity of subproblem II in DS-DSRRP. The best solution is obtained using DS-DSRRP with PH, where the objective value is around \$8,000 less than $\mathrm{F}(x^R, \boldsymbol{\xi})$ and the computation time is less than 900 seconds. By using PH, we obtained a high quality solution in a short time. Next, we compare the routing solutions on 5 random realizations. Let x^S be the routing solution obtained by solving DS-DSRRP with PH (Fig. 5.4). We set x^S to be constant and generate a random scenario to simulate an actual event. The objective value and the quality of the routing solution can then be found by solving $\mathrm{F}(x^S, \xi)$. The results for 5 cases are shown in Table 5.4. In addition to DS-DSRRP (PH) and Reoptimization, we solve the test cases using Dynamic

Reoptimization, where the solution is updated as new information is obtained. The optimal solution (last column in Table 5.4) is obtained by solving the deterministic problem for each case, with perfect information on the random variables. In the first test case, Reoptimization outperformed DS-DSRRP. In all other cases, the stochastic method achieved higher quality solutions, which is highlighted by the optimality gaps. This further signifies the importance of uncertainty in our decision-making process. However, the dynamic approach outperformed both DS-DSRRP and static Reoptimization. Therefore, we can conclude that a dynamic method is the best approach for this problem in terms of quality and speed. The downside of the dynamic approach is that it requires constant communication with all crews, which may not be available after extreme events.

Table 5.4 The objective value for the IEEE 123-bus system (14 damaged lines) with constant routing solutions and different scenario realizations

Case	DS-DSRRP (PH)		Static-Reoptimization		Dynamic-Reoptimization		Optimal
	F(x^S, ξ_{case})	% Gap	F(x^R, ξ_{case})	% Gap	F(x^D, ξ_{case})	% Gap	
1	\$256,104.7	10.84%	\$241,661.9	4.59%	\$232,728.8	0.72%	\$231,065.4
2	\$248,671.7	6.98%	\$299,586.4	28.88%	\$245,558.6	5.64%	\$232,447.7
3	\$269,505.5	6.85%	\$291,036.7	15.38%	\$259,189.3	2.76%	\$252,235.3
4	\$251,256.7	13.27%	\$268,590.5	21.08%	\$236,415.2	6.58%	\$221,828.2
5	\$240,549.3	15.22%	\$246,431.5	18.04%	\$221,790.7	6.24%	\$208,772.2

5.6 Summary

In this chapter, we proposed a two-stage stochastic approach for the repair and restoration of distribution networks. The scenarios are generated using Monte Carlo sampling, considering the uncertainty of the repair time, load, and solar irradiance. We developed a decomposition approach to solve the stochastic problem. The approach starts by solving an assignment problem, and then operates the system and routes the crews in the second subproblem. Both subproblems are formulated as two-stage stochastic programs. Parallel Progressive Hedging is employed in the algorithm for the second subproblem where the subproblem for each scenario is solved separately. The results demonstrate the effectiveness of the proposed approach in balancing computational

burden and solution quality. In addition, we showed the importance of including uncertainty in the decision-making process. Using a stochastic or dynamic method for handling the uncertainties leads to better routing solutions.

CHAPTER 6. CONCLUSIONS AND FUTURE WORK

6.1 Conclusion and Research Contribution

Major weather events can cause significant damage to the infrastructure of distribution networks. Utilities must efficiently plan the recovery operation to repair the assets in a quick and effective manner. Utilities schedule the repairs using predefined restoration priority lists based on previous experiences. Some utilities use simple greedy algorithms to determine the restoration sequence [12], and others rely on the experience of the operators. After an extreme event, a sudden influx of crews can overwhelm operators and storm planners when they route the crews. Efficient restoration of the system is only possible if the crews are utilized properly. This involves coordinating repair crews with the recovery operation of distribution networks. Crews must be dispatched to repair the most critical lines, and power should be rerouted by reconfiguring the network to achieve a quick restoration process. In addition, the effectiveness of the recovery response depends on the preparation processes that are taken before extreme events hit. Pre-staging crews, equipment and other resources safely before a severe event allows for a proactive response and efficient resource management. This dissertation uses mathematical programming for disaster preparation in distribution systems and for co-optimizing repair scheduling and the recovery operation of distribution networks. An optimization process can help the operator to greatly decrease the restoration time. Effective response to weather events can lead to faster restoration time, as demonstrated in Fig. 4.16. Simulation results in Table 4.7 showed the importance of coordinating DGs and switches in the restoration process. The main contributions of this dissertation are listed as follows:

- A new two-stage SMIP model is developed and used to select depots and allocate crews and equipment. The model considers different types of crews (line and tree crews) and equipment (poles, transformers, and conductor). Mathematical equations for modeling the interdependencies of the depots, crews, equipment, and damaged components are formulated,

in addition to symmetry-breaking constraints to improve the performance of the model. Also, we provide a procedure for estimating the number and types of required equipment after extreme weather events.

- A novel MILP model for combining the repair crew routing and distribution network operation problems is developed. To the best of our knowledge, the proposed model is the first formulation that combines the two problems in the literature. The designed model captures the nature of the repair problem by modeling the coordination of line and tree crews, resource logistics, and isolation of the damaged components. Isolation of the damaged components is necessary because crews cannot repair live wires. The developed model can be applied on balanced and unbalanced distribution networks. This model can assist utilities in scheduling the repairs and restore normal operations after natural disasters.

- A mathematical formulation is developed for fault isolation and service restoration. Most of the studies on distribution system restoration assume that every line is equipped with switches to isolate the faults, which is not the case in practice. The developed formulation allows the network to isolate the faults and divides the network into microgrids. The proposed model can be incorporated into various distribution system studies, such as those relating to distribution system planning, networked microgrids, and distribution system repair and restoration.

- A framework for modeling different types of PV systems and their connectivity is developed. The idea of the proposed approach is to use virtual sources, loads, and flow to identify energized buses in distribution systems.

- A new hybrid algorithm that combines mathematical programming and the neighborhood search method is designed to solve DSRRP. The proposed tri-stage method starts by solving an assignment problem, where the crews are assigned to the damaged components, and in the second stage, crews are dispatched to the assigned components from the first stage. An adaptive neighborhood search method is then designed to iteratively improve the solution. The algorithm updates the crew schedule as more information is obtained regarding the network

and damaged components. The proposed algorithm achieved the best repair schedule when compared to solutions obtained using other methods, including commercial solvers.

- A two-stage stochastic framework is developed for optimizing service restoration in distribution networks. The designed method shows how stochastic programs can be efficiently solved using decomposition methods and Monte Carlo sampling. The stochastic DSRRP is simplified by first solving a stochastic assignment problem, and then solving the stochastic co-optimization problem. The results showed the importance of including uncertainty, as both stochastic and dynamic methods outperform the deterministic method.

6.2 Future Research

6.2.1 Coordination Between Utilities for Disaster Preparation

The preparation study in Chapter 3 presented a preparation plan for a single utility. However, in some cases where the natural disaster hits multiple regions, preparation should be coordinated between all utilities in the region. In addition, the Federal Emergency Management Agency (FEMA) will provide support for those utilities. Thus, it is necessary to coordinate the available resources between all involved parties. One possible approach is to modify the model presented in Chapter 3 and use it in a multi-agent based approach.

6.2.2 Mobile Generators

Advanced weather forecasting methodologies and fragility models provide utilities the ability to predict the severity of the damage to the system and the affected areas. If the available flexible resources such as mobile generators and mobile battery energy storage systems are coordinated strategically with distributed solar energy and other system components, we can reduce the disaster outcome and decrease the restoration time. Efficient utilization of mobile generators is hindered after extreme events due to difficult road conditions. Therefore, it is imperative that power

companies preposition the mobile sources. In current research, we are developing a two-stage SMIP to preposition the mobile generators before extreme events.

6.2.3 Machine Learning for Repair Time Estimation

In order to devise a plan for power restoration, it is necessary for utilities to estimate the repair time for the damaged components. The dispatchers can then direct the repair crews more efficiently and release the estimated restoration time to the public. Few studies have tackled the prediction of repair and restoration times. Instead, studies have focused on predicting the locations, size, and number of outages.

In previous work [123], we used Deep Neural Network to predict the repair and restoration times of outages. We presented and analyzed 6 years of distribution network outage data that were obtained from one utility in the United States. The data showed that there existed a clear correlation between the repair/restoration time and the number of customers interrupted. In addition, both repair and restoration times tended to be higher after extreme weather events. The repair time prediction model achieved satisfactory performance, where the mean error was only 18 minutes. The mean error for the restoration time predictive model was 2 hours. However, the work in [123] is only for one utility, and may not be replicated on other datasets. Therefore, further investigation is needed to determine whether we can accurately predict the repair time.

6.2.4 Sequential Operation of Switching Devices

In Section 4.2.2.4, a model was developed for the optimal topology configuration of distribution systems after outages. However, the purpose of the model was to find the final configuration of the switches and not the sequence of switching actions that must be taken. Due to the different characteristics of switching devices, the switches must be operated in a specific sequence to obtain the optimal configuration. For example, a sectionalizing switch cannot interrupt currents, therefore, circuit breakers or reclosers have to cut off the power before operating the sectionalizer. In future work, we will develop a MILP model for finding the optimal sequence of switching operations.

6.2.5 Rebuilding the Distribution System

In extreme cases, natural disasters may completely destroy parts of the grid. The problem for the utilities would then become a rebuilding one, rather than repair and restoration. Rebuilding after major events is challenging, utilities must organize and manage all their resources while ensuring that the electricity is restored as fast as possible. However, the rebuilding process presents an opportunity for the utility to rebuild a smarter and more resilient network, instead of reconstructing the same network. Destroyed equipment can be rebuilt with upgraded assets, and new controllable switches can be installed. In addition, the new grid should be built with smart communication technologies to facilitate the use of microgrids and renewable generators.

There are several research directions that can be explored on this topic. In terms of logistics, crews and their accommodations, equipment, and work schedules must all be coordinated and managed. For the distribution systems, utilities must decide where and what types of technologies to install. The objective of the rebuilding process is to construct a more resilient system within the budget.

6.3 Publications

Journal Paper

1. **A. Arif**, Z. Wang, C. Chen, and B. Chen "A stochastic multi-commodity logistic model for disaster preparation in distribution systems," *IEEE Trans. Smart Grid*, accepted for publication.

2. **A. Arif**, Z. Wang, J. Wang, and C. Chen, "Repair and resource scheduling in unbalanced distribution systems using neighborhood search," *IEEE Trans. Smart Grid*, accepted for publication.

3. **A. Arif**, S. Ma, Z. Wang, J. Wang, S. M. Ryan and C. Chen, "Optimizing service restoration in distribution systems with uncertain repair time and demand," *IEEE Trans. Power Syst.*, vol. 33, no. 6, pp. 6828–6838, Jul. 2018.

4. **A. Arif**, Z. Wang, J. Wang, B. Mather, H. Bashualdo, and D. Zhao, "Load modeling - a review," *IEEE Trans. Smart Grid*, vol. 9, no. 6, pp. 5986–5999, Nov. 2018.

5. **A. Arif**, Z. Wang, J. Wang, and C. Chen, "Power distribution system outage management with co-optimization of repairs, reconfiguration, and DG dispatch," *IEEE Trans. Smart Grid*, vol. 9, no. 5, pp. 4109–4118, Sept. 2018.

6. **A. Arif** and Z. Wang, "Networked microgrids for service restoration in resilient distribution systems," *IET Gener., Transm. Distrib.*, vol. 11, no. 14, pp. 3612–3619, Sep. 2017.

Conference Paper

1. S. Ma, N. Carrington, **A. Arif**, Z. Wang,"Resilience assessment of self-healing distribution systems under extreme weather events," *IEEE PES General Meeting*, Atlanta, GA, 2019, pp. 1-5.

2. S. Ma, S. Li, Z. Wang, **A. Arif** and K. Ma,"A novel MILP formulation for fault isolation and network reconfiguration in active distribution systems," *IEEE PES General Meeting*, Portland, OR, 2018, pp. 1-5.

3. **A. Arif**, S. Ma, Z. Wang, "Distribution network outage data analysis and repair time prediction using deep learning," *IEEE Int Conf. Probabilistic Methods Appl. Power Syst.*, Boise, ID, 2018, pp. 1-6.

4. **A. Arif**, S. Ma, Z. Wang, "Dynamic reconfiguration and fault isolation for a self-healing distribution system," *IEEE PES Transm. Distrib. Conf. Expo.*, Denver, CO, 2018, pp. 1-5.

5. **A. Arif**, S. Ma, Z. Wang, "Online decomposed optimal outage management after natural disasters," *IEEE PES General Meeting*, Chicago, IL, 2017, pp. 1-5.

6. **A. Arif**, S. Ma, Z. Wang, "Optimization of transmission system repair and restoration with crew routing," *IEEE North Amer. Power Symp.*, 2016, Denver, CO, pp. 1-6.

7. **A. Arif** and Z. Wang, "Service restoration in resilient power distribution systems with networked microgrid," *IEEE PES General Meeting*, Boston, MA, 2016, pp. 1-5.

BIBLIOGRAPHY

[1] "Economic Benefits of Increasing Electric Grid Resilience to Weather Outages," Executive Office of the President, Tech. Rep., 2013.

[2] D. Darling, S. Hoff. "Average frequency and duration of electric distribution outages vary by states." Internet: https://www.eia.gov/todayinenergy/detail.php?id=35652, Apr. 5, 2018 [May 1, 2018].

[3] T. DiChristopher. "Texas utilities struggle to restore power as Harvey hampers progress." Internet: https://www.cnbc.com/2017/08/28/texas-utilities-struggle-to-restore-power-as-harvey-hampers-progress, Aug. 28, 2017 [Aug. 1, 2018].

[4] P. Sullivan, M. Berman, and K. Zezima. "After Irma, Florida prepares for days - and maybe weeks - without power." Internet: https://www.washingtonpost.com/news/post-nation/wp/2017/09/12/florida-struggles-with-top-job-in-irmas-wake-restoring-power-to-millions, Sep. 13, 2017 [Aug 1, 2018].

[5] A. B. Smith. "2017 U.S. billion-dollar weather and climate disasters: a historic year in context." Internet: https://www.climate.gov/news-features/blogs/beyond-data/2017-us-billion-dollar-weather-and-climate-disasters-historic-year, Jan. 28, 2017 [Aug. 9, 2018].

[6] A. B. Smith. "2018's Billion Dollar Disasters in Context." Internet: https://www.climate.gov/news-features/blogs/beyond-data/2018s-billion-dollar-disasters-context, Feb. 7, 2019 [Mar. 13, 2019].

[7] S. Ma, B. Chen, and Z. Wang, "Resilience enhancement strategy for distribution systems under extreme weather events," *IEEE Trans. Smart Grid*, vol. 32, no. 2, pp. 1440-1450, Mar. 2017.

[8] S. Ma, S. Liu, Z. Wang, F. Qiu, and G. Guo, "Resilience enhancement of distribution grids against extreme weather events," *IEEE Trans. Power Syst.*, to be published.

[9] FirstEnergy. "Storm restoration process" Internet: http://www.firstenergycorp.com/content/customer/help/outages/storm_restorationprocess.html, Mar. 18, 2016 [Aug. 1, 2018].

[10] T. Taylor and J. Kazemzadeh, "Integrated SCADA/DMS/OMS: increasing distribution operations efficiency ," *Electric Energy T&D*, no. 2, vol. 13, Apr. 2009.

[11] G. J. Lim, S. Kim, J. Cho, Y. Gong and A. Khodaei, "Multi-UAV pre-positioning and routing for power network damage assessment," *IEEE Trans. Smart Grid*, vol. 9, no. 4, pp. 3643-3651, Jul. 2018.

[12] P. Van Hentenryck and C. Coffrin "Transmission system repair and restoration," *Math. Program.*, vol. 151, no. 1, pp. 347-373, Jun. 2015.

[13] H. O. Mete and Z. B. Zabinsky, "Stochastic optimization of medical supply location and distribution in disaster management," *Int. J. Prod. Econ.*, vol. 126, no. 1, pp. 76-84, 2010.

[14] A. Verma and G. M. Gaukler, "Pre-positioning disaster response facilities at safe locations: an evaluation of deterministic and stochastic modeling approaches", Comput. Oper. Res., vol. 62, pp. 197-209, Oct. 2015.

[15] O. Rodriguez-Espindola, P. Albores, C. Brewster, "Disaster preparedness in humanitarian logistics: a collaborative approach for resource management in floods," *Eur. J. Oper. Res.*, vol. 264, no. 3, pp. 978-993, Feb. 2018.

[16] J. Salmeron and A. Apte, "Stochastic optimization for natural disaster asset prepositioning," Prod. Oper. Manage., vol. 19, no. 5, pp. 561-574, 2010.

[17] C. Rawls, M. Turnquist, "Pre-positioning and dynamic delivery planning for short-term response following a natural disaster", Socio-Economic Planning Sciences, vol.46, no.1, pp. 46-54, 2012.

[18] L. Zhen, K. Wang, and H. C. Liu, "Disaster relief facility network design in metropolises," IEEE Trans. Syst., Man, Cybern., Syst., vol. 45, no. 5, pp. 751-761, May 2015.

[19] A. Ben-Tal, B. D. Chung, S. R. Mandala, T. Yao, "Robust optimization for emergency logistics planning: risk mitigation in humanitarian relief supply chains," *Transp. Res. Part B*, vol. 45, no. 8, pp. 1177-1189, Sep. 2011.

[20] Ali Bozorgi-Amiri, M. S. Jabalameli, S. M. J. Mirzapour Al-e-Hashem, "A multi-objective robust stochastic programming model for disaster relief logistics under uncertainty," *OR Spectrum*, vol. 35, no. 4, pp. 905-933, Nov. 2013.

[21] M. Fereiduni, K. Shahanaghi, "A robust optimization model for distribution and evacuation in the disaster response phase," *J Ind Eng Int*, vol. 13, no. 1, pp. 117-141, Mar. 2017.

[22] W. Ni, J. Shu, M. Song, "Location and emergency inventory pre-positioning for disaster response operations: min-max robust model and a case study of Yushu Earthquake," *Prod. Oper. Manage.*, vol. 27, no. 1, pp. 160-183, Jan. 2018.

[23] S. Wang, B. R. Sarker, L. Mann, Jr., and E. Triantaphyllou, "Resource planning and a depot location model for electric power restoration," *Eur. J. Oper. Res.*, vol. 155, no. 1, pp. 22-43, May 2004.

[24] P. V. Hentenryck, R. Bent, C. Coffrin, "Strategic planning for disaster recovery with stochastic last mile distribution," in *Proc. Int. Conf. CPAIOR, Bologna, Italy*, Jun. 2010, pp. 318-333.

[25] C. Coffrin, P. V. Hentenryck, and R. Bent, "Strategic stockpiling of power system supplies for disaster recovery," in *Proc. IEEE Power Eng. Soc. Gen. Meeting*, San Diego, CA, USA, 2011, pp. 1-8.

[26] M. Khomami, M. Sepasian, "Pre-hurricane optimal placement model of repair teams to improve distribution network resilience," *Elect. Power Syst. Res.*, vol. 165, pp. 1-8, Dec. 2018.

[27] K. Braekers, K. Ramaekers, and I. V. Nieuwenhuyse, "The vehicle routing problem: State of the art classification and review," *Comput. Ind. Eng.*, vol. 99, pp. 300 – 313, Sep. 2016.

[28] G. Ozbaygin, O. E. Karasan, M. Savelsbergh, and H. Yaman, "A branch-and-price algorithm for the vehicle routing problem with roaming delivery locations," *Transp. Res. B, Methodological*, vol. 100, pp. 115 – 137, Jun. 2017.

[29] M. T. Godinho, L. Gouveia, and T. L. Magnanti, "Combined route capacity and route length models for unit demand vehicle routing problems," *Discrete Optimization*, vol. 5, no. 2, pp. 350 – 372, May 2008, in Memory of George B. Dantzig.

[30] T.-C. Chiang and W.-H. Hsu, "A knowledge-based evolutionary algorithm for the multiobjective vehicle routing problem with time windows," *Comput. Oper. Res.*, vol. 45, pp. 25 – 37, May 2014.

[31] S. Yan, J. C. Chu, F.-Y. Hsiao, and H.-J. Huang, "A planning model and solution algorithm for multi-trip split-delivery vehicle routing and scheduling problems with time windows," *Comput. Ind. Eng.*, vol. 87, pp. 383 – 393, Sep. 2015.

[32] H. Hojabri, M. Gendreau, J.-Y. Potvin, and L.-M. Rousseau, "Large neighborhood search with constraint programming for a vehicle routing problem with synchronization constraints," *Comput. Oper. Res.*, vol. 92, pp. 87 – 97, Apr. 2018.

[33] Y. Zhang and X. Chen, "An optimization model for the vehicle routing problem in multi-product frozen food delivery," *J. Appl. Res. Tech.*, vol. 12, no. 2, pp. 239 – 250, Apr. 2014.

[34] C. Archetti and M. G. Speranza, "A survey on matheuristics for routing problems," *EURO J. Comput. Optim.*, vol. 2, no. 4, pp. 223–246, Nov 2014.

[35] H. Chen, "Combinatorial clock-proxy exchange for carrier collaboration in less than truck load transportation," *Transp. Res. E, Logistics Transp. Rev.*, vol. 91, pp. 152 – 172, Jul. 2016.

[36] E. Choi and D.-W. Tcha, "A column generation approach to the heterogeneous fleet vehicle routing problem," *Comp. Oper. Res.*, vol. 34, no. 7, pp. 2080 – 2095, Jul. 2007.

[37] P. Hokama, F. K. Miyazawa, and E. C. Xavier, "A branch-and-cut approach for the vehicle routing problem with loading constraints," *Expert Syst. Appl.*, vol. 47, pp. 1 – 13, Apr. 2016.

[38] Y. Zhong and M. H. Cole, "A vehicle routing problem with backhauls and time windows: a guided local search solution," *Transp. Res. E, Logistics Transp. Rev.*, vol. 41, no. 2, pp. 131 – 144, Mar. 2005.

[39] V. F. Yu, A. P. Redi, Y. A. Hidayat, and O. J. Wibowo, "A simulated annealing heuristic for the hybrid vehicle routing problem," *Appl. Soft Comput.*, vol. 53, pp. 119 – 132, Apr. 2017.

[40] S. R. A. Haddadene, N. Labadie, and C. Prodhon, "A grasp x ils for the vehicle routing problem with time windows, synchronization and precedence constraints," *Expert Syst. Appl.*, vol. 66, pp. 274 – 294, Dec. 2016.

[41] H. Jia, Y. Li, B. Dong, and H. Ya, "An improved tabu search approach to vehicle routing problem," *Procedia Social Behavioral Sci.*, vol. 96, pp. 1208 – 1217, Nov. 2013, intelligent and Integrated Sustainable Multimodal Transportation Systems Proceedings from the 13th COTA International Conference of Transportation Professionals (CICTP2013).

[42] P. Grangier, M. Gendreau, F. Lehuede, and L.-M. Rousseau, "A matheuristic based on large neighborhood search for the vehicle routing problem with cross-docking," *Comput. Operations Res.*, vol. 84, pp. 116 – 126, Aug. 2017.

[43] M. A. Mohammed, M. K. A. Ghani, R. I. Hamed, S. A. Mostafa, M. S. Ahmad, and D. A. Ibrahim, "Solving vehicle routing problem by using improved genetic algorithm for optimal solution," *J. Comput. Sci.*, vol. 21, pp. 255 – 262, Jul. 2017.

[44] B. Yu, Z.-Z. Yang, and B. Yao, "An improved ant colony optimization for vehicle routing problem," *Eur. J. Oper. Res.*, vol. 196, no. 1, pp. 171 – 176, Jul. 2009.

[45] Y. Marinakis, G.-R. Iordanidou, and M. Marinaki, "Particle swarm optimization for the vehicle routing problem with stochastic demands," *Appl. Soft Comput.*, vol. 13, no. 4, pp. 1693 – 1704, Apr. 2013.

[46] P. Toth and D. Vigo, "A heuristic algorithm for the symmetric and asymmetric vehicle routing problems with backhauls," *Eur. J. Oper. Res.*, vol. 113, no. 3, pp. 528 – 543, Mar. 1999.

[47] C. Liu, *et al.*, "Development and evaluation of system restoration strategies from a blackout," PSERC Publication 09-08, Sep. 2009.

[48] Y. Wang, C. Chen, J. Wang, and R. Baldick, "Research on resilience of power systems under natural disasters - a review," *IEEE Trans. Power Syst.*, vol. 31, no. 2, pp. 1604-1613, March 2016.

[49] S. Toune, H. Fudo, T. Genji, Y. Fukuyama, and Y. Nakanishi, "Comparative study of modern heuristic algorithms to service restoration in distribution systems," *IEEE Trans. Power Del.*, vol. 17, no. 1, pp. 173-181, Jan. 2002.

[50] R. E. Perez-Guerrero, G. T. Heydt, N. J. Jack, B. K. Keel, and A. R. Castelhano, "Optimal restoration of distribution systems using dynamic programming," *IEEE Trans. Power Del.*, vol. 23, no. 3, pp. 1589-1596, Jul. 2008.

[51] J. M. Solanki, S. Khushalani, and N. N. Schulz, "A multi-agent solution to distribution systems restoration," *IEEE Trans. Power Syst.*, vol. 22, no. 3, pp. 1026-1034, Aug. 2007.

[52] K. L. Butler, N. D. R. Sarma, and V. R. Prasad, "Network reconfiguration for service restoration in shipboard power distribution Systems," *IEEE Trans. Power Syst.*, vol. 16, no. 4, pp. 653-661, Nov. 2001.

[53] R. A. Jabr, R. Singh, and B. C. Pal, "Minimum loss network reconfiguration using mixed-integer convex programming," *IEEE Trans. Power Syst.*, vol. 27, no. 2, pp. 1106-1116, May 2012.

[54] E. Romero-Ramos, A. G. Exposito, J. R. Santos, and F. L. Iborra, "Path-based distribution network modeling: Application to reconfiguration for loss reduction," *IEEE Trans. Power Syst.,* vol. 20, no. 2, pp. 556–564, May 2005.

[55] M. Al Owaifeer and M. Al-Muhaini, "MILP-based technique for smart self-healing grids," *IET Gener. Transm. Distrib.*, vol. 12, no. 10, pp. 2307–2316, May 2018.

[56] X. Chen, W. Wu and B. Zhang, "Robust restoration method for active distribution networks," *IEEE Trans. Power Syst.,* vol. 31, no. 5, pp. 4005-4015, Sept. 2016.

[57] A. Abel Hafez, W. A. Omran and Y. G. Hegazy, "A decentralized technique for autonomous service restoration in active radial distribution networks," *IEEE Trans. Smart Grid*, vol. 9, no. 3, pp. 1911-1919, May 2018.

[58] Z. Wang, B. Chen, J. Wang, and C. Chen, "Networked Microgrids for Self-healing Power Systems," *IEEE Trans. Smart Grid*, vol. 7, no. 1, pp. 310-319, Jan. 2016.

[59] A. Arif and Z. Wang, "Networked microgrids for service restoration in resilient distribution systems," *IET Gener., Transm. Distrib.*, vol. 11, no. 14, pp. 3612-3619, Sep. 2017.

[60] H. Gao, J. Liu, L. Wang, and Z. Wei, "Decentralized energy management for networked microgrids in future distribution systems," *IEEE Trans. Power Syst.,* vol. 33, no. 4, pp. 3599-3610, July 2018.

[61] C. Chen, J. Wang, and F. Qiu, "Resilient distribution system by microgrids formation after natural disasters," *IEEE Trans. Smart Grid*, vol. 7, no. 2, pp. 958-966, March 2016.

[62] Z. Wang and J. Wang, "Self-healing resilient distribution systems based on sectionalization into microgrids," *IEEE Trans. Power Syst.*, vol. 30, no. 6, pp. 3139-3149, Nov. 2015.

[63] D. N. Trakas and N. D. Hatziargyriou, "Optimal distribution system operation for enhancing resilience against wildfires," *IEEE Trans. Power Syst.*, vol. 33, no. 2, pp. 2260-2271, Mar. 2018.

[64] M. J. Ghorbani, M. A. Choudhry and A. Feliachi, "A multiagent design for power distribution systems automation," *IEEE Trans. Smart Grid*, vol. 7, no. 1, pp. 329-339, Jan. 2016.

[65] R. Romero, J. F. Franco, F. B. Leao, M. J. Rider and E. S. de Souza, "A new mathematical model for the restoration problem in balanced radial distribution systems," *IEEE Trans. Power Syst.*, vol. 31, no. 2, pp. 1259-1268, Mar. 2016.

[66] D. Cui, L. Li, Z. Mu, Z. Hu, G. Yuan and C. Zhang, "Fault isolation and reconfiguration of multi-voltage level distribution network based on PSO algorithm," *Asia-Pacific Power and Energy Eng. Conf.*, Shanghai, 2012, pp. 1-4.

[67] A. Arab, A. Khodaei, Z. Han, and S. K. Khator, "Proactive recovery of electric power assets for resiliency enhancement," *IEEE Access*, vol. 3, pp. 99-109, Feb. 2015.

[68] N. Xu, S. D. Guikema, R. A. Davidson, L. K. Nozick, Z. Cagnan, and K. Vaziri, "Optimizing scheduling of post-earthquake electric power restoration tasks," *Earthquake Eng. Struct. Dyn.*, vol. 36, no. 2, pp. 265-284, Feb. 2007.

[69] C. J. Zapata, S. C. Silva, H. I. Gonzalez, O. L. Burbano and J. A. Hernandez, "Modeling the repair process of a power distribution system," in *Trans. Distribution Conf.*, Latin America, Bogota, 2008, pp. 1-7.

[70] P. M. S. Carvalho, F. J. D. Carvalho and L. A. F. M. Ferreira, "Dynamic restoration of large-scale distribution network contingencies: crew dispatch assessment," in *Power Tech Conf.*, Lausanne, 2007, pp. 1453-1457.

[71] A. Arif, Z. Wang, J. Wang, and C. Chen, "Power distribution system outage management with co-optimization of repairs, reconfiguration, and DG dispatch," *IEEE Trans. Smart Grid*, vol. 9, no. 5, pp. 4109-4118, Sept. 2018.

[72] A. Arif, S. Ma, Z. Wang, J. Wang, S. M. Ryan, and C. Chen, "Optimizing service restoration in distribution systems with uncertain repair time and demand," *IEEE Trans. Power Syst.*, vol. 33, no. 6, pp. 6828–6838, Nov. 2018.

[73] Y. Lin, B. Chen, J. Wang and Z. Bie, "A combined repair crew dispatch problem for resilient electric and natural gas system considering reconfiguration and DG islanding," *IEEE Trans. Power Syst.*, to be published.

[74] S. Lei, C. Chen, Y. Li and Y. Hou, "Resilient disaster recovery logistics of distribution systems: co-optimize service restoration with repair crew and mobile power source dispatch," *IEEE Trans. Smart Grid*, to be published.

[75] B. Chen, Z. Ye, C. Chen, J. Wang, T. Ding and Z. Bie, "Toward a synthetic model for distribution system restoration and crew dispatch," *IEEE Trans. Power Syst.*, to be published.

[76] A. Arif, Z. Wang, J. Wang, C. Chen, "Repair and resource scheduling in unbalanced distribution systems using neighborhood search," arXiv:1808.10548 [math.OC], Aug. 2018.

[77] A. W. Mohamed, "Solving stochastic programming problems using new approach to differential evolution algorithm," *Egyptian Informat. J.*, vol. 18, no. 2, pp. 75 – 86, Jul. 2017.

[78] J. Kaplan and M. De Maria, "A simple empirical model for predicting the decay of tropical cyclone winds after landfall," *J. Appl. Meteorol.*, vol. 34, no. 11, pp. 2499-2512, Nov. 1995.

[79] P. Javanbakht, "Risk-based generation dispatch in the power grid for resilience against extreme weather events," Ph.D dissertation, Elect. Eng. Comput. Sci. Dept., Colorado School of Mines, Golden, CO, 2015. Accessed on: December 12, 2018. [Online]. Available: https://mountainscholar.org/handle/11124/17126.

[80] R. Brown, "Cost-benefit analysis of the deployment of utility infrastructure upgrades and storm hardening programs," *Quanta Technology*, Tech. Rep. 36375, 2009.

[81] M. Ouyang and L. Duenas-Osorio, "Multi-dimensional hurricane resilience assessment of electric power systems," *Struct. Safety*, vol. 48, pp. 15-24, Feb. 2014.

[82] J. Winkler, L. Duenas-Osorio, R. Stein, and D. Subramanian, "Performance assessment of topologically diverse power systems subjected to hurricane events," *Rel. Eng. Syst. Safety*, vol. 95, no. 4, pp. 323-336, Apr. 2010.

[83] C. Bayliss, *Transmission and Distribution Electrical Engineering*. London, U.K.: Butterworth, 1996, pp. 95-106.

[84] C. D. Canham, M. J. Papaik, and E. F. Latty, "Interspecific variation in susceptibility to windthrow as a function of tree size and storm severity for northern temperate tree species," *Can. J. Forest Res.*, vol. 31, no. 1, pp. 1-10, Jan. 2001.

[85] S. D. Ritenour, "Gulf Power Company's vegetation management for storm hardening," Gulf Power Company, Sep. 25, 2006. [Online]. Available: http://www.psc.state.fl.us/library/filings/2006/08950-2006/. Accessed on: January 12, 2019.

[86] R. T. Rockafellar and R. J.-B. Wets, "Scenarios and policy aggregation in optimization under uncertainty," *Math. Oper. Res.*, vol. 16, no. 1, pp. 119-147, 1991.

[87] J.-P. Watson and D. L. Woodruff, "Progressive hedging innovations for a class of stochastic mixed-integer resource allocation problems," *Comput. Manage. Sci.*, vol. 8, no. 4, pp. 355-370, Jul. 2010.

[88] K. Cheung, D. Gade, S. Ryan, C. Silva-Monroy, J.-P. Watson, R. Wets, D. L. Woodruff, "Toward scalable stochastic unit commitment - part 2: assessing solver performance," *Energy Syst.*, vol. 6, pp. 417-438, Apr. 2015.

[89] W. E. Hart, C. Laird, J. P. Watson, and D. L. Woodruff, *Pyomo - optimization modeling in Python (Springer optimization and its applications)*. New York, NY, USA: Springer, 2012, vol. 67.

[90] R. Fourer, D. M. Gay, and B. Kernighan, "AMPL: a mathematical programming language," *Algorithms and Model Formulations in Math. Programming*, S. W. Wallace, Ed. New York, NY, USA: Springer-Verlag, 1989, pp. 150-151.

[91] GAMS/SCENRED2. Documentation. [Online]. Available: https://www.gams.com/24.8/docs/tools/scenred2/index.html.

[92] J.-P. Watson, D. L. Woodruff, W. E. Hart, "PySP: modeling and solving stochastic programs in Python ," *Math. Program.*, vol. 4, no. 2, pp. 109-149, Jun. 2012.

[93] IEEE PES AMPS DSAS Test Feeder Working Group, "123-bus feeder." Internet: http://sites.ieee.org/pes-testfeeders/resources/, Feb. 3, 2014 [May 12, 2018].

[94] Southwire Company. (2012, Apr. 19). Aluminum Conductor. Steel Reinforced. [Online]. Available: https://www.southwire.com/ProductCatalog/XTEInterfaceServlet?contentKey=prodcatsheet16.

[95] L. Kempner Jr., *Substation Structure Design Guide (ASCE Manuals and Reports on Engineering Practice*, 113). Reston, VA, USA: ASCE, 2007.

[96] W. Klibi, S. Ichoua, A. Martel, "Prepositioning emergency supplies to support disaster relief: A case study using stochastic programming," *INFOR: Inform. Syst. Oper. Res.*, vol. 56, no. 1, pp. 50-81, Jun. 2017.

[97] H. R. Lu, A. El Hanandeh, "Environmental and economic assessment of utility poles using life cycle approach," *Clean Techol. Environ. Policy*, vol 19, pp. 1047-1066, Oct. 2016.

[98] Garret Engineers. (Sep. 2015). The cost of a power pole. [Online]. Available: https://garrett-engineers.com/cases-of-the-month/the-cost-of-a-power-pole/.

[99] Synapse Energy Economics, Avoided energy supply components in New England: 2018 report. (2018). [Online]. Available: http://www.synapse-energy.com/sites/default/files/AESC-2018-17-080-Oct-ReRelease.pdf.

[100] M. Kaut and S. W. Wallace, "Evaluation of scenario-generation methods for stochastic programming," *Pacific J. Optimization*, vol. 3, no. 2, pp. 257-271, May 2007.

[101] K. Fleszar, I. H. Osman, and K. S. Hindi, "A variable neighborhood search algorithm for the open vehicle routing problem," *Eur. J. Oper. Res.*, vol. 195, no. 3, pp. 803-809, Jun. 2009.

[102] T. Malakar and S. K. Goswami, "Active and reactive dispatch with minimum control movements," *Int. J. Electr. Power Energy Syst.*, vol. 44, no. 44, pp. 78-87, Jan. 2013.

[103] M. Nagpal, G. Delmee, A. El-Khatib, K. Stich, D. Ghangass and A. Bimbhra, "A practical and cost effective cold load pickup management using remote control," in *Proc. Western Protective Relay Conf.*, Spokane, WA, 2014, pp. 1-25.

[104] B. Chen, C. Chen, J. Wang, and K. L. Butler-Purry, "Multi-Time Step Service Restoration for Advanced Distribution Systems and Microgrids," *IEEE Trans. Smart Grid*, to be published.

[105] B. Chen, C. Chen, J. Wang, and K. L. Butler-Purry, "Sequential service restoration for unbalanced distribution systems and microgrids," *IEEE Trans. Power Syst.*, vol. 33, no. 2, Mar. 2018.

[106] R. R. Gonçalves, J. F. Franco, and M. J. Rider, "Short-term expansion planning of radial electrical distribution systems using mixed-integer linear programming," *IET Generation, Transmission & Distribution*, vol. 9, no. 3, pp. 256–266, 2014.

[107] A. Arif, S. Ma, Z. Wang, "Dynamic reconfiguration and fault isolation for a self-healing distribution system," *IEEE PES Transm. Distrib. Conf. Expo.*, Denver, CO, 2018, pp. 1-5.

[108] A. Borghetti, "A mixed-integer linear programming approach for the computation of the minimum-losses radial configuration of electrical distribution networks," *IEEE Trans. Power Syst.*, vol. 27, no. 3, pp. 1264-1273, Aug. 2012.

[109] J. Kirk, "Count loops in a graph," Internet: https://www.mathworks.com/matlabcentral/fileexchange/10722-count-loops-in-a-graph, Mar. 18, 2016 [May. 1, 2017].

[110] C. Meehan. "What types of solar power systems can I get for my home?" Internet: https://www.solar-estimate.org/news/2017-11-15-types-solar-power-systems-homes-111517, Nov. 15, 2017 [Nov. 1, 2018].

[111] T. Kenning. "Australia's first large-scale grid-connected solar and battery project comes online." Internet: https://www.pv-tech.org/news/australias-first-large-scale-grid-connected-solar-and-battery-project-comes, Feb. 19, 2018 [Nov. 1, 2018].

[112] Q. Zhang, K. Dehghanpour and Z. Wang, "Distributed CVR in unbalanced distribution systems with PV penetration," *IEEE Trans. Smart Grid*, to be published.

[113] H. H. Abdeltawab, Y. A. I. Mohamed, "Mobile energy storage scheduling and operation in active distribution systems," *IEEE Trans. Ind. Electron.*, vol. 64, no. 9, pp. 6828-6840, Sept. 2017.

[114] E. W. Dijkstra, "A note on two problems in connexion with graphs," Numerische Mathematik, vol. 1, no. 1, pp. 269-271, Dec. 1959.

[115] G. Laporte, "Fifty years of vehicle routing," *Transp. Sci.*, vol. 43, no. 4, pp. 408-416, Oct. 2009.

[116] Pennyrile Electric. "Power restoration procedures." Internet: http://www.precc.com/content/power-restoration-procedures, [May 25, 2018].

[117] IBM, "ILOG CPLEX Optimization Studio." Internet: https://www.ibm.com/products/ilog-cplex-optimization-studio, [May 25, 2018].

[118] *National Solar Radiation Data Base (NSRDB)*. Available: https://nsrdb.nrel.gov/nsrdb-viewer.

[119] C. J. Zapata, S. C. Silva and O. L. Burbano, "Repair models of power distribution components," in *Proc. IEEE Transmission and Distrib. Conf. and Expo.*, Latin America, Bogota, 2008, pp. 1-6.

[120] Electronic Reliability Design Handbook, Military Handbook, MILHDBK-338B, 1998, Department of Defense, USA.

[121] N. Lu, R. Diao, R. P. Hafen, N. Samaan and Y. Makarov, "A comparison of forecast error generators for modeling wind and load uncertainty," *IEEE PES General Meeting*, Vancouver, BC, 2013, pp. 1-5.

[122] R. Torquato, Q. Shi, W. Xu, et al., "A Monte Carlo simulation platform for studying low voltage residential networks," *IEEE Trans. Smart Grid*, vol. 5, no. 6, pp. 2766-2776, July 2014.

[123] A. Arif, S. Ma, Z. Wang, "Distribution network outage data analysis and repair time prediction using deep learning," *IEEE Int Conf. Probabilistic Methods Appl. Power Syst.*, Boise, ID, 2018, pp. 1-6.